

MIT Open Access Articles

50th Anniversary Perspective: Polymers and Mixed Matrix Membranes for Gas and Vapor Separation: A Review and Prospective Opportunities

The MIT Faculty has made this article openly available. *Please share* how this access benefits you. Your story matters.

As Published: 10.1021/ACS.MACROMOL.7B01718

Publisher: American Chemical Society (ACS)

Persistent URL: <https://hdl.handle.net/1721.1/134685>

Version: Final published version: final published article, as it appeared in a journal, conference proceedings, or other formally published context

Terms of Use: Article is made available in accordance with the publisher's policy and may be subject to US copyright law. Please refer to the publisher's site for terms of use.



50th Anniversary Perspective: Polymers and Mixed Matrix Membranes for Gas and Vapor Separation: A Review and Prospective Opportunities

Michele Galizia,[†] Won Seok Chi,[‡] Zachary P. Smith,[‡] Timothy C. Merkel,[§] Richard W. Baker,[§] and Benny D. Freeman^{*,||,⊥}

[†]Department of Chemical, Biological and Materials Engineering, The University of Oklahoma, 100E Boyd Street, Norman, Oklahoma 73019, United States

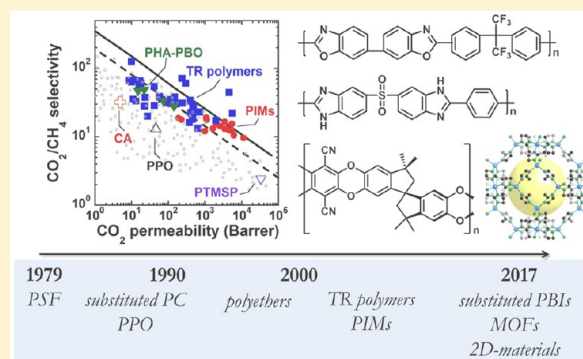
[‡]Department of Chemical Engineering, Massachusetts Institute of Technology, 77 Massachusetts Avenue, Cambridge, Massachusetts 02139, United States

[§]Membrane Technology and Research, Inc., 39630 Eureka Drive, Newark, California 94560, United States

^{||}John J. McKetta Jr. Department of Chemical Engineering, The University of Texas at Austin, 200 E. Dean Keeton Street, Austin, Texas 78712, United States

[⊥]Center for Energy and Environmental Resources, The University of Texas at Austin, 10100 Burnet Road, Building 133 (CEER), Austin, Texas 78758, United States

ABSTRACT: Membrane gas separation is a mature and expanding technology. However, the availability of better membrane materials would promote faster growth. In this Perspective we analyze the state of the art of membrane materials, including polymers and hybrid materials, as well as the current issues and barriers, and finally, we outline future research directions in membrane science. Development of new membrane materials for large scale separations will rely on a multidisciplinary approach that embraces the broad fields of chemical and materials engineering, polymer science, and materials chemistry.



1. INTRODUCTION

1.1. Background. Today's membrane gas separation industry grew out of the development of membrane technology for water treatment.¹ From 1959 to 1962, Sidney Loeb and Sirivasan Sourirajan created the first asymmetric reverse osmosis membrane. This membrane consisted of a dense, thin selective polymer layer on top of a much thicker microporous support layer. The microporous support provided mechanical strength, while the thin dense skin performed the separation. These membranes had 20 times the permeance of any membrane then known and good water/salt selectivity. This breakthrough made desalination by reverse osmosis potentially economical. It took another 10 years to develop the technology required to fabricate the membranes on a large scale and package them into large membrane area modules. By the late 1970s, reverse osmosis and the related membrane water treatment process of ultrafiltration were off the ground, and the market was supplied by established companies. The time was then ready for this base technology to be applied to gas separation.

The first commercially successful gas separation membranes were developed by Permea, now a division of Air Products.² An early application was the separation of hydrogen from nitrogen,

argon, and methane in ammonia plant purge gas. This was soon expanded to hydrogen/light hydrocarbon separations in refineries and hydrogen/carbon monoxide ratio adjustment in synthesis gas plants. These were all good applications because hydrogen is very permeable and membranes are able to easily separate it from many gas mixtures.

Over the decade from 1980 to 1990, a number of other applications were developed. The big four membrane gas separation applications developed by 1990 are listed in Table 1. These four applications continue to represent 80–90% of the current gas separation membrane industry. The market has expanded very significantly over the past 25 years, and current sales are in the range of \$1.0–1.5 billion/year, but no large new application has been added to the list in Table 1. Recently, some new applications, such as air and natural gas dehydration, have shown some commercial success. Also, the bulk of today's market is supplied by essentially the same handful of polymers used for these applications in 1990. This apparent stagnation has occurred

Received: August 8, 2017

Revised: September 11, 2017

Published: October 3, 2017

Table 1. Current Big Four Commercial Gas Separation Membrane Applications

application	separation performed	selective layer polymer	approximate market size
hydrogen recovery	H ₂ /N ₂ , H ₂ /CH ₄ , H ₂ /CO	polysulfone, polyimides	\$200 million/year
N ₂ production	O ₂ /N ₂	polyimides, polysulfone, polyphenylene oxide, substituted polycarbonates	\$800 million/year
natural gas treatment	CO ₂ /CH ₄ , H ₂ S/CH ₄ , He/CH ₄	cellulose acetates, polyimides	\$300 million/year
vapor recovery	C ₃ H ₆ /N ₂ , C ₂ H ₄ /N ₂ , C ₂ H ₄ /Ar, C ₃₊ /CH ₄ , CH ₄ /N ₂ , gasoline/air	silicone rubber	\$100 million/year

despite a flood of reports describing new polymers—many of which, based on the authors' data, appear to be better than those used industrially.

There are several reasons for this lack of success. One reason is that the big, and relatively easy, applications shown in Table 1 are mostly solved problems. For example, the separation of nitrogen from air represents about half of the current gas separation market. The same polymers—polysulfone, polyimides, substituted polycarbonate, and poly(phenylene oxide)—all with membrane selectivities of 4–7 have been used for more than 20 years. In nitrogen plants, the membrane skid represents about a third of the cost, the air compressor is another half, and balance of the plant components is the remainder. Membranes with increased selectivity at the same permeance will reduce the compressor size, and membranes with increased permeance at the same selectivity will reduce the membrane skid size, but these improvements will require a significant development effort and are likely to only reduce the total process cost by 5–10%. Such an improvement would be commercially useful for the company making the breakthrough but is unlikely to significantly expand the overall membrane market against the competitive technologies of cryogenic distillation or pressure swing adsorption. For this reason, industrial membrane producers have focused most of their development efforts on optimizing the production of their current membrane products.

Even in applications where better materials would make a difference and expand or open new markets, industry has been slow to pick up novel membrane materials. In this case, an important issue is that developers of new membrane materials have not fully appreciated that when they measure the permeability of these new candidates as a 100 μm thick film with pure gases and get encouraging results, they are at the beginning of the development program, not at the end. Few industrial companies are ready to invest the millions of dollars required to commercialize a new membrane application based on a simple laboratory film test result. If materials researchers and their funding sponsors want to see their polymers used, they must go further down the development path than they have done to date, either by themselves or with industrial partners. By this route, we would hope that some of the new materials described later in this review can be used to expand the Table 1 application list.

1.2. This Paper. This paper is divided into ten parts. In section 2, a brief review of the fundamental principles of membrane gas transport is provided. This section sets the stage for understanding the membrane materials and application challenges as well as some of the proposed solutions that follow. In section 3, we describe a number of large gas separation applications where development of better membranes could make a difference. This description will suggest performance targets that, if achieved, might get the technology off the ground. These permeance and selectivity targets are for *real* membranes,

used with industrially relevant gas mixtures under the conditions of temperature, pressure, and contaminant composition expected in the industrial application. It is possible that some of these problem applications may be solved with a variant of the conventional polymer membranes already available. However, over the past 25 years, hundreds of conventional polymers have been suggested without much success. It seems likely, therefore, that most of these unsolved applications will require development of new types of advanced membranes. Sections 4, 5, 6, 7, 8, and 9 of this paper review some of the promising new materials that may help membrane gas separation technology break out of its box. Finally, in section 10 we summarize present and future research directions in membrane materials science.

2. FUNDAMENTALS OF MEMBRANE GAS TRANSPORT

2.1. Solution-Diffusion Model. The solution-diffusion model has been used successfully to describe gas, vapor, liquid, and ion transport in dense membranes.^{3,4} A basic assumption of this model is that no permanent pores exist in the membrane selective layer, so different chemical species are separated based on their different solubility and diffusivity through the membrane material. Based on this picture, gas molecules dissolve in the high pressure face of the membrane, diffuse through the membrane down a chemical potential (or concentration) gradient, and finally desorb from the low-pressure face of the membrane. Another basic assumption of this model is that equilibrium conditions hold between the fluid and the membrane material on both sides of the membrane. A partition coefficient, S_i , also called solubility coefficient, is introduced to relate penetrant concentration in the membrane with the external penetrant partial pressure:³

$$S_i = \frac{C_{i,0}}{p_{i,0}} = \frac{C_{i,1}}{p_{i,1}} \quad (1)$$

where $p_{i,0}$ is the penetrant partial pressure at the feed side and $p_{i,1}$ is the corresponding value at the permeate side. The terms $C_{i,0}$ and $C_{i,1}$ represent the penetrant concentration at the feed and permeate face of the membrane, respectively.

The permeability of a penetrant, P_i , through the membrane is defined as follows:³

$$P_i = \frac{J_i l}{p_{i,0} - p_{i,1}} \quad (2)$$

where l is the membrane thickness. When penetrant diffusion is described by the Fick's law, the following expression holds, at steady state, for the penetrant flux, J_i :³

$$J_i = D_i S_i \frac{p_{i,0} - p_{i,1}}{l} \quad (3)$$

where D_i is the penetrant diffusion coefficient through the membrane material. By comparing eqs 2 and 3, the penetrant

permeability can be expressed as the product of penetrant diffusion and solubility coefficients:^{3,4}

$$P_i = D_i \times S_i \quad (4)$$

Permeability is an intrinsic material property corresponding to a thickness and pressure normalized permeant flux. Permeability is often expressed in units of barrer, where 1 barrer = 1×10^{-10} cm³ (STP) cm/(cm² s cmHg).

A parameter related to permeability and used more frequently in the membrane industry is gas permeance, where permeance = permeability/thickness (P_i/l).⁵ Permeance is frequently expressed in gas permeance units (GPU), where 1 GPU = 1×10^{-6} cm³ (STP)/(cm² s cmHg). Gas permeance impacts the membrane area required to perform a separation. Higher permeances reduce the size of the membrane system and thus lower the capital cost of a membrane unit. Permeance can be increased either by increasing intrinsic permeability through changes to membrane chemistry or by reducing the thickness of the membrane.

The separating ability of a membrane is determined by the selectivity, $\alpha_{1/2}$, defined as the ratio of the gas permeabilities, P_1/P_2 , or permeances. Based on eq 4, selectivity can be expressed as

$$\alpha_{1/2} = \frac{P_1}{P_2} = \left(\frac{D_1}{D_2} \right) \times \left(\frac{S_1}{S_2} \right) \quad (5)$$

Generally, in conventional glassy polymers, the dominant contribution to selectivity is the ratio of the diffusion coefficients, D_1/D_2 , which primarily depends on the ratio of the molecular sizes. In rubbery polymers, the dominant contribution is from the ratio of the sorption coefficients, S_1/S_2 , which is largely proportional to the ratio of the permeant condensabilities.⁵ However, diffusivity and selectivity of glassy and rubbery polymers are quite similar when compared at similar diffusion coefficients, i.e., at similar fractional free volume.

The selectivity of a membrane impacts the energy required to perform a given separation and thus is related to the operating cost of a membrane system.

2.2. Membrane Structure. The structure of a typical thin-film composite membrane used for industrial gas and liquid separations is shown in Figure 1. A microporous, highly

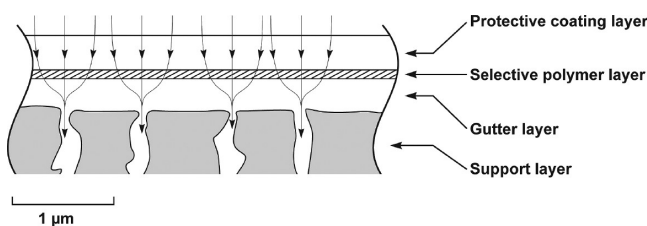


Figure 1. Schematic drawing of the structure of a thin-film composite membrane.

permeable support material provides mechanical strength for the membrane.^{5,6} This support makes up the bulk of the membrane thickness and often has an asymmetric structure with a relatively low-porosity “skin” on one side and a more open structure on the opposite side. The low-porosity side of the support is typically coated with one or more polymer layers including a gutter layer, a selective layer, and a protective or sealing layer.⁵ The gutter layer is formed from a highly permeable polymer and is used to improve the compatibility between the microporous support and selective layer as well as directing the

permeating gas to the support membrane pores. The gutter layer is then coated with a selective layer composed of a polymer with the desired separation properties. For typical industrial gas separation membranes, the selective layer varies between 0.1 and 1 μm in thickness. Finally, a high-permeability protective or sealing layer can be applied to plug any defects in the selective layer and prevent damage during handling. Gas permeation through such composite membranes follows a resistance-in-series model, but when properly designed, the overall separation performance largely depends on the properties of the selective layer.

Our focus throughout this Perspective is on the properties of advanced materials that have potential to be used as the selective layer in an industrial composite membrane. It should be noted that in addition to promising transport properties (permeability, selectivity), ideally these materials would be amenable to reproducible fabrication of thin, defect-free layers by conventional membrane coating methods. For commercial applications, hundreds and even thousands of square meters of defect-free membrane are typically required. If a new material cannot be fabricated at scale cost-effectively, it will not be used. Lack of attention to these practical scale-up issues will hinder progress on new membrane material adoption.

2.3. Trade-Off Relationship. An ideal selective layer polymer combines high permeability (permeance) with high selectivity to minimize membrane system capital and operating costs, respectively. However, nature appears to limit the combinations of polymer permeability and selectivity that can be achieved, resulting in a trade-off relationship. Membrane materials generally exhibit high permeability and low selectivity, or vice versa. This point was first recognized by Robeson,^{7,8} with Freeman later providing a theoretical basis for this behavior.⁹

Figure 2 shows an example of a Robeson-type trade-off plot for CO₂/CH₄. The CO₂/CH₄ selectivity is plotted against the CO₂

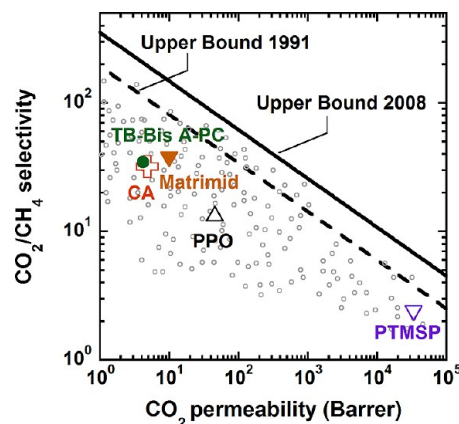


Figure 2. CO₂/CH₄ Robeson diagram for conventional glassy polymers. Data were taken from refs 10–14. PTMSP: poly(trimethylsilylpropyne); PPO: poly(phenylene oxide); CA: cellulose acetate; TB-Bis A-PC: tetrabromobisphenol A poly(carbonate). Pure gas permeabilities were measured between 25 and 35 °C and pressures ranging from 1 to 20 bar. Continuous line represents the 2008 upper bound, and dashed line represents the 1991 upper bound.

permeability for all polymers reported in the open literature, resulting in a diagonal upper bound line beyond which no materials appear. This type of plot has been widely used to judge the relative potential of new membrane materials with a goal of finding polymers exceeding the upper bound line. As research

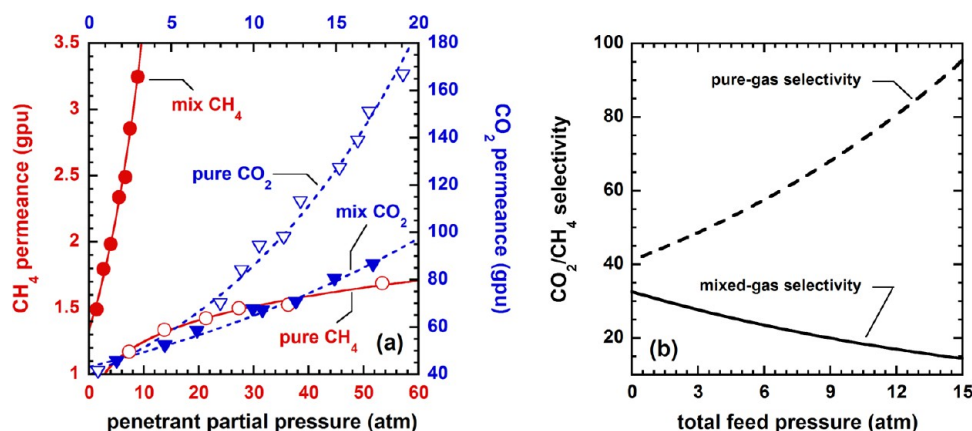


Figure 3. (a) Pure and mixed gas CO₂ and CH₄ permeance in cellulose acetate at room temperature as a function of partial pressure of component *i* in the feed. The CO₂/CH₄ percent mole ratio in the feed mixture is 70/30. Solid and dotted lines serve to guide the eye. (b) Pure gas and mixed gas CO₂/CH₄ selectivity at room temperature. Data after Donohue et al.¹⁷

efforts produced new membrane materials with improved separation performance, the original upper bound devised in 1991 shifted toward the upper-right corner in the Robeson plot.

While trade-off plots like Figure 2 are a useful new material screening tool, they have limitations if the objective is to develop a new commercial membrane. Almost all of the trade-off plots described in literature are for pure gases. As described in the next section, real-world phenomena like plasticization can change the relative positions of different membrane materials when tested with gas mixtures under application conditions. In this sense, finding a promising material with pure gas properties above the upper bound is not the end but only the beginning of new membrane development.

2.4. Plasticization and Physical Aging. A frequently encountered issue that impacts mixed-gas performance of membranes is plasticization.^{5,15,16} Plasticization occurs when the membrane is exposed to highly soluble species that produce significant swelling of the polymer matrix. As a consequence, polymer chain mobility and free volume are increased, which results in a loss of the polymer size-sieving ability, especially at high pressures. A common indicator of plasticization is an increase in pure (or mixed) gas permeability as the total upstream pressure (or the partial pressure of one component) increases.¹⁶

An example of polymer plasticization that has been investigated extensively is that caused by CO₂. In Figure 3a, pure and mixed-gas CO₂ and CH₄ permeances in cellulose acetate membranes, reported by Donohue et al.,¹⁷ are shown as a function of penetrant partial pressure. The presence of plasticizing CO₂ causes the methane mixed-gas permeance to be much higher than the pure gas methane permeance. For example, at 10 atm and room temperature, CH₄ permeance increases by over 2.5 times, relative to the pure gas CH₄ permeance, when a 70/30 mol CO₂/CH₄ mixture is fed to the membrane. As a consequence, a severe loss in CO₂/CH₄ selectivity was observed during mixed gas permeation experiments (cf. Figure 3b). This result highlights the importance of measuring gas permeability at realistic conditions when evaluating new membrane materials.

Another application where the effects of plasticization are detrimental is the olefin–paraffin separation. Some polyimides, such as BPDA-TmPD (BPDA = 3,3',4,4'-biphenyl-tetracarboxylic dianhydride, TmPD = 2,4,6-trimethyl-1,3-phenylenediamine), have high propylene–propane pure gas selectivity (50 or more).¹⁸ Such high ideal selectivity is largely

due to diffusion selectivity (cf. eq 5). Propylene and propane have similar condensability and solubility levels in polymers, while showing greater differences in diffusion coefficient, due to the smaller size of propylene relative to that of propane.¹⁸ However, when tested in mixed propylene–propane conditions, the selectivity of these polyimides is reduced by 1 order of magnitude. This effect is due to plasticization induced by propylene and propane sorption.¹⁸

Another frequently encountered issue that impacts membrane performance is physical aging. Glassy polymer chains pack inefficiently, leaving excess free volume in the polymer matrix. Over time, polymer chains gradually reorder to fill this excess free volume, reducing the specific volume of the polymer matrix. Improved packing efficiency ultimately reduces excess free volume and penetrant diffusion coefficients.¹⁹ Viewed another way, excess free volume elements migrate toward the membrane surface as air bubbles in a viscous liquid, with a migration rate proportional to the square of the membrane thickness.⁵ In thick films (50–100 μm), this process takes long times to become important, and so, in the typical time frame of laboratory experiments, the effects of physical aging on gas permeability appear negligible. In contrast, thin membranes (<1 μm) show the effects of physical aging on gas permeability within a few days, if not hours.¹⁹

Rowe and Paul investigated the effect of physical aging on gas permeability in thin Matrimid films.¹⁹ In Figure 4, CH₄ normalized permeability (i.e., the ratio of permeability at time *t* to permeability of freshly cast film) in Matrimid films 18–550 nm thick is reported as a function of time. Such ultrathin films lose up to 70% of their original permeability after 1000 h (~40 days) of aging. This decay in membrane permeability is due to the relaxation of the nonequilibrium free volume and to the subsequent reordering of polymer chains, which ultimately reduces the number and size of free volume holes available for gas transport in the membrane.

Covalent cross-linking has been tried as a way to stabilize polymer membranes against plasticization and physical aging. In rubbery polymers, covalent cross-linking either leaves permeability unchanged or may reduce it, while in glassy polymers, cross-linking can either increase or decrease gas permeability. The final properties of cross-linked glassy polymers depend on the cross-linking agent length and flexibility as well as on the cross-linking route. For example, Koros and co-workers²⁰ showed that plasticization can be successfully controlled by

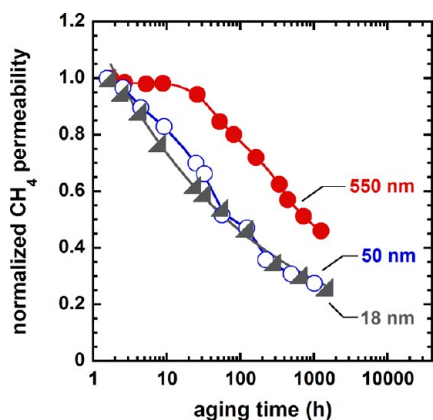


Figure 4. CH₄ normalized permeability in Matrimid at 35 °C and 2 atm as a function of time and thickness. Data after Rowe and Paul.¹⁹ Permeability was normalized to the value measured for a freshly cast sample.

reducing polymer chain mobility (and not by simply suppressing gas sorption). In these studies, membranes based on 6FDA-DAM:DABA polyimide (6FDA = 4,4'-(hexafluoroisopropylidene)diphthalic anhydride, DAM = 2,4,6-trimethyl-1,3-phenylenediamine, DABA = 4,4'-diaminobenzanilide) were cross-linked via monoesterification and transesterification reactions. After cross-linking, CO₂ permeability increased by a factor of 3, and CO₂/CH₄ pure gas selectivity increased from 34 to 37. A significant gain in CO₂/CH₄ selectivity (up to 44.8) was observed during mixed gas permeation experiments, which is due to the effect of competitive sorption. In Figure 5a, pure CO₂ permeability isotherms in cross-linked and un-cross-linked 6FDA-DAM:DABA films are reported as a function of pressure. In the un-cross-linked sample, severe plasticization occurs at pressures greater than 10 atm, while the cross-linked film does not show any plasticization up to 30 atm.

3. UNSOLVED APPLICATIONS

Table 2 lists a series of large gas separation applications where better membranes would either greatly expand their use or allow entry into a new market. Included in this table is an estimate of the membrane permeance and selectivity required to achieve commercial viability. As noted earlier, these performance values

are for industrial composite or asymmetric membranes operating with real mixtures at application conditions.

3.1. CO₂ Removal from Natural Gas. Many natural gas sources contain high levels of CO₂.¹ This excess CO₂ must be reduced to ≤2% CO₂ before the gas can be transported to the users. About 10% of U.S. gas reserves are out of specification for this reason. In the rest of the world, there are large gas fields in the Middle East, Malaysia, Indonesia, and Australia that are also difficult to use because of high CO₂ content. A related application is the use of membranes in enhanced oil recovery (EOR) using CO₂ injected into the oil formation. EOR allows significant amounts of otherwise unextractable oil to be collected. However, the oil is recovered with associated gas that contains some of the injected CO₂. A CO₂/gas separation is then used to recover natural gas and reinject the CO₂.

In some ways, CO₂ separation from natural gas is a solved problem. Membranes currently have about 10% of the CO₂/natural gas separation market; amine absorption has the rest. The reason membranes have only a small market share is a combination of factors including the relatively low permeance and low selectivity of today's membranes. Because of insufficient membrane performance, energy-intensive two-stage processes are usually required to do the separation. A block flow diagram of a representative system for removing CO₂ from natural gas at typical conditions (10% CO₂ in feed at 1000 psig and 50 °C) is shown in Figure 6a. The membrane unit in the first calculation is based on today's commercial cellulose acetate-based (CA) membrane with a CO₂ permeance of 100 GPU and a selectivity of 12. Also shown in Figure 6b is a block diagram of a process using a yet-to-be-developed advanced membrane with a permeance of 200 GPU and a selectivity of 24.

The initial cost of membrane systems fitted with today's cellulose acetate membranes is often competitive with amine technology. The principal barrier to more widespread membrane use is the loss of ~4% of the feed methane with the CO₂ permeate stream. The methane loss of an amine system is much lower (often ~1%). Figure 6b shows the impact of a better membrane; the methane loss is reduced by almost two-thirds to 1.7%. The size of the second-stage compressor is also cut by 28% and the membrane area by 40%. A membrane with these properties in operation would significantly increase the market

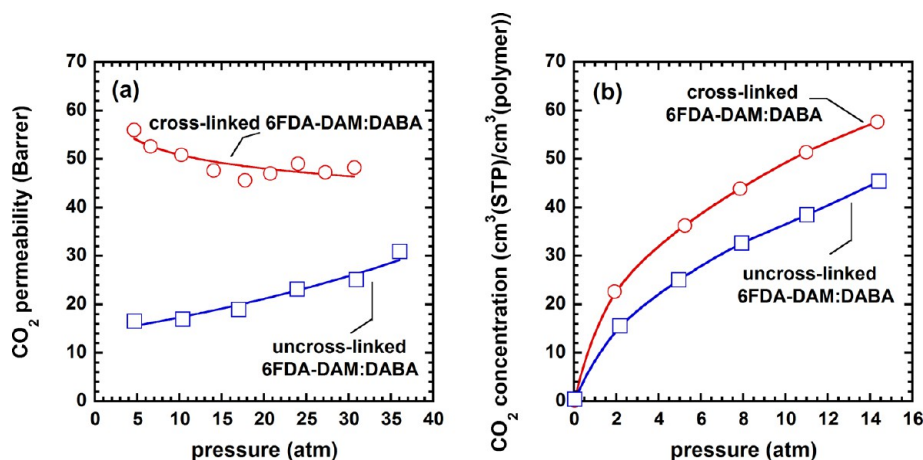


Figure 5. (a) CO₂ permeability at 35 °C in cross-linked and un-cross-linked 6FDA-DAM:DABA. (b) CO₂ sorption isotherms at 35 °C in cross-linked and un-cross-linked 6FDA-DAM:DABA. Membrane cross-linking was achieved by annealing pristine samples at 200 °C for 24 h under vacuum. Data after Hillock and Koros.²⁰

Table 2. Potential Large New Applications and Target Membrane Performance

application	separation required	desired membrane performance		comments
		selectivity	permeance (GPU)	
CO ₂ removal from natural gas	CO ₂ /CH ₄	20–30	>100	already an established membrane application; goal would be to capture a portion of the much larger amine absorption market
olefin/paraffin separation	C ₂ ⁺ /C ₂ ⁰	>5	>50	near-term market is reactor purge streams; larger application is processing steam cracker gas or fluid catalytic cracking unit (FCCU) off-gas
	C ₃ ⁺ /C ₃ ⁰			
CO ₂ capture	CO ₂ /N ₂	30–50	1000–5000	CO ₂ capture from power and industrial exhaust gases
	H ₂ /CO ₂	>10	>200	syngas separations, coal or gas-to-chemical applications
	CO ₂ /H ₂	>20		
vapor/vapor	H ₂ O/ethanol, H ₂ O/IPA	50–100	1000–3000	solvent dehydration, has to be done as a high temperature vapor to be commercially significant
	aromatic/aliphatic, polar/nonpolar	>10	>500	vapor/vapor separation to reduce cost and energy consumption of distillation

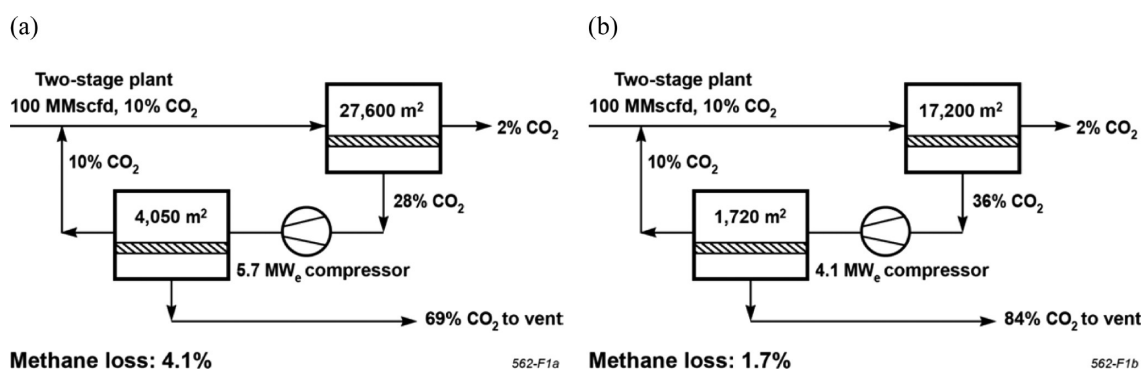


Figure 6. (a) Today's standard CA membrane with CO₂ permeance = 100 GPU and CO₂/CH₄ selectivity = 12. (b) A possible future membrane with CO₂ permeance = 200 GPU and CO₂/CH₄ selectivity = 24.

share of membrane technology. Unfortunately, despite many years of effort, no such membrane has been developed.

Pure-gas data measured with thick films show cellulose acetate to be a rather mediocre membrane material (cf. Figure 2). Many other materials, when plotted on Robeson's selectivity/permeability trade-off curve, are clearly better. However, pure-gas measurements are a poor predictor of real world mixed-gas performance for this application. Cellulose acetate membranes generally have a CO₂/CH₄ selectivity of 35–40 when measured with pure methane and pure CO₂. Thin membranes measured with simple CO₂/methane gas mixtures at high pressure and 50 °C will generally have a selectivity of 15–20. Measured with real natural gas containing a range of C₂ to C₆ hydrocarbons and traces of BTEX components (benzene, toluene, ethylbenzene, and xylenes), the membrane selectivity drops to 10–14.

The key issue is plasticization of the membrane material by carbon dioxide and other hydrocarbons, including the BTEX aromatics usually present at a few hundred ppm. Sorption of these plasticizing components swells the membrane, causing a severe loss in size selectivity (i.e., diffusion selectivity). This point is highlighted in Figure 3. In some cases, the mechanical integrity of the membrane module can even be compromised by sorption of highly plasticizing components. Plasticization has proved to be particularly troublesome for some of the highly size-selective polyimides that have been proposed as a replacement for CA. Cross-linking has been tried as a way to mitigate plasticization, with some success in the lab, but it has proved difficult to scale-up and field experience has been disappointing. The commercial availability of a better membrane material for this application

remains an unsolved problem. Some of the possibilities that may lead to success are discussed later.

3.2. Olefin/Paraffin Separations. Ethylene and propylene are the two largest hydrocarbon feedstocks of the chemical industry. Some of this olefin is produced as a byproduct of refinery operations, but most is produced by steam crackers from ethane, propane, and other light hydrocarbons. As part of these production processes, propylene/propane or ethylene/ethane mixtures must be separated. This is done by distillation, even though the components' boiling points differ by only 4–5 deg.²² These olefin/paraffin splitter columns contain 100–150 stages and are normally the largest column in a petrochemical plant.

Membrane separation has been suggested as an alternative or supplement to olefin/paraffin distillation for many years, but despite much effort, no membrane with the required properties has been developed. To completely or partially replace distillation, membranes with an olefin/paraffin selectivity of >10 and permeances of several hundred GPU for the olefin are likely needed. These permeation properties are far better than the properties of today's membrane materials. However, there are combination membrane/distillation debottlenecking processes or purge stream applications where membranes with selectivities of 5–10 and permeances of around 50–100 GPU could be used. Development of these membranes over time might help to displace distillation.

As an example of a possible purge stream membrane application, Figure 7 shows the synthesis of isopropyl alcohol by direct hydration. Chemical grade propylene (~95% propylene, 5% propane) is reacted with superheated steam over a phosphoric acid catalyst held on an inert support. The

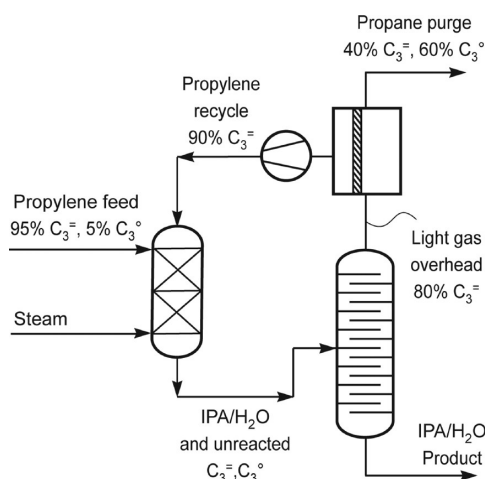


Figure 7. Simple process flow diagram of isopropyl alcohol (IPA) synthesis including a selective purge membrane for propylene ($C_3^=$)/propane ($C_3^°$) separation.

reaction product consisting of water, isopropyl alcohol, unreacted propylene, and propane is separated in a recovery column. The column overhead is a propylene/propane mixture. Only a portion of this gas can be recycled without separation to the feed. The remainder must be purged to stop the buildup of inert propane in the loop. A membrane system having a C_3 selectivity as low as 5 could be used to selectively recycle propylene. Such a system could recover about 90% of the propylene that would otherwise be lost in the purge gas. Similar purge-gas streams are produced in the synthesis of cumene, polypropylene, and polyethylene. Membrane systems are ideally suited for these streams, which can have a value of a few million dollars/year, but are still too small for distillation to be economic.

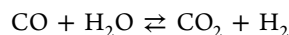
Robeson trade-off plots created using pure-gas data with propylene and propane show that many polymers are available that easily meet the performance targets described above. Unfortunately, mixed-gas membrane selectivity for propylene/propane or ethylene/ethane is almost always a fraction of the pure-gas film data due to severe plasticization. A few very rigid, solvent-resistant polymers such as P84-type polyimides do have selectivities in the target range when tested with olefin/paraffin mixtures at real conditions. However, because of their extreme rigid nature, membrane permeances are very low and uneconomical. Other conventional membrane materials have adequate permeances, but selectivities are too low to be useful in gas mixtures. These olefin/paraffin separations appear difficult to perform with any conventional polymer. As a result, significant effort has been devoted to developing more exotic membranes, including facilitated transport, various mixed-matrix, and inorganic materials. These membranes often show target properties in initial tests, but due to stability, reproducibility, and cost issues, they have yet to leave the laboratory.

3.3. CO₂ Capture. The capture of CO₂ from power plants and industrial exhaust gases could significantly reduce man-made CO₂ emissions.²³ Widespread adoption of this technology would go a long way to solving the global climate change issue. Currently, the most mature CO₂ capture technology is amine absorption. Two large commercial demonstration plants have been built and more are planned. However, the high capital and operating costs, large footprint, and the need to handle large amounts of hazardous chemicals that have their own environmental issues are making it increasingly clear that amine

absorption is unlikely to be widely used. Membrane separation is being developed as a potential alternative approach.

Flue gas streams from power plants typically contain 4–20% CO₂ in mostly N₂ and are at atmospheric pressure. The objective of the separation process is to produce >99% pure liquid CO₂, at a pressure of 100–150 bar at a cost in the range of \$40–60/ton of CO₂ captured. This is a tough cost target for any process to meet. The best approach seems to be to use a membrane system to perform a bulk separation that produces a CO₂-concentrate stream containing 60–80% CO₂. A membrane-assisted condensation process is then used to produce liquid CO₂. Because of the prohibitive cost of compressing the flue gas feed stream to generate a driving force across the membrane, vacuum operation with a pressure of 0.2–0.3 bar on the permeate is the approach generally used. The pressure difference across the membrane is then only about 1 bar, so very high permeance membranes must be used. Today's best membranes made from rubbery polar polymers have a CO₂ permeance of about 2000 GPU and a mixture CO₂/N₂ selectivity of 20–30 at application conditions (30 °C, water saturated). Increased selectivity is not particularly helpful because of pressure ratio limitations, but membranes with higher permeances would help reduce cost. For example, a membrane system for a typical 500 MW_e coal power plant is likely to have ~1 million m² of membranes, which would be a significant fraction of the plant cost. A doubling of membrane CO₂ permeance without selectivity loss would roughly cut the required membrane area in half, significantly reducing cost and increasing the competitiveness of the membrane process.

Another area where CO₂ capture membranes may prove useful is in the treatment of synthesis gas or syngas. A number of large petrochemical processes start with the conversion of coal, petroleum coke, or natural gas with steam and oxygen to produce syngas, which typically contains about 30% CO₂, 20% CO, 45% H₂, and 5% other inerts. There are two main uses of syngas. Many times, the gas is used as a source of hydrogen in refinery and petrochemical processes or as a fuel for power production. In this application, the CO in the high-pressure syngas is converted to more hydrogen and CO₂ by the water gas shift reaction:



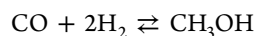
The resulting mixture contains ~50% hydrogen, with most of the balance being CO₂. The second application is when the syngas is being used as the feedstock for chemical synthesis, for example:

Fischer–Tropsch:



or

methanol synthesis:



In both of these applications, separation of H₂ from CO₂ is required. Large syngas streams at pressures above 20 bar are usually treated by physical absorption processes, such as Rectisol using cold methanol or Selexol using dimethyl ether derivatives of polyethylene glycol oligomers.²⁴ Physical absorption is preferred because no reactions are involved and the energy cost of regenerating the CO₂-laden absorbent solution is not high. At pressures below 20 bar, a stronger chemical absorbent is required to capture the CO₂, so amine absorption is typically used. A good separation is obtained, although the regeneration energy is higher. Pressure swing adsorption is sometimes used as

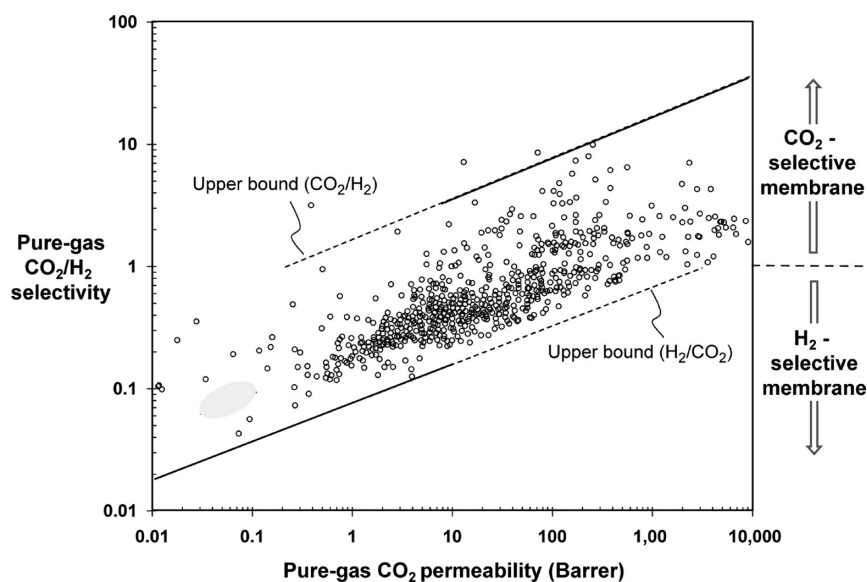


Figure 8. Pure gas trade-off plot of CO_2/H_2 selectivity versus CO_2 permeability for polymer membranes at about room temperature. The performance of CO_2 -selective membranes improves as the temperature decreases; the performance of H_2 -selective membranes improves as the temperature increases.

a final polishing step to remove the last few percent of CO_2 if needed.

Membranes have not been widely used for this application. The problem is the modest selectivity of today's polymeric membranes shown by the Robeson plot in Figure 8. Hydrogen (kinetic diameter of 2.9 Å) is smaller than CO_2 (kinetic diameter of 3.3 Å), so the diffusion selectivity always favors permeation of hydrogen. But, CO_2 (sublimes at 195 K) is far more condensable than hydrogen (boiling point of 20 K), so solubility selectivity always favors permeation of CO_2 . This means rubbery polymers (with low diffusion selectivity) are generally CO_2 -selective, while glassy polymers are generally hydrogen-selective.

Today's best CO_2 -selective membranes are close to being able to compete with conventional absorption technology. The most promising materials are polar rubbers based on derivatives of polyethylene glycol. CO_2 permeabilities are in the range of a few hundred barrer, implying permeances of 200–500 GPU, which are good enough for most applications. Pure-gas selectivities are in the range of 10–12, perhaps increasing to 15–20 if the gas is cooled.²⁵ Unfortunately, mixed-gas selectivities are normally not more than 6–8 at room temperature. This is good enough to do a useful bulk separation with a two-stage process, but the process economics would be significantly improved if the selectivity could be increased to the 15–20 range. A number of membranes using reactive amine groups to facilitate CO_2 transport have been proposed and appear to show some promise, but testing under realistic conditions is required.

Although most syngas membrane applications involve CO_2 -selective membranes, there are a few applications where a hydrogen permeable membrane can be used. Conventional glassy polymers usually have mixed-gas H_2/CO_2 selectivities of less than 5. However, a few very rigid glassy polymers such as polybenzimidazole (PBI) have higher selectivities. Diffusion selectivity is dominant in these materials, so at room temperature pure-gas selectivities of ~ 10 can be obtained, but hydrogen permeabilities are low, in the range of 1–10 barrer. Fortunately, operation at higher temperatures (100–150 °C) increases both the hydrogen permeability and selectivity. Membranes with a permeance of more than 100 GPU and a mixed-gas selectivity of

20 have been made. This type of performance, if successfully scaled up, would make membranes attractive for H_2/CO_2 separations in various chemical synthesis processes.

3.4. Vapor/Vapor Separations. The separation of organic mixtures is a huge and still unmet opportunity for membranes. There are 40 000 distillation columns in the U.S., which together use 40–60% of the energy needed by the chemical and refinery industries. Distillation is widely used because the same familiar equipment, appropriately sized, can be used to separate many mixtures. Membrane processes generally require different membranes to be developed for each category of mixture. This has significantly slowed development of the technology. The one category of separation where membranes have begun to find a place is dehydration of solvents, such as ethanol, isopropanol, acetone, THF, and acetonitrile. All of these solvents form azeotropes with water, and so distillation is no longer a simple one-column solution.

The first membrane ethanol dehydration separation system was a pervaporation unit built by GFT in 1982. This system used cross-linked poly(vinyl alcohol) membranes, and over the years, a small business for separating ethanol/water and isopropanol/water mixtures has developed. Initially, most plants were pervaporation-based, but more recently, there has been a trend toward vapor permeation systems using zeolite membranes. More than 100 small zeolite membrane plants processing 2000 to 10 000 tons per year of wet solvent have been installed, mostly in China.

Dehydration applications using membrane are beginning to grow, although it is unclear whether polymeric or zeolite membranes will emerge as the winner. In these applications, water/solvent selectivities of 100–300 are easily achieved because water is so much smaller than the nonpermeating organic solvent. The hope is that over time similar membranes will be used for other separations, such as, for example, aromatics from aliphatics, linear from branched paraffins, and olefins from their equivalent saturated hydrocarbons. In these applications, selectivities are much less than for water/solvent mixtures. However, if selectivities of 10 or more can be obtained, combined with permeances of ≥ 500 GPU, then there will likely be a place

for these processes. Membrane and module stability in the high temperature, aggressive environment of use is likely to be the most difficult problem to solve. Developing this technology is going to be a long-term process that few companies have the patience to stick with and requires a combination of membrane material know-how, process design, and application development experience not easily found in universities. For this reason, industry/academic collaborations are likely to be the best route to moving the technology forward.

4. ROUTES TO BETTER MEMBRANES

Thus far, we have given a brief description of the development of the membrane gas separation industry, provided a review of how these membranes perform a separation, and introduced some large applications where better membranes could be used. In the following sections, we will describe some of the new advanced materials that offer promise to yield better membranes. Looking back, the history of gas separation membrane development is a story of some successes and some failures. A billion dollar per year industry has been created, and most chemical engineering textbooks now have a section on membrane gas separations. However, in the past 30 years, hundreds, even thousands, of polymers have been evaluated as potential membrane materials, and yet the best of these new materials are no better than the dozen or so polymers that were in use by 1990. It is instructive to review what has been done in these intervening years before describing the route forward.

An overall theme of development work in past decades has been systematic pure-gas testing of polymer families to create polymer structure–property relationships. An example of this approach is polyimides where flexibility of chemistry has allowed hundreds of different polymers to be rapidly synthesized and studied. The hope was that by understanding structure–property relationships, it would then be possible to tailor-make membrane materials with the desired permeation properties. This appealing idea has produced useful empirical rules and correlations but has failed to yield breakthrough materials.^{26,27} Understanding has certainly improved, but the bottom line is that the polymers identified 30 years ago by industry had close to the best balance of properties for existing membrane applications. Breaking through this impasse will require moving beyond these so-called conventional polymers.

In the following sections we will describe five approaches to better materials that may yet work:

- Unconventional–conventional polymers. By this we mean polymer chemistries that are so different from the conventional materials that a different result may be possible; ultrarigid polybenzimidazoles or fully fluorinated polymers are examples.
- Nanoporous polymers. These materials have an extremely fine nanoporous structure, and laboratory results show promising results often above the gas pair upper bounds. Examples include polymers of microporosity (PIMs) and thermally rearranged (TR) polymers.
- Facilitated transport. In these materials, normal permeation is enhanced by incorporating chemical groups in the polymer matrix that react reversibly with one of the permeating species. Facilitated transport membranes have been around for 40 years, and spectacular separations have been achieved in the laboratory. The unsolved problem is membrane stability. However, a breakthrough is still possible.

- Mixed matrix materials. These membranes seek to combine the processability of polymers with the separation properties of molecular sieves. Early work focusing on inorganic zeolites proved unsuccessful primarily due to incompatibility between phases, but this area has been revitalized by new sieve materials such as metal–organic frameworks (MOFs).
- Inorganic membranes. These materials have been around for decades and often combine extraordinary transport properties with excellent thermal and chemical stability. Their Achilles heel has been scale-up difficulties leading to high cost. New approaches offer hope for the future.

5. NEW CONVENTIONAL POLYMERS

Over the past 30 years, many new membrane materials based on dense and nanoporous polymers, as well as composite polymers, were synthesized. We will not review this huge body of literature here. Rather, we will highlight a few cases of new conventional polymers that may be sufficiently different to find an application where so many other polymers have not. Poly(benzimidazoles) (PBIs) are an example of this category of polymer. They exhibit outstanding chemical, mechanical, and thermal stability, which make them attractive as membrane materials for separations in harsh environments and high temperatures.^{28–31} mPBI, commercialized by Celanese under the trade name of Celazole, is prepared from 3,3'-diaminobenzidine and isophthalic acid. The physical, chemical, and thermal stability of Celazole, which is uncommon among glassy polymers, comes from its rigid aromatic structure and intermolecular hydrogen bonding.³² However, these structural features and intermolecular forces make Celazole poorly soluble in most organic solvents, which hinders the use of standard solution casting techniques to form thin membranes.³⁰ For at least this reason, Celazole is not currently employed for gas separations. However, novel, substituted PBIs bearing flexible sulfonyl linkages on their backbone were recently synthesized using 3,3',4,4'-tetraamino-diphenylsulfone (TADPS) as a monomer.³⁰ These materials exhibit good solubility in solvents typically used to cast or spin coat membranes, such as DMAc and DMSO, while maintaining a thermal, mechanical, and chemical stability comparable to those of Celazole. Moreover, PBIs can be covalently cross-linked, which helps to control swelling and plasticization. Recently, Livingston and co-workers²⁹ used dibromoxylene (DBX) and dibromobutane (DBB) to cross-link Celazole for application in organic solvent nanofiltration (OSN, sometimes referred to as organic reverse osmosis). PBIs cross-linked using DBX exhibited improved resistance to solvents, such as dichloroacetic acid, acetonitrile, dimethylformamide, and 20 wt % HCl in water, with a maximum weight loss of about 2%, as well as improved chemical stability in the entire pH range (0–14).²⁹ However, despite its rigidity and the presence of interchain hydrogen bonds, cross-linked Celazole is still susceptible to physical aging when exposed to high temperatures for several hours.³¹ TADPS-PBIs are not yet commercially available, but there are significant research efforts underway to characterize these materials, especially in the realm of understanding their aging behavior in thin films, making these processable PBIs an emerging material for applications as gas separation membranes.

Block copolymers with hard and soft segments have also attracted considerable interest as membrane materials.^{33,34} Hard (glassy) segments, generally polyimide units, provide mechanical strength and good resistance to swelling and plasticization. Soft

(rubbery) segments, such as PEO units, provide high permeability. Chemical cross-linking can be exploited to further control swelling and plasticization. Even though their characterization is in its infancy, these materials appear promising. For example, Tena et al.³⁵ synthesized random block copolymers based on BPDA-ODA (ODA = 4,4'-oxydianiline) and poly(propylene oxide) (PPO) with good performance in CH₄/N₂ separation. Specifically, these materials exhibited a methane permeability of over 20 barrer and a CH₄/N₂ selectivity of 4.2. As reported in Table 3, lower CH₄/N₂ selectivity was reported in the

Table 3. CH₄/N₂ Ideal Selectivity of Selected Membrane Materials at Room Temperature

material	CH ₄ /N ₂ selectivity	reference
BPDA-ODA/PPO	4.2	35
PDMS	3.3	36
PSF	1.7	37
PIM-PI	1.6	38
cellulose acetate	1.2	37
PC	1.2	37
6FDA-m-PDA	0.4	39

literature for other conventional and advanced materials. Moreover, the authors demonstrated that permeability and selectivity can be tuned by properly changing the PPO/BPDA-ODA ratio.

Target applications of tough materials are separations in harsh environments as well as separations at high temperatures. Separations in harsh environments typically include vapor permeation, pervaporation, and an emerging process, organic solvent nanofiltration.²⁹ In these applications, materials that withstand aggressive solvents in the pH range from 0 to 14 are needed. If suitable materials can be developed, these applications represent the most technologically disruptive potential for membrane-based separations by providing a pathway to eventually implement membrane-distillation hybrid systems or, of much greater impact, replace certain distillation processes in their entirety.⁵ Likewise, the possibility of separating H₂ from precombustion syngas at high temperature (150–300 °C) in the integrated gasification combustion cycle (IGCC) would increase the overall process efficiency.³⁰ At these conditions, nearly all commercial polymers for gas separations would severely degrade, while PBIs exhibit good stability up to 550 °C. However, the effects of physical aging and water vapor at high temperature on the performance of PBIs require further investigation before these materials can move to the pilot scale.

Research efforts are underway to develop materials for olefin–paraffin separation. The upper bound for these applications is defined by 6FDA-based polyimides, but these materials are all susceptible to plasticization under relevant industrial conditions. Koros and co-workers⁴⁰ demonstrated that entropic-selective materials, such as dense carbon molecular sieve (CMS) membranes derived from pyrolysis of glassy polyimides, exhibit superior ethylene/ethane selectivity (up to 12), combined with fair ethylene permeability (15 barrer). Such high selectivity is termed as “entropic” since smaller ethylene molecules preferentially pass through the rigid CMS slit-shaped pores compared to larger ethane molecules.

Fluorinated polymers, such as Cytop, exhibit stable propylene–propane selectivity (about 5) up to 12 atm.¹⁸ Unfortunately, this selectivity is not quite high enough to be commercially attractive. To date, the relatively limited number of

perfluoropolymers available has hindered the search for higher selectivity members of this polymer family. However, work is continuing in this area, and some recent results appear promising.

Mixed matrix membranes offer many opportunities to tune transport properties of conventional polymers for target applications.⁴¹ This aspect is discussed in detail in section 8.

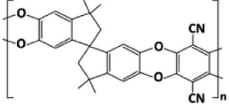
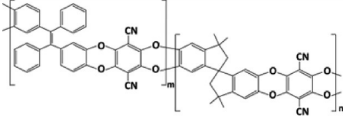
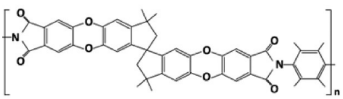
The examples cited above provide an invaluable lesson learned from the decades of research in the membrane field: today the painstaking search for materials that cross the upper bound is of little technological importance. The actual priority is identifying materials that maintain acceptable and stable separation performance over time.

6. NANOPOROUS POLYMERS

6.1. Polyacetylenes and High Free Volume Glassy Polymers. Nanoporous materials (i.e., materials with a pore size <2 nm) are attracting increasing interest in molecular separations and heterogeneous catalysis.⁴² Polyacetylenes were the first examples of this family of polymers.⁴³ Polyacetylenes tend to have extremely rigid and sterically hindered backbones, which prevent the polymer chains from packing efficiently. As a result, these polymers have very high free volume (up to 30%) and large surface areas, which often exceeds 1000 m²/g. Poly(trimethylsilylpropyne) (PTMSP), first synthesized by Masuda et al.,⁴⁴ is the most well-known nanoporous polymer. It has received significant attention in view of its exceptionally high gas permeability, which is 2–3 orders of magnitude higher than that exhibited by conventional glassy polymers. Freshly prepared PTMSP samples exhibit large free volume fractions (30%), with free volume elements interconnected to form a nanoporous structure.⁴² However, the high permeability exhibited by PTMSP rapidly declines over time due to structural compaction and densification.⁴⁵ Several attempts have been made to mitigate the tendency of PTMSP to age, primarily chemical cross-linking and addition of rigid, inorganic nanoparticles. However, none of these attempts ultimately solved the problem. For example, gas permeability is reduced by 70% after PTMSP cross-linking,⁴⁶ which makes the polymer productivity no longer competitive with that of conventional glassy polymers. In 2014, Lau et al.⁴⁵ reported that addition of ultraporos additives, such as a porous aromatic framework (PAF), stops aging in superglassy polymers, such as PTMSP and poly(methylpentyne) (PMP). They demonstrated that a portion of the polymer chain is absorbed in the PAF pores, thereby freezing the polymer in its initially open, loosely packed structure. This recent discovery could open the door to commercial application of superglassy polymers in vapor/gas separation.

Raharjo et al.^{47,48} reported pure and mixed C₄H₁₀/CH₄ solubility, diffusivity, and permeability coefficients in PTMSP at multiple temperatures. Methane permeability decreases up to 1 order of magnitude with increasing butane activity in the feed. In contrast, butane permeability is substantially unaffected by the presence of methane in the feed mixture. Such depression in methane permeability in mixed conditions is due to cooperative effects of competitive sorption and blocking. Indeed butane, which is more condensable than methane, occupies preferentially the Langmuir sites, thus reducing methane solubility in PTMSP in mixed gas conditions (competitive sorption). For the same reason, methane diffusion in the free volume of the polymer is hindered in mixed gas conditions, which causes a substantial decrease of the methane diffusion coefficient (blocking). Interestingly, mixed gas C₄H₁₀/CH₄ selectivity increases with

Table 4. Chemical Structure and Gas Permeation Properties of Selected PIM Materials

Material	Structure	Permeability (Barrer)				Selectivity	
		CO ₂	CH ₄	O ₂	N ₂	CO ₂ /CH ₄	O ₂ /N ₂
PIM-1 [†]		5922	495	1103	350	12.0	3.2
TPE-PIM [†]		862	41	138	33.4	20.9	4.2
PIM-PI [‡]		1100	77	150	47	14.3	3.2

[†]Permeability tests were run at 35 °C and 2 bar.⁵⁷ [‡]Permeability tests were run at 30 °C and 1 bar.⁵⁶

increasing butane activity in the feed, and it is much greater than the ideal selectivity calculated from pure gas permeability data. For example, the ratio of mixed-to-pure gas C₄H₁₀/CH₄ selectivity is 32 at -20 °C (i.e., 167 vs 5.2) and 7 at 35 °C (i.e., 38 vs 5.6). Pinnau et al.¹⁴ also reported enhanced butane/methane mixed gas selectivity (i.e., 30) compared to pure gas selectivity (i.e., 5) in PTMSP.

In recent years a novel high free volume glassy polymer, poly(trimethylsilylnorbornene) (PTMSN), first synthesized by Yampolskii et al.,⁴⁹ exhibited high gas and vapor solubility, diffusivity, and permeability coefficients, combined with good vapor/gas selectivity and fair chemical stability.^{49–51} Polynorbornenes are attracting commercial interest in C₃ removal from natural gas.⁵² Reverse selective membranes based on polynorbornenes maintain a C₄H₁₀/CH₄ and a C₃H₈/CH₄ selectivity equal to 5 over 5 days of exposure to a multi-component mixture (CH₄, C₂H₆, C₃H₈, C₄H₁₀, CO₂) at 55 atm.⁵² Moreover, real selectivity in polynorbornenes depends little on the feed pressure, suggesting that the effects of plasticization are not as detrimental as in common diffusion selective glassy polymers. In contrast, vapor/gas selectivity rapidly declines in rubbery PDMS at high pressures.

Fundamental studies of structure–property correlations in glassy polymers reveal that highly permeable, high performance polymers should exhibit (i) bulky substituent groups, which prevent the polymer chains from packing effectively, and (ii) high chain rigidity.⁵ Based on this rule of thumb, in recent years new nanoporous polymers appeared in the literature, such as polymers of intrinsic microporosity (PIMs) and thermally rearranged (TR) polymers.

6.2. Polymers of Intrinsic Microporosity. McKeown and Budd exploited a unique condensation reaction involving a double aromatic nucleophilic substitution to form dioxane linkages in an aromatic polymer backbone. These polymers are typically synthesized with (1) a ladder-type monomer composed of two aromatic rings linked by a single tetrahedral carbon atom and (2) tetrafluoroterephthalonitrile (e.g., 5,5',6,6'-tetrahydroxy-3,3,3',3'-tetramethyl-1,1'-spirobisindane and tetrafluoroterephthalonitrile for PIM-1).⁴² The resulting polymer has a rigid, ladder-type structure, thereby resulting in frustrated polymer chain packing to form polymers of intrinsic microporosity (PIMs) with exceptionally high free volume.⁵³ These

materials also exhibit good solubility in organic solvents, making it possible to process them by solution-casting. The microporosity of these polymers is referred to as “intrinsic” since it arises directly from their structure instead from the processing protocol. Gas permeability in PIM-1 has a 100-fold enhancement compared to conventional glassy polymers for gas separation, with no detrimental effects on selectivity. The high gas permeability exhibited by PIMs is due essentially to high solubility coefficients, whereas diffusion coefficients are quite modest. Generally speaking, separation performance of PIMs lies between the 1991 and 2008 Robeson upper bound,^{7,8} with even better performance being observed for some gas pairs (O₂/N₂, CO₂/CH₄, CO₂/N₂). As recently demonstrated by Robeson et al.,⁵⁴ the upper bound performance of PIMs is essentially due to high gas solubility and diffusivity, which increases gas permeability with no detrimental effects on selectivity, as well as high diffusion selectivity. Interestingly, during CO₂/CH₄ or CO₂/N₂ mixed gas permeation experiments, PIMs exhibit greater selectivities than those calculated from pure gas permeability data. For example, CO₂/N₂ mixed gas selectivity for a 50:50 mixture at 10 atm CO₂ partial pressure is 38, which is 36% greater than the value calculated from pure CO₂ and N₂ permeability data at the same temperature and penetrant partial pressure.⁵⁵

More recently, new modified PIMs and PIM polyimides (PIM-PI) were synthesized, whose transport properties reach or surpass the 2008 Robeson upper bound⁵⁶ (cf. Figure 11). In 2016, Pinnau and co-workers⁵⁷ synthesized a novel intrinsically microporous polymer from tetrahydroxytetraphenylethylene and tetrafluoroterephthalonitrile (TPE-PIM). TPE-PIM exhibits higher thermal stability than PIM-1, coupled with lower permeability and better selectivity. This behavior was attributed to enhanced rotational freedom of TPE-PIM chains compared to PIM-1, which causes a more packed structure, as indicated by the smaller *d*-spacing detected by WAXD analysis.⁵⁷

Despite their rigid structure, all PIMs materials are subject to significant physical aging.⁵⁸ For example, thick films based on PIM-1 lose 70% of O₂ permeability after 1400 days of operation, with a gain in O₂/N₂ selectivity of 40%. Chemically modified PIMs lose 50% of their O₂ permeability in 300 days, with a gain in O₂/N₂ selectivity of about 30%. However, the overall performance of aged membranes in O₂/N₂ separation still lies on the

Table 5. Chemical Structure and Gas Permeation Properties of HAB-6FDA Polyimide and Its TR Analogues^a

material ^a	structure	TR conversion ^l (%)	Permeability [†] (Barrer)		CO ₂ /CH ₄ selectivity [†]
			CO ₂	CH ₄	
HAB-6FDA		/	12.0	0.313	38.0
TR350-1h		39	35.3	0.77	46.0
TR400-1h		60	160	5.60	28.6
TR450-30min		76	410	18.2	22.5

^aTR samples are labeled TRX-Y, where X and Y are the temperature (in units of °C) and the duration of the thermal treatment, respectively. Thermal treatment was performed under N₂ purge. ^lTR conversion was calculated as 100 × (actual mass loss)/(theoretical mass loss). The actual mass loss was measured via thermogravimetric analysis. The theoretical mass loss is the stoichiometric mass loss expected in the case of complete thermal conversion. [†]Pure gas permeability and selectivity were measured at 35 °C and 10 atm using a constant volume/variable pressure device.⁶⁷

2008 upper bound. A major issue with PIMs is dimensional stability, since their rigidity does not alone mitigate plasticization in the presence of CO₂.^{58,59}

Scholes investigated effects of condensable contaminants on gas separation properties of PIM-1.^{60,61} Specifically, CO₂/N₂ mixed gas permeability was measured at different values of relative humidity (i.e., water vapor activity). For a water activity of 0.71, CO₂ mixed permeability is reduced by 38% with respect to the value in dry conditions, and N₂ permeability is reduced by 39%. Since water vapor affects CO₂ and N₂ permeability to a similar extent, CO₂/N₂ selectivity does not change compared to its value in dry conditions (i.e., 33). The global decrease in gas permeability observed in humid conditions is presumably due to the interplay of competitive sorption (which reduces CO₂ and N₂ solubility), plasticization (which increases CO₂ and N₂ diffusivity), and antiplasticization (which reduces CO₂ and N₂ diffusivity). The latter effect is favored by the appearance of water clusters. Similar qualitative trends were observed during mixed gas CO₂/N₂ permeability experiments in the presence of organic contaminants, such as *n*-hexane and toluene.⁶¹ However, no information is reported about the reversibility of these effects.

In recent years, aromatic polymers containing iptycene units are attracting significant attention.^{62–64} Among iptycenes, triptycenes especially exhibited promising transport properties.⁶³ Triptycenes are three-dimensional structures made by three benzene rings in a paddlewheel-like configuration. The introduction of such highly open structures on the backbone of aromatic polymers increases free volume available for penetrant transport thanks to their “internal volume”. Moreover, it is possible to tune the internal volume by properly selecting the functional groups neighboring the triptycene units. So, triptycene-containing polymers represent an interesting platform of materials whose properties can be opportunely tuned to maximize the separation performance based on the species to be separated. Performance of polyimides of intrinsic microporosity prepared using diisopropyltriptycene surpasses the 2008 upper bound for several gas pairs,⁶⁴ such as CO₂/CH₄, H₂/CH₄, O₂/N₂, and H₂/N₂.

6.3. Thermally Rearranged Polymers. Thermally rearranged (TR) polymers based on polybenzoxazoles (PBOs), first reported by Park and co-workers, are also attracting interest for gas separation, since their performance, especially for CO₂ separation, surpasses the 2008 Robeson upper bound. The outstanding transport properties of PBOs, uncommon among glassy polymers, were first highlighted by Wolfe⁶⁵ in the early

1980s, but the lack of solubility in most organic solvents prevented a systematic study of PBOs as potential membrane materials for gas separation. This issue was circumvented in 2007 by Park et al.,⁶⁶ who demonstrated that PBO films can be formed by the solid-state thermal decarboxylation reaction of aromatic polyimides containing ortho-positioned hydroxyl groups at elevated temperatures (i.e., 350–450 °C) and for a prescribed time (i.e., 30 min to 1 h) under an inert atmosphere. The resulting thermally rearranged polymers have a very rigid, perhaps cross-linked structure, which improves resistance to plasticization in chemically challenging environments. While the high gas permeability is attributed to poor chain packing, the unusually high CO₂/CH₄ selectivity is believed to be due to the regular distribution of free volume size after thermal rearrangement.^{66–69} This well-tuned distribution of free volume size was demonstrated by positron annihilation lifetime spectroscopy (PALS), which revealed a decrease in the number of free volume cavities accompanied by an increase in cavity size after thermal conversion. So, coalescence of smaller cavities to form larger cavities is believed to take place during conversion of polyimides to PBOs.⁶⁹ The high size-sieving ability of TR polymers was recently demonstrated using macroscopic modeling of gas transport behavior.^{70,71}

Pure gas solubility, diffusivity, and permeability coefficients in three thermally rearranged polymers obtained from HAB-6FDA (HAB = 3,3'-dihydroxy-4,4'-diaminobiphenyl)polyimide were measured at multiple temperatures and up to 27 atm. H₂, N₂, CH₄, and CO₂ solubility, diffusivity, and permeability coefficients increase with increasing thermal conversion. In the more converted sample (i.e., TR450-30min), sorption coefficients exhibit an approximately 2-fold increase compared to the polyimide precursor (i.e., HAB-6FDA), and diffusion coefficients increase by an order of magnitude.^{67,68} So, the high permeability exhibited by TR polymers stems mostly from increased diffusion coefficients. As confirmed by different experimental and theoretical investigations,^{67–71} fractional free volume increases substantially with increasing temperature and duration of thermal treatment, which ultimately produces the observed increase in gas transport rate.

Gleason et al.⁷² measured pure and mixed CO₂/CH₄ permeability at 35 °C in TR450-30min, a TR polymer prepared from HAB-6FDA polyimide, using a 50:50 mol CO₂/CH₄ mixture. CO₂ permeability in mixed conditions changes little compared to pure gas permeability, while a severe depression is observed for CH₄ permeability (cf. Figure 9a,b). For example, at

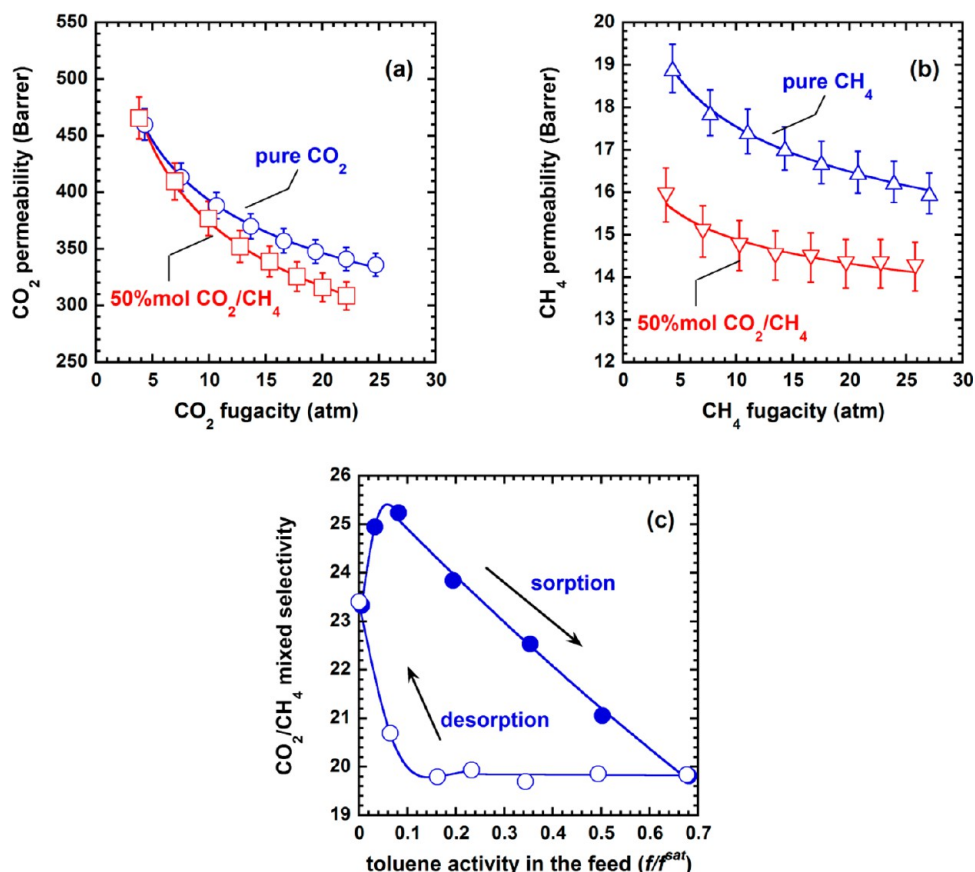


Figure 9. (a) Pure and mixed CO₂ permeability in TR450-30min at 35 °C. (b) Pure and mixed CH₄ permeability in TR450-30min at 35 °C. Data after Gleason et al.⁷² (c) CO₂/CH₄ mixed gas permselectivity at 4.7 atm fugacity of CO₂ (9.9 atm total pressure) and 35 °C in TR450-30min as a function of toluene activity in the feed. The effect of toluene is reversed upon toluene removal from the feed (desorption). Data after Liu et al.⁷³

10 atm, mixed gas CH₄ permeability is 20% lower than pure gas permeability at the same partial pressure, so mixed gas selectivity is enhanced relative to ideal selectivity. This effect was ascribed to competitive sorption.

Liu et al.⁷³ investigated the influence of toluene, a model contaminant in natural gas, on pure and mixed CO₂ and CH₄ permeability in TR450-30 min (cf. Figure 9c). As the polymer is exposed to an equimolar mixture CO₂/CH₄ at a toluene activity of 0.2, CO₂ and CH₄ permeability decreased by 93% compared to the toluene-free permeability, as a result of competitive sorption and antiplasticization. Indeed toluene, which is significantly more condensable than both CO₂ and CH₄, occupies preferentially the Langmuir sites and reduces CO₂ and CH₄ solubility. Moreover, due to its large size, toluene hinders polymer chains mobility, thus reducing diffusion coefficients for CO₂ and CH₄ (antiplasticization). These effects produce an increase in mixed CO₂/CH₄ selectivity by about 8% with respect to the toluene-free selectivity. When toluene activity is increased up to 0.7, mixed CO₂/CH₄ selectivity decreases by 27% with respect to the toluene-free selectivity due to the interplay of antiplasticization, competitive sorption, and plasticization. Indeed, toluene vapor sorption experiments show that when Langmuir sites become completely saturated (at a toluene activity greater than 0.2), vapor sorption starts to occur in the Henry mode, which produces severe plasticization. However, the effects of contaminant were largely reversed upon toluene removal from the feed.

Wang et al.⁷⁴ exploited gas permeability measurements to track physical aging of thick and thin films of TR polymers. As

expected, thin (1–2 μm) films exhibit accelerated physical aging compared to thick (20 μm) films. For example, methane permeability through a thin film decreases by 80% after 2000 h with a prominent increase in pure gas selectivity, which indicates pronounced size sieving associated with polymer densification. Plasticization of thin TR polymer films by CO₂ was also investigated. CO₂ permeability increases over the first several hours of exposure and then rapidly declines, indicating that, over longer times, physical aging dominates over plasticization. Thick films exhibit a stronger increase in CO₂ permeability over time, indicating that plasticization overwhelms physical aging within the typical experimental time frame. Interestingly, thick films (15 μm) of TR polymers were rapidly plasticized when exposed to condensable hydrocarbons, such as propane. However, after a few hours of exposure to swelling vapors, the rate of plasticization outpaces that of physical aging. For example, plasticization increases propane permeability by 100% with respect to the pre-exposure value within the first 30 h of exposure; then permeability drops by 10% compared to the pre-exposure value after 250 h.

The same authors demonstrated that, at fixed temperature and duration of thermal treatment, thin samples reach a greater TR conversion than thick films.⁷⁵ Thus, at early times, i.e., in the absence of significant aging effects, thin films are more permeable than thick films, owing to the greater degree of thermal conversion. However, as mentioned above, thin films age more rapidly than thick films, so, over longer times, thick films become more permeable than thin films.

The aforementioned examples further illustrate that many high performance polymers are susceptible to plasticization and physical aging, especially when they are tested under realistic conditions, i.e., in the presence of swelling penetrants (carbon dioxide, propane) and as thin films.

High-temperature treatments (up to 450 °C), which are required to obtain PBOs with an optimal combination of permeability and selectivity, have a detrimental effect on mechanical performance. Indeed, highly converted samples appear quite brittle since, at these temperatures, polymer thermal degradation may start to occur.⁷⁶ In 2015, Kushwaha et al.⁷⁷ synthesized fully converted PBOs by cyclodehydration of poly(hydroxyamide)s (PHAs) at a temperature 100 °C lower than that reached during TR reaction. The resulting films have gas separation properties comparable to those of some of the more traditional, albeit lower-performance, polyimide-derived TR polymers (cf. Figure 10) and exhibit much better mechanical

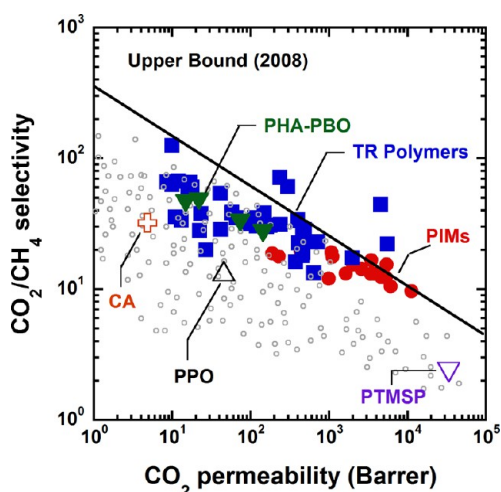


Figure 10. CO₂/CH₄ Robeson diagram for PBOs, PIMs, and conventional glassy polymers (CA, PPO, and PTMSP). The diagram was generated using pure-gas permeability data.^{10–12,14,66,78,86,79,80}

properties. Moreover, PHAs dehydration can occur in both air and inert atmosphere. The use of air, rather than an inert atmosphere, can reduce the complexity and cost of manufacturing membranes from such materials.

Target applications of nanoporous membrane materials are natural gas sweetening, O₂/N₂ separation, and vapor/gas separation. For example, TR polymers based on PBOs exhibit outstanding performance in CO₂/CH₄ separation, even though their brittleness, high monomer cost, and intensive thermal treatment to reach good separation performance have hampered their industrial acceptance. Additionally, their high permeability, coupled with moderate selectivity for gas pairs such as O₂/N₂, has attracted interest for use in applications needing high flux without requiring high selectivity, such as on-board inert gas generation (OBIGGS) aboard aircraft.⁸¹ PIMs do not require intensive treatments, but their overall performance is somewhat lower than that of TR polymers. They are especially appealing for O₂/N₂ and CO₂/N₂ separation. The possibility of using PIMs for natural gas sweetening still requires further research. While the effects of contaminants on PIMs separation properties have been investigated,^{60,61} no information is currently available about the reversibility of such effects after exposure. Moreover, a general issue in PIMs synthesis is limited structural diversity, since few

monomers are capable of being reacted to sufficiently high molecular weight to form strong and ductile films.

Polyacetylenes and other high free volume glassy polymers could be good candidates for vapor/gas and vapor/vapor separations, in view of their reverse selective behavior. However, the stability of transport properties remains an open question. As previously mentioned, work by Lau et al.⁴⁵ on mitigating ultrafast physical aging in these materials using PAFs might open the door to the industrial application of reverse selective polymers.

6.4. Evidence of Gas Transport/Mechanical Properties Trade-Off. In large scale industrial separations, membrane materials are sought that exhibit favorable combinations of transport and mechanical properties. For example, the failure pressure, p_f , of hollow fiber membranes depends on the Young's modulus (E) and Poisson ratio (ν) of the membrane material as follows:⁸²

$$p_f = \frac{2E}{1 - \nu^2} \left(\frac{\delta}{d_0} \right)^3 \quad (6)$$

where δ is the wall thickness and d_0 is the fiber outer diameter. Mechanical properties of commercially relevant membrane materials are reported in Table 6 and compared to those of

Table 6. Mechanical Properties of Selected Polymers for Gas Separation

material	Young's modulus (GPa)	tensile stress (MPa)	elongation at break (%)	ref
cellulose acetate ^a	4.90	14	17	11
polysulfone (Udel P-1700)	2.76	54.2	48	84
Matrimid	2.41	87.1	21.1	85
HAB-6FDA	3.54	153	7.1	76
HAB-6FDA-TR350-1h	2.68	107	4.9	76
HAB-6FDA-TR400-1h	2.51	86	4.0	76
HAB-6FDA-TR450-30min	2.52	62	2.9	76
APAF-6FDA	2.90	65	2.5	76

^aDegree of substitution = 2.84.

new generation materials, such as polyimides and TR polymers. New generation rigid polymers, such as 6FDA-based polyimides and corresponding TR samples, are generally more brittle than commercial polymers, such as polysulfone or cellulose acetate.⁷⁶ For example, despite surpassing the 2008 Robeson upper bound for CO₂/CH₄ separation, the Young's modulus and elongation break of TR450-30min are 95% and 490%, respectively, lower than those of cellulose acetate. Similar conclusions can be drawn comparing the overall performance of 6FDA-polyimide with that of well-established commercial membrane materials. This result suggests that an apparent trade-off exists between gas transport and mechanical properties. The existence of such a trade-off was recently confirmed by Scholes et al.⁸³ They prepared new copolymers blending TR-able polyimides (HAB-6FDA) with non-TR-able polyimides (4MPD-6FDA, 4MPD = 2,3,5,6-tetramethyl-1,4-phenylenediamine), which exhibited improved mechanical properties but poorer gas transport properties compared to TR samples based on pure HAB-6FDA polyimide.

Liu et al.⁷⁶ compared gas transport and mechanical properties of TR polymers based on HAB-6FDA and APAF-6FDA polyimides (APAF = 2,2'-bis(3-amino-4-hydroxyphenyl)-

hexafluoropropane). Bulky hexafluoroisopropylidene groups in the APAF monomer produced an increase in pure gas permeability and selectivity with increasing APAF content. However, since APAF is a less reactive monomer than HAB, APAF-derived polymers exhibited lower molecular weights and, ultimately, poorer mechanical properties.

7. FACILITATED TRANSPORT

Superior separation properties can be achieved using membranes based on the facilitated transport mechanism, which exploits reversible chemical reactions between the target species and active sites available on the polymer backbone to enhance membrane permeability and selectivity. Meanwhile, other species that do not react with the active sites permeate through the membrane by a simple solution-diffusion mechanism.^{86,87} Active sites that are covalently bound to the polymer backbone are referred to as fixed carriers. Conversely, active sites that have the ability to move throughout the membrane material are referred to as mobile carriers. In mobile carrier membranes (MCMs), the target component X reacts reversibly with the carrier Y to form the adduct XY. The latter diffuses through the membrane down its concentration (or chemical potential) gradient, and in the downstream membrane face, it decomposes liberating the species X. Ideal facilitated transport membranes exhibit moderate equilibrium constant for the reaction $X + Y \rightleftharpoons XY$ and a fast XY decomposition rate at the downstream side. The overall flux of the target species, X, is expressed as the sum of Fickian flux plus the carrier-mediated flux:⁸⁶

$$J_X = -D_X \frac{dC_X}{dz} - D_{XY} \frac{dC_{XY}}{dz} \quad (7)$$

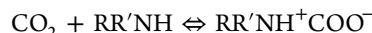
where D_X and D_{XY} are the diffusion coefficients of species X and XY, respectively, and C_X and C_{XY} are the concentrations of the two species. In eq 7, C_{XY} is a function of the equilibrium constant of the reaction $X + Y \rightleftharpoons XY$. When considering fixed site carrier membranes (FSCMs), the second term in eq 7 is null.

Fixed-site carrier membranes exhibit better stability than mobile carrier membranes. The latter are, generally, supported liquid membranes obtained upon immersion of the supporting layer in the carrier solution. Industrial application of MCMs is hampered by at least two issues: (i) the evaporation of liquid phase over long times and (ii) the deactivation of the mobile carrier, which, in most of cases, is a complexing agent.^{86,87} To prevent these issues, the carrier can be immobilized by electrostatic interactions in an ion exchange membrane, according to the protocol reported by LeBlanc et al.,⁸⁸ or covalently bound to the polymer backbone. In FSCMs, the target molecule jumps from one fixed carrier to another down the concentration (i.e., chemical potential) gradient.

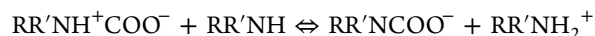
Facilitated transport membranes, first introduced by Scholander⁸⁹ in 1960 for O₂ separation, are today the subject of intense research efforts. Scholander reported that O₂ permeability in supported liquid membranes containing hemoglobin is enhanced 8-fold relative to liquid membranes containing water. Similarly, Ward and Robb⁹⁰ reported a CO₂/O₂ selectivity of over 4000 for a liquid membrane containing bicarbonate solutions. In the early 1970s, Steigelmann and Hughes at Standard Oil discovered that embedding silver ions in cellulose acetate membranes facilitates alkene over alkane transport.⁹¹ So, target applications of facilitated transport membranes are CO₂ separation, olefin–paraffin separation, and O₂/air separation.

7.1. CO₂ Separation. In CO₂ capture from flue gas, CO₂/N₂ selectivity greater than 50 and CO₂ permeability over 100 barrer

are required for economic operation.⁹² Facilitated transport membranes for CO₂ separation help meet this requirement. CO₂ transport can be selectively enhanced inserting basic carriers (generally, amines) in the membrane material. Since CO₂ is an acid gas, it will form with basic carriers a complex which permits facilitated transport of CO₂ through the membrane. Amines react reversibly with CO₂ according to a zwitterion mechanism:



where R is a functional group and R' can be either a functional group of hydrogen. Then, zwitterion deprotonates to produce a carbamate ion, which represent the adduct, according to the following scheme:



Huang et al.⁹² prepared composite membranes by casting PVA with mobile and fixed amine carriers on a PTFE porous support. Mobile carrier (2-aminoisobutyric acid) enhances membrane permeability by promoting the carrier–CO₂ adduct diffusivity, and fixed carrier (polyallyamine) enhances membrane stability. A CO₂ permeability of 6200 barrer and a CO₂/N₂ selectivity of 500 were measured at 110 °C, with a feed containing 20% CO₂, 40% H₂, and 40% N₂ on dry basis. CO₂ permeability and CO₂/N₂ selectivity dropped at 2000 barrer and 40, respectively, at 170 °C.

Peng et al.⁹³ developed novel fixed-site carrier membranes by incorporating multiwalled carbon nanotubes (MWCNs) functionalized with Cu²⁺, Fe³⁺, Ca²⁺, and Mg²⁺ ions in Matrimid polyimide. CO₂ permeability in composites loaded with Cu²⁺ and Fe³⁺ containing MWCNs was enhanced by 90% relative to the neat polymer, with an increase in CO₂/CH₄ selectivity up to 25%. Membranes loaded with Ca²⁺ and Mg²⁺ containing MWCNs exhibited modest improvement of separation properties. Such membranes exploit the ability of transition metal ions to interact with CO₂ molecules via a π -complexation mechanism, which permits a CO₂ facilitated transport over methane.

7.2. Olefin–Paraffin Separation. Transition metals can interact reversibly with alkenes through a π -complexation mechanism. The strength of this interaction is obviously related to the electronegativity of the transition metal. When the carrier electronegativity is too high, it can strongly attract electrons of alkene molecules, so the reaction is irreversible. Likewise, when the carrier electronegativity is too low, the interaction with alkene molecules is weak. In these two extreme cases, facilitated transport of alkenes over alkanes cannot take place. The carrier electronegativity should range from 1.6 to 2.3 to permit optimal facilitated transport of alkenes.⁹⁴ Silver (electronegativity = 1.93) exhibits the best performance in this application. Silver ions dispersed in the high pressure side of the membrane form reversible complexes with alkenes, which diffuse through the membrane down a concentration gradient. In the low-pressure side, decomplexation occurs. Alkene molecules are released in the gas phase, and the regenerated carrier diffuses back to the high-pressure face, down its concentration gradient. Then, the facilitated transport cycle is repeated. Based on this mechanism, alkene over alkane solubility in the membrane is significantly enhanced.⁹⁴

In 1997, BP Amoco developed a pilot plant for olefin–paraffin separation based on polypropylene–silver salt hollow fibers. Since then, many other researchers developed facilitated transport membrane dispersing silver salts in polymers. Interesting results were observed for the systems cellulose acetate/AgBF₄⁹⁵ and poly(acrylamide)/AgBF₄⁹⁶ whose mixed gas propylene–propane selectivity was 200 and 170, respectively.

Membranes based on CA/AgBF₄ exhibited a mixed gas ethylene–ethane selectivity of 280. Tomé et al.⁹⁷ reported that addition of silver salt (AgNTf₂) in polymeric ionic liquids based on poly([pyr11][NTf₂]) enhances ethylene solubility in the membrane and, in turn, ethylene/ethane pure gas selectivity. The separation performance of these membranes surpasses the 2008 upper bound.

Despite huge research efforts, facilitated transport membranes for olefin–paraffin separation never went beyond the pilot scale because of the instability of the carrier, which is readily deactivated upon exposure to light or poisoning agents, such as H₂ or H₂S. For example, Merkel et al.⁹⁸ showed that the mixed gas ethylene–ethane selectivity of membranes based on Pebax and AgBF₄ declines from 40 to 1.1 after 34 days of exposure to light due to photoreduction of silver ions. However, the membrane can be regenerated in situ upon exposure to hydrogen peroxide/tetrafluoroboric acid vapor or liquid mixtures, which readily oxidize the reduced silver ions.

7.3. O₂/Air Separation. O₂/N₂ separation by solution-diffusion membranes is quite difficult to achieve due to the similar size and condensability of these two gases. Transition metal complexes, such as cobalt Schiff bases, form reversible adducts with O₂, which can be exploited to boost O₂ facilitated transport over N₂.⁹⁹ Drago et al.¹⁰⁰ reported that O₂/N₂ selectivity of polystyrene-based membranes with cobalt–*N,N'*-bis[(3-salicylideneamino)propyl]methylamine complexes bound to the polymer backbone is significantly enhanced relative to that of the neat polymer. Similarly, a 2-fold increase in O₂ permeability and O₂/N₂ selectivity (from 2.9 to 6.2) after adding cobalt Schiff bases to a rubbery epoxidized styrene–butadiene–styrene block copolymer was reported by Yang et al.¹⁰¹ However, these complexes are prone to oxidative degradation during repeated oxygen absorption–desorption cycles,¹⁰² which hampers their use in practical reality.

8. MIXED-MATRIX MEMBRANES

One key requirement for industrial gas separation membranes is processability. These membranes require a thin film selective layer of 0.1–1.0 μm thick and surface areas on the order of 1000–500 000 m².⁵ To economically form such films at scale, all commercial membranes have been necessarily made from dense polymers, but these polymers have property sets bound by the solution-diffusion model. To harness the processability of polymers while simultaneously overcoming the upper bound trade-off between permeability and selectivity, inorganic materials have been added to polymers as composites to form hybrid materials known as mixed-matrix membranes (MMMs, cf. Figure 11). Since inorganic materials may possess specific pore sizes of precise shape and geometry or narrow pore size distributions, these materials may act as efficient molecular sieves to improve diffusivity selectivity, thereby forming polymer–inorganic hybrids with property sets that surpass those of pure polymers alone. Moreover, inorganic materials may possess specific chemical or coordinative functionality that are not found in organic polymers, allowing these materials to act as selective adsorbents to increase solubility selectivity, which can also improve membrane separation performance.

Effective permeabilities of inorganic materials are difficult to determine experimentally, so simplistic models are often used to deconvolute individual property sets within the polymeric and filler phases of MMMs. To this end, the most commonly employed model, by far, is the Maxwell model, which was

(a) Polymer membrane (b) Inorganic membrane (c) Mixed-matrix membrane

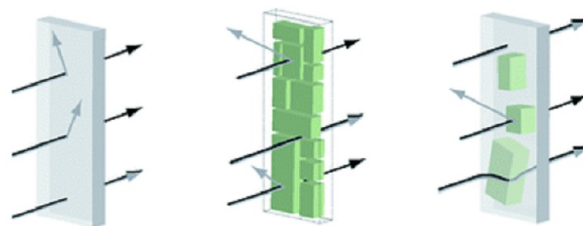


Figure 11. Schematic illustrating three membrane systems: (a) pure polymer membrane where transport is governed by the solution-diffusion model, (b) pure inorganic membrane where transport is governed by molecular sieving or preferential sorption, and (c) MMM composed of dispersed inorganic fillers in a polymer where transport is governed by the composite characteristics of the polymer and the inorganic phase. This figure was adapted from ref 132.

originally developed in 1873 for estimating dielectric properties of composites:¹⁰³

$$P_{\text{eff}} = P_c \left[\frac{nP_d + (1-n)P_c - (1-n)\Phi_d(P_c - P_d)}{nP_d + (1-n)P_c + n\Phi_d(P_c - P_d)} \right] \quad (8)$$

where P_{eff} is the effective permeability, P_c and P_d represent the permeabilities of the continuous (i.e., polymer) and dispersed (i.e., filler) phase, Φ_d is the volume fraction of the dispersed phase, and n is a shape factor for the dispersed phase ($n = 1/3$ for spherical particles).

For small volume fractions of well-dispersed and compatible inorganic fillers, the Maxwell model has been employed with a high level of success for predicting effective transport properties of MMMs with a variety of inorganic materials such as carbons, zeolites, and MOFs.^{104–108} However, when the volume fraction of inorganic filler increases, nonidealities result due to the connectivity of the inorganic phase and the presence of interfacial defects between the polymer and inorganic particles. The reader is directed to recent reviews that have covered these topics in depth.^{109,110} Moreover, the Maxwell model does not consider nonuniform distributions of particle shapes, and from a statistical mechanics perspective, it is unable to decouple directional permeabilities in anisotropic materials. Nevertheless, modifying the shape factor, n , in this model has been used as a crucial tool to explain transport properties in MMMs containing particles of various aspect ratios.^{111–115} Given some of the aforementioned limitations, more sophisticated models based on a modified Maxwell model have been reported to more accurately reflect the physics of inorganic–organic hybrids and particle geometries.^{104,116,117}

Zeolites are often investigated as a filler phase for MMMs because of their unique molecular sieving characteristics,^{118,119} and many encouraging papers have reported promising transport performance. Mahajan et al. prepared MMMs using zeolite 4A and various polymer matrices (e.g., Matrimid, Ultem, poly(vinyl acetate), etc.) for O₂/N₂ separation.^{120,121} With the small pore aperture of zeolite 4A (3.8–4.0 Å), O₂/N₂ selectivities as high as 37 were reported. Even considering the correspondingly small O₂ permeability of 0.8 barrer, materials with these property sets are still of tremendous interest to the membrane community. However, despite these promising results, polymer/zeolite MMMs have not gained commercial acceptance, illustrating some practical challenges for deploying these systems. Perhaps most importantly, zeolite–polymer composites often suffer from issues of poor interfacial compatibility,¹²² which results in the

formation of nonselective interfacial defects and concomitantly poor mechanical properties,^{123,124} especially for thin film formation.^{125,126} Moreover, high zeolite loadings often result in nonuniform dispersions in MMMs.¹²⁷ Additionally, for polymers that interact strongly with zeolites, polymer rigidification and pore blocking effects have also been noted.¹²⁸ As a final consideration, zeolites are often strongly adsorbing, and adsorption of gases into binding sites can result in immobilization (i.e., reduced diffusion) of condensable gases and vapors. This effect is somewhat analogous to sorption of molecules in Langmuir sites of glassy polymers.¹²⁹ Paul and Kemp investigated this effect for zeolite 5A/polydimethylsiloxane (PDMS) MMMs for CO₂/CH₄ separation and quantified the change in diffusion time lag that resulted from adding zeolites to PDMS.¹³⁰ The key takeaway from this work is that diffusion of sufficiently polarizable penetrants can be slowed by strongly binding inorganic adsorbents, particularly for materials with small pore apertures (i.e., the molecular sieve needed to achieve MMM selectivity). In the extreme case, pores can be blocked and effectively deactivated for transport in these MMM systems through a phenomena known as capillary condensation.¹³¹ Therefore, much recent research has shifted from zeolites to other materials such as graphene-based materials and metal–organic frameworks, which will be highlighted in this Perspective.

8.1. Metal–Organic Frameworks (MOFs). Metal–organic frameworks are composed of metal ions or metal clusters coordinatively bridged by organic ligands. Because of the diversity of accessible metals and ligands used in MOF synthesis, a variety of structures with unique chemical and physical property sets can be formed, making these materials of interest for membrane-based separations. MOFs can be formed with ultrahigh porosities and internal surface areas up to 10 000 m²/g, tunable pore architectures, and, in many cases, mechanical and chemical stability toward aggressive gas feeds (e.g., high partial pressures of CO₂ of ~1000 psia).¹³³ Compared to zeolites or carbons, the organic linkers in MOFs provide a tunable feature to their structure, enabling potentially better interaction with polymers, thereby reducing nonselective defects at the MOF–polymer interface. Therefore, new design strategies have been developing rapidly to form MOF-based MMMs to optimize gas diffusion and selectivity. To date, a variety of MOFs have been investigated for their transport performance. For this Perspective, we will highlight some of the most commonly studied MOFs used for MMMs with a particular emphasis on ZIF-8, HKUST-1, MIL-53, MIL-101, MOF-74, and UiO-66. Crystal structures for these MOFs and some common features are presented in Figure 12 and Table 7, respectively.

ZIF-8. Zeolitic imidazolate frameworks (ZIFs) are formed from metal ions (typically zinc or cobalt) tetrahedrally coordinated to imidazolate linkers. Their name (i.e., “zeolitic”) originates from topological and bond angle similarities between these materials and zeolites. For example, analogous to zeolites, ZIFs can be formed into Sodalite (SOD), Chabazite (CHA), and Linde Type A (LTA) topologies, and they have 145° metal–imidazole–metal bond angles. Within the subclass of ZIFs, ZIF-8 is the most extensively studied for gas separation membranes. Crystallographically, ZIF-8 has a 3.4 Å pore aperture and 11.6 Å cages.¹³⁴ The small pore aperture makes this material a molecular sieve with length scales of interest for gas separations. Interestingly, the methyl group in the organic linker of ZIF-8, which extends into the pore aperture, can rotate within the pores, creating a somewhat flexible pore-gate opening mechanism that

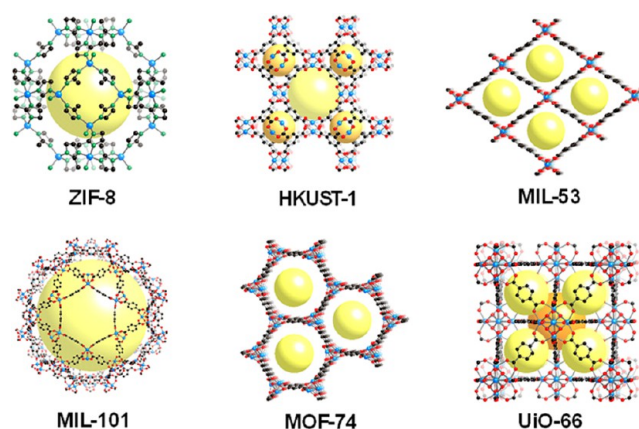


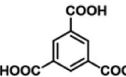
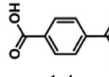
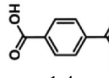
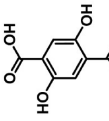
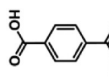
Figure 12. Crystal structures of MOFs considered in this paper.

permits gases with kinetic diameters larger than 3.4 Å (e.g., C₃H₈, C₃H₆) to diffuse through the ZIF-8 pore system.^{145,146}

Some of the early MMM work on ZIF-8 targeted propylene/propane separations using a 6FDA-DAM polyimide as the continuous phase. Zhang et al. prepared MMMs from commercially available ZIF-8 nanoparticles (~200 nm in diameter), which were dried after synthesis and dispersed in 6FDA-DAM.¹⁴⁷ Even though there were small clusters of ZIF-8 particles (~600 nm in diameter) in these MMMs, the clusters were well-dispersed, a feature that was ascribed to the hydrophobic nature of ZIF-8 in a hydrophobic 6FDA-based polyimide. Up to 48 wt % of ZIF-8 nanoparticles were loaded in the polymer, which resulted in a C₃H₆ permeability of 56 barrer (260% improvement compared to pure 6FDA-DAM) and a C₃H₆/C₃H₈ selectivity of 31 (150% improvement compared to pure 6FDA-DAM) (cf. Figure 13c). Despite these high loadings, transport performance still closely matched the Maxwell model prediction, indicating excellent dispersion and no percolation of the MOF phase. However, binary gas permeation experiments showed a decrease in C₃H₆ permeability, explained by the authors as potentially resulting from competitive sorption effects.

In addition to identifying materials of interest with beneficial transport properties for the filler phase, an equally important challenge is effectively dispersing particles without interfacial defects into a polymer. Similar to the aforementioned work by Zhang et al.,¹⁴⁷ most researchers form MMM by first drying particles and redispersing them in a casting solution. However, this approach can often lead to particle agglomerations, and notably, even the work by Zhang et al. with ZIF-8, which closely matched Maxwell model predictions, still showed some particle agglomerations by microscopy. To overcome this compatibility issue, Song et al. synthesized ZIF-8 nanocrystals (~60 nm in diameter and surface area ~1300–1600 m²/g) (Figure 13b) and dispersed their ZIF-8 colloidal suspension directly into a solution of dissolved Matrimid. This approach resulted in uniform distributions of ZIF-8 nanocrystals, even at high ZIF-8 loadings (30 wt %).¹⁴⁸ Compared to the typical aggregation of ZIF-8 nanocrystals with the conventional “dry-first” method (i.e., drying the ZIF-8 nanocrystals and resuspending them in a polymer solution), this direct mixing approach showed evenly dispersed particles with good adhesion between the filler and the continuous phase. The authors concluded that these favorable interactions resulted from increased interfacial surface area between the ZIF and polymer, as noted by a reduction in polymer chain packing efficiency from positron annihilation lifetime spectroscopy (PALS) analysis.¹⁴⁸ Of particular note,

Table 7. Common Name, Alternative Name(s), Available Metal Cations, Ligands, and Physical Characteristics for Commonly Investigated MOFs^a

Common name	Alternative name(s)	Metal Cation(s)	Ligand	Limiting Pore aperture (Å)	BET Surface area (m ² /g)
ZIF-8	Zn(2-methylimidazolate) ₂ or Zn(MeIm) ₂	Zn ²⁺	 (2-methylimidazole)	3.4	1813
HKUST-1	Cu ₃ (BTC) ₂	Cu ²⁺	 benzene-1,3,5-tricarboxylate (BTC)	9	1500-2100
MIL-53	M(OH)(BDC)	Al ³⁺	 1,4-benzenedicarboxylate (BDC)	8.5	1100-1500
MIL-101	Cr ₃ O(H ₂ O) ₂ F(BDC) ₃	Cr ³⁺	 1,4-benzenedicarboxylate (BDC)	29, 34	2800-4230
MOF-74	M ₂ (dobdc) or CPO-270-M	Mg ²⁺ , Mn ²⁺ , Fe ²⁺ , Co ²⁺ , Ni ²⁺ , Zn ²⁺	 2,5-dioxido-1,4-benzenedicarboxylate (dobdc)	12	1277-1957
UiO-66	Zr ₆ O ₄ (OH) ₄ (BDC) ₆	Zr ⁴⁺	 1,4-benzenedicarboxylate (BDC)	6	1067

^aThe information in this table was adapted from refs 134–144.

these measurements indicate the importance of assessing the physical structure of the polymer at the MOF–polymer interface. For pure gas measurements with H₂, CO₂, O₂, N₂, and CH₄, ZIF-8/Matrimid MMMs showed enhanced permeability without loss in selectivity. Japip et al. also circumvented particle agglomeration issues using a similar direct mixing approach with ZIF-71 nanoparticles (~100 nm in diameter), which are composed of Zn²⁺ and 4,5-dichloroimidazole, dispersed in a 6FDA-Durene polyimide (Durene = 2,3,5,6-tetramethylbenzene-1,4-diamine).¹⁴⁹ Interestingly, hydrogen bonding between the small ZIF-71 particles and 6FDA-Durene revealed an additional benefit: when polymer chain mobility can be reduced, improvements can result in CO₂ plasticization resistance, as the authors noted by shifts in the plasticization pressure point between the pure polymer at 16 atm and the MMM at 30 atm. Other ZIFs have been used with some degree of success in forming MMMs. For example, Bae et al. prepared MMMs with 6FDA-DAM polyimides and submicrometer-sized ZIF-90 particles (~0.8 μm), which are composed of Zn²⁺ cations and imidazolate-2-carboxyaldehyde ligands, thereby improving both CO₂ perme-

ability and CO₂/CH₄ selectivity to 720 barrer and 37, respectively, compared to the pure 6FDA-DAM polymeric membrane (CO₂ permeability = 390 barrer and CO₂/CH₄ selectivity = 24).

HKUST-1. Named after an acronym for the Hong Kong University of Science and Technology, HKUST-1 is composed of a Cu²⁺ paddlewheel structure coordinated with benzene-1,3,5-tricarboxylate (BTC) ligands. HKUST-1 has a cubic, twisted boracite topology with a 9 Å diameter main pore channel surrounded by 5 Å diameter tetrahedral pockets.¹⁵⁰ HKUST-1 is stable up to 300 °C under nitrogen atmosphere¹⁵¹ and has coordinatively unsaturated (open) metal sites that can be exposed by removing weakly bound solvent or water molecules through solvent exchange and/or heating.^{152,153} These coordinatively unsaturated metal sites act as Lewis acids, providing additional gas sorption capacity compared with their coordinatively saturated counterparts. Basu et al. incorporated cubic crystalline HKUST-1 particles (size ~10 μm) in Matrimid and Matrimid/polysulfone blends to form asymmetric MMMs for CO₂ separation.¹⁵⁴ However, the size of HKUST-1 particles was

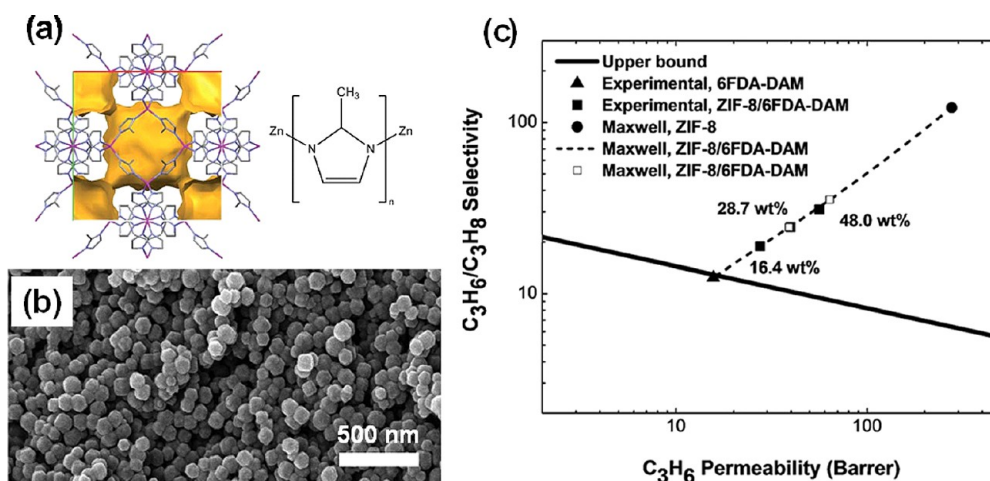


Figure 13. (a) Crystal and chemical structure of ZIF-8 nanoparticles including accessible pore structure (shown in the yellow region). (b) SEM image of ZIF-8 nanoparticles. (c) Pure-gas C_3H_6/C_3H_8 upper bound plot with property sets for the pure 6FDA-DAM polymer, Maxwell model prediction for pure ZIF-8, and experimental and Maxwell model predictions for ZIF-8/6FDA-DAM MMMs with various ZIF-8 loadings. This figure was reproduced from refs 147 and 148.

too large to form defect-free membranes at an experimental scale, and interfacial defects between the polymer and HKUST-1 particles resulted in insufficient improvements in separation performance. To address these interfacial defects, Lin et al. incorporated 1-ethyl-3-methylimidazolium bis(trifluoromethylsulfonyl)imide ionic liquids (ILs) as binders on HKUST-1/6FDA-Durene MMMs to reduce interfacial void formation during membrane casting.¹⁵⁵ In these MMMs composed of HKUST-1 with surfaces covered in ionic liquids, the volume fraction of interfacial voids between HKUST-1 and 6FDA-Durene was significantly reduced compared to the uncoated MOFs from 0.028% to 0.0023%, as calculated from analysis of FIB-SEM images. The HKUST-IL MMM showed a high CO_2 permeability of 1100 barrer with increased CO_2/N_2 selectivity of 27 and CO_2/CH_4 selectivity of 29 compared to pure 6FDA-Durene (CO_2 permeability of 770 barrer with CO_2/N_2 and CO_2/CH_4 selectivities of 21 and 22, respectively). MMMs formed with HKUST-1 for gas capture applications have also yielded some interesting results, which may eventually be translatable to new membrane applications. DeCoste et al. fabricated HKUST-1/poly(vinylidene difluoride) (PVDF) MMM composite blends for ammonia capture. Ammonia is a base which can adsorb strongly onto the coordinatively unsaturated metal sites.¹⁵⁶ Because HKUST-1 shows some instability under sufficiently humid conditions,¹⁵¹ the hydrophobic PVDF polymer was introduced as a protective layer. Although the surface of the MOF was in contact with the polymer binder, gravimetric adsorption measurements confirmed that the internal pore structure was fully accessible to ammonia gas.

MIL-53 and MIL-101. The MIL-53 series MOFs (named after the Materials Institute Lavoisier) are composed of trivalent metal cations (typically Al¹⁵⁷ for MMM, but also Cr,¹⁵⁸ Fe,¹⁵⁹ Sc,¹⁶⁰ and Ga¹⁶¹) and terephthalic acid (i.e., 1,4-benzenedicarboxylate) ligands. MIL-53 has a three-dimensional structure composed of infinite trans chains of corner-sharing MO_6 polyhedra lined with dicarboxylate ligands, resulting in rhombic channels and large pore sizes up to 8.5 Å.^{162,163} Interestingly, the MIL-53 framework is flexible and exhibits a so-called “breathing effect” in that the pore structure opens and closes during adsorption or desorption of specific gases (i.e., H_2O , CO_2), analogous to an accordion

expanding and being compressed.^{162,164–166} This effect results in unique framework configurations depending on temperature, pressure, and guest molecule insertion, although this transition is fully reversible. A related series of MOFs, known as MIL-101, do not have a structure amenable to the breathing phenomena but do have coordinatively unsaturated metal sites. Similar to MIL-53, these MOFs are composed of Cr^{3+} cations and terephthalic acid ligands but have large pore cages (29 and 34 Å) and excellent stability to high temperatures, aggressive chemical environments, and humidity.^{167–170}

One important factor for lab-scale MMM formation is controlling the rate of solvent evaporation so that homogeneous, uniform MMMs can be formed. Such experimental factors are even more critical for flexible MOF frameworks. Rodenas et al. investigated these effects with an amine-functionalized MIL MOF, NH_2 -MIL-53(Al), by modifying casting techniques (e.g., using a doctor blade, controlling solvent evaporation rates, etc.).¹⁷¹ NH_2 -MIL-53 is a breathable framework, so casting a MMM by slow evaporation of chloroform at 0 °C with Matrimid results in the MOF retaining its characteristic open structure. However, rapid removal of solvent from the pore structure using a doctor-blade technique results in significant contributions of the closed pore structure. Sabetghadam et al. controlled the morphology of NH_2 -MIL-53(Al) (e.g., forming nanoparticles, nanorods, and microneedles) to understand the impact of particle shape and geometry on MMMs formed with Matrimid and 6FDA-DAM.¹⁷² Because of increased interfacial contact between the MOF and polymer, nanoparticles resulted in more polymer chain rigidification than nanorods, resulting in lower free volume of the polymer phase. The MMMs containing 20 wt % NH_2 -MIL-53(Al) nanoparticles in 6FDA-DAM showed the most improved gas separation performance for a 1:1 CO_2/CH_4 mixtures with a CO_2 permeability of 660 barrer and a CO_2/CH_4 separation factor of 28.

MIL-101(Cr) can interact with a variety of polymer functionalities, which has been shown to improve compatibility of this MOF in MMMs. Xin et al. incorporated polyethylenimine (PEI) into the carefully activated mesoporous cages of MIL-101(Cr) and dispersed these MOFs into a poly(ether ether ketone) (SPEEK) polymer. At the polymer–MOF interface, interactions were improved by hydrogen bonding and electro-

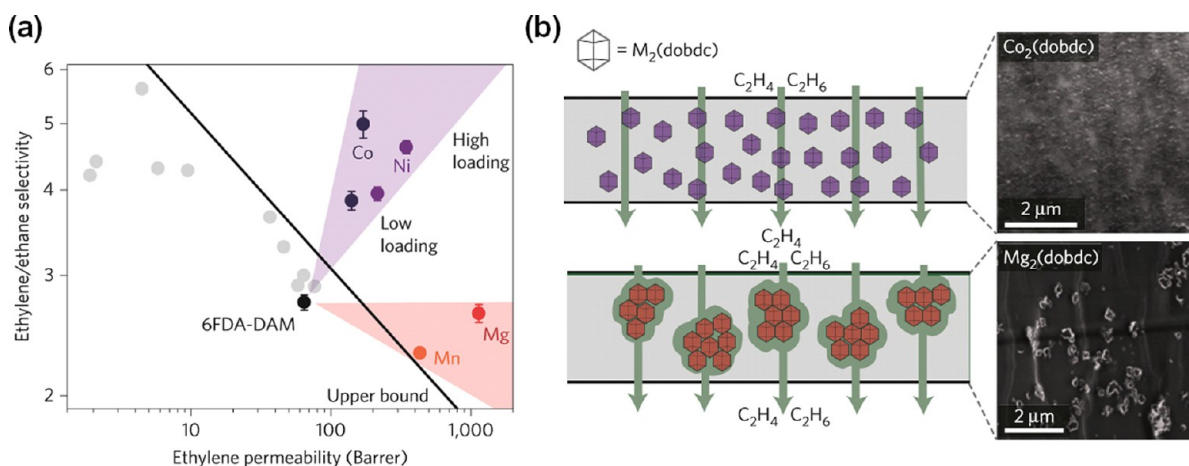


Figure 14. (a) Pure-gas ethylene/ethane upper bound with pure 6FDA-DAM and several 6FDA-DAM MMMs containing $M_2(\text{dobdc})$ nanoparticles with different metal centers (i.e., Co, Ni, Mn, and Mg). The weight loadings of the MMMs are 10% and 33% for Co, 6% and 25% for Ni, 23% for Mg, and 13% for Mn. References for pure polymers are presented as gray circles. (b) Cross-sectional TEM images of $\text{Co}_2(\text{dobdc})$ and $\text{Mg}_2(\text{dobdc})$ incorporated MMMs and illustration of gas transport mechanism based on particle dispersion. Well-dispersed purple hexagonal nanocrystals represent $\text{Co}_2(\text{dobdc})$ or $\text{Ni}_2(\text{dobdc})$ and aggregated red hexagonal nanocrystals represent $\text{Mg}_2(\text{dobdc})$ or $\text{Mn}_2(\text{dobdc})$. This figure was taken from ref 180.

static interactions between PEI on the MIL-101(Cr) surface and the sulfonic acid group in the polymer.¹⁷³ Although the surface area was reduced, likely from pore blocking, under humid conditions, CO_2 permeability increased from 545 to 2490 barrer and CO_2/CH_4 and CO_2/N_2 selectivities improved from 24.7 and 36.0 to 72 and 80, respectively. The authors concluded that the presence of PEI bound to the coordinatively unsaturated metal sites improved permeability and selectivity under humid conditions through a reversible reaction between the PEI amine groups and CO_2 .

MOF-74. Also commonly referred to as $M_2(\text{dobdc})$, MOF-74 is composed of Mg, Mn, Fe, Co, Ni, Cu, or Zn metal cations coordinated with 2,5-dioxido-1,4-benzenedicarboxylate (dobdc) ligands to form ~ 12 Å wide hexagonal channels.^{174,175} MOF-74 has some of the highest known concentrations of coordinatively unsaturated metal sites, which, analogous to HKUST-1 and MIL-101, can act as Lewis acids and significantly increase gas adsorption.^{176–178} Bachman et al. reported plasticization resistance of MMMs composed of $\text{Ni}_2(\text{dobdc})$ in various polyimide-based MMMs for CO_2 separation.¹⁷⁹ Even with small amounts of $\text{Ni}_2(\text{dobdc})$, all of these MMMs showed improvements in selectivities and plasticization resistance for mixed-gas permeation tests. The mechanism behind their stability was hypothesized to arise from interactions between imide functionality and coordinatively unsaturated metal sites in $\text{Ni}_2(\text{dobdc})$ nanocrystals, which was supported by an increase in the glass transition temperature for the MMMs compared to the pure polymers (e.g., $T_g = 393$ °C for pure 6FDA-DAM compared to $T_g = 397$ °C for a 25 wt % $\text{Ni}_2(\text{dobdc})$ MMM). Bachman et al. also synthesized a series of $M_2(\text{dobdc})$ ($M = \text{Mg}, \text{Mn}, \text{Ni}, \text{Co}$) nanoparticles and dispersed them in 6FDA-DAM polyimides to form MMMs for ethylene/ethane separation.¹⁸⁰ The smallest particles were formed with $\text{Co}_2(\text{dobdc})$ or $\text{Ni}_2(\text{dobdc})$ nanocrystals, and due to their small size and excellent dispersion in the polyimide, these MMMs showed significant improvement in C_2H_4 permeability and $\text{C}_2\text{H}_4/\text{C}_2\text{H}_6$ selectivity compared to the pure-gas polymer upper bound. For the Ni and Co samples, ethylene permeabilities increased by factors of 2.6 and 5.3, respectively, and ethylene/ethane selectivities were almost doubled (4.6 and 5.0 compared to pure 6FDA-DAM polyimide at 2.7). Pure-gas results and a schematic illustrating particle

dispersion for these MMMs are highlighted in Figure 14. In addition to these promising pure-gas results at low-pressures (i.e., 2 bar), plasticization was further suppressed as noted by a shift in the ethylene plasticization pressure point at 35 °C from 10 bar for the pure 6FDA-DAM polymer to greater than 20 bar for a 6FDA-DAM MMM containing 25 wt % $\text{Ni}_2(\text{dobdc})$ nanocrystals, and similar selectivities were noted for mixed-gas $\text{C}_2\text{H}_4/\text{C}_2\text{H}_6$ experiments.

Pre- and postsynthetic functionalization of MOFs provides a promising opportunity to form new MMMs with previously inaccessible transport characteristics. One interesting and undeveloped subcategory in this field relates to an extended $M_2(\text{dobdc})$ -type MOF structure, which is formed with a biphenyl ligand. By functionalizing the coordinatively unsaturated metal sites in these MOFs with diamines, unusual sorption characteristics have been observed. The most commonly investigated form of this MOF, mmen- $M_2(\text{dobpcd})$ ($M = \text{Mg}, \text{Mn}, \text{Fe}, \text{Co}, \text{Zn}$; mmen = N,N' -dimethylethylenediamine; $\text{dobpcd} = 4,4'$ -dioxidobiphenyl-3,3'-dicarboxylate), reported by McDonald et al. undergoes a phase change with a stoichiometrically equivalent addition of CO_2 per amine at pressures and temperatures of interest for adsorption-based separations.¹⁸¹ This phase change results in a step-shaped isotherm exclusive to CO_2 and inaccessible to N_2 , thereby achieving record CO_2 adsorption and CO_2/N_2 adsorption selectivities.¹⁸¹ If successfully incorporated into MMMs, such an approach could redefine expectations for the limits of current sorption enhancements from porous fillers.

UiO-66. Named after the University of Oslo, UiO-66 consists of $\text{Zr}_6\text{O}_4(\text{OH})_4$ clusters coordinated with six 1,4-benzenedicarboxylate ligands. The octahedral and tetrahedral cages construct a three-dimensional topology with 6 Å triangular windows.¹⁸² UiO-66 has high thermal,¹⁸³ chemical,¹⁸⁴ and water stability.¹⁸⁵ Moreover, topologically similar frameworks can be easily formed with substituted variations of 1,4-benzenedicarboxylate (i.e., $-\text{NH}_2$, $-\text{COOH}$, $-\text{OH}$). Given the accessible functionalities in UiO-66, excellent gas capture/separation and interfacial interactions between modified UiO-66 fillers and polymer matrices are often reported. Anjum et al. modulated the growth of UiO-66 using monosubstituted carboxylic acid modulators such as benzoic acid and 4-aminobenzoic acid to

change the internal/external chemistry of the MOF. In doing so, MOF-polymer compatibility, mechanical stability, and selectivity for CO₂ separations were improved compared to the unmodified UiO-66 MOF in MMMs formed with Matrimid.¹⁸⁶ The authors suggested that the modulated MOF had more internal unsaturated metal sites resulting from missing linkers due to competitive coordination between the modulator and ligand. The MMM formed from amino-functionalized UiO-66 (i.e., UiO-66-NH₂) dispersed in Matrimid had a CO₂ permeability of 19 barrer and CO₂/CH₄ selectivity of 48 for CO₂/CH₄ mixed-gas experiments (50:50 mol %). Compared to pure Matrimid, which under identical conditions had a CO₂ permeability of 6 and CO₂/CH₄ selectivity of 31, these MMMs showed improved transport performance, indicating fast transport through the UiO-66 pore framework and increased sorption selectivity for CO₂ due to dipole–quadrupole interactions between CO₂ and the NH₂ groups. Venna et al. postsynthetically modified the amino group on the surface of UiO-66-NH₂ with phenyl acetyl, decanoyl acetyl, and succinic acid groups.¹⁸⁷ The phenylacetyl-functionalized UiO-66-NH₂ had two types of favorable interactions with Matrimid, including π – π stacking and hydrogen bonding, thereby improving adhesion and compatibility between the polymer and functionalized UiO-66-NH₂, resulting in improved gas separation performance compared to unmodified UiO-66-NH₂ MMM. Su et al. synthesized UiO-66-NH₂ via a microwave-assisted technique and prepared a hybrid UiO-66-NH₂/polysulfone membrane through a “priming” process by adding a polysulfone solution directly to a UiO-66-NH₂ suspension and sonicating. MOF loading was enhanced from 30 to 40 wt %, and CO₂ permeability increased significantly from 19 barrer for the MMM with 30 wt % UiO-66-NH₂ to 46 barrer for the MMM with 40 wt % UiO-66-NH₂ with minimal changes in selectivity (i.e., CO₂/N₂ selectivity increased from 27 to 28 and CO₂/CH₄ selectivity remained unchanged at 24), suggesting the formation of a MOF percolation network and dual transport pathways leading to improved gas separation performance.¹⁸⁸ Of note, at high MOF loadings (especially between 30 and 40 wt %), the percolation limit was surpassed resulting in an interconnected network through the membrane. For loadings above 30 wt %, the Maxwell model could only fit the data if an adjustment was made to account for a dispersed phase shape factor of 0.14 (for spherical geometry, the shape factor is 1/3), indicating that UiO-66-NH₂ had formed an ellipsoid percolation network with orientation parallel to the direction of gas transport. Consequently, a “molecular transport highway” was introduced by UiO-66-NH₂ that provided higher diffusivity compared to traditional solution-diffusion transport.

8.2. Two-Dimensional Metal–Organic Frameworks.

Properly designed morphology and dimensionality of inorganic fillers can lead to improvements in MMM performance. One area of interest is for two-dimensional (2D) MOF nanosheets. In contrast to three-dimensional (3D) materials such as spherical nanoparticles, transport in 2D materials is strongly affected by orientation. Naturally, the in-plane and out-of-plane orientations of the pore systems, in particular, pores with orientation parallel to the gas diffusion pathway, can maximize gas permeability and selectivity. An interesting example of a 2D material that can improve CO₂/CH₄ separation performance is presented in Figure 15. In this work, Rodenas et al. prepared copper 1,4-benzenedicarboxylate (CuBDC) MOF nanosheets via a bottom-up interfacial synthesis technique based on density and solubility differences of the BDC ligand and Cu²⁺ in a three-phase system of *N,N*-dimethylformamide (DMF) and acetonitrile (CH₃CN).

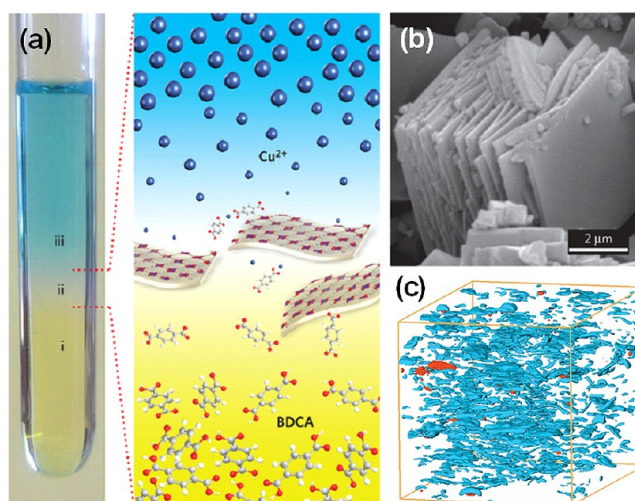


Figure 15. (a) Schematic of bottom-up synthesis of CuBDC MOF nanosheets. Layer I is a solution of benzene and 1,4-dicarboxylic acid (BDCA, referred to as BDC in the text), layer II is the boundary layer containing ligand and copper ion, and layer III is a copper ion solution. For visualization, yellow 2-amino 1,4-benzenedicarboxylic acid was added to phase I and a schematic illustrating the boundary layer is presented to the right. (b) SEM image of the CuBDC MOF. (c) 3D reconstructed, orthogonal cross-sectional image from FIB-SEM tomogram of CuBDC MOF in Matrimid. Blue indicates CuBDC MOF particles, and red indicates void spaces. This figure was reproduced from ref 111.

The first phase, added to the bottom of a glass tube, consisted of BDC in a 2:1 (v/v) mixture of DMF:CH₃CN. Next, a small amount of 1:1 (v/v) DMF:CH₃CN was added as the interfacial phase, and finally, a 1:2 (v/v) mixture of DMF:CH₃CN with Cu(NO₃)₂·3H₂O was added as the top phase. Copper metal ions diffused from the top phase and BDC diffused from the bottom phase, meeting at the interfacial layer to form CuBDC nanosheets with aspect ratios over 20 (width of square sheets was 0.5–4 μm and thickness of sheets was 5–25 nm). These sheets had a perpendicular stacking direction of the CuBDC layers as confirmed by XRD.¹¹¹ The CuBDC nanosheets, which preferentially orient and uniformly distribute in MMMs (Figure 15b,c), resulted in increased gas selectivity compared to low aspect ratio materials and materials dispersed without orientation. Mechanistically, these materials increased the tortuosity of gas transport, forcing penetrants to navigate between the CuBDC nanosheets in the MMM. In a related study, Kang et al. used a bottom-up synthesis method to synthesize a “jungle-gym-like” [Cu₂(ndc)₂(dabco)]_n (ndc = 1,4-naphthalenedicarboxylate, dabco = 1,4-diazabicyclo[2.2.2]octane) MOF with various morphologies (bulk crystals, nanocubes, and nanosheets).¹⁸⁹ The MOF [Cu₂(ndc)₂(dabco)]_n had characteristically narrow pore channels along the (100) and (001) direction of 5.4 Å × 6.2 Å and 3.7 Å × 3.7 Å, respectively. Interestingly, the MMM with [Cu₂(ndc)₂(dabco)]_n nanosheets showed relatively stronger peak intensity in the (001) plane rather than (100) plane, indicating an oriented stacking structure of the MOFs in the MMM. This orientation suggested that the (001) planes were oriented in the direction of gas diffusion such that separation of H₂/CO₂ could be achieved via selective diffusion of H₂ (kinetic diameter = 2.89 Å) compared to CO₂ (kinetic diameter = 3.3 Å). Crystallographically, CO₂ could still diffuse through the pore aperture, but the size difference was enough to improve selectivity. Wang et al. fabricated nanometer thick molecular sieving membranes using two-dimensional

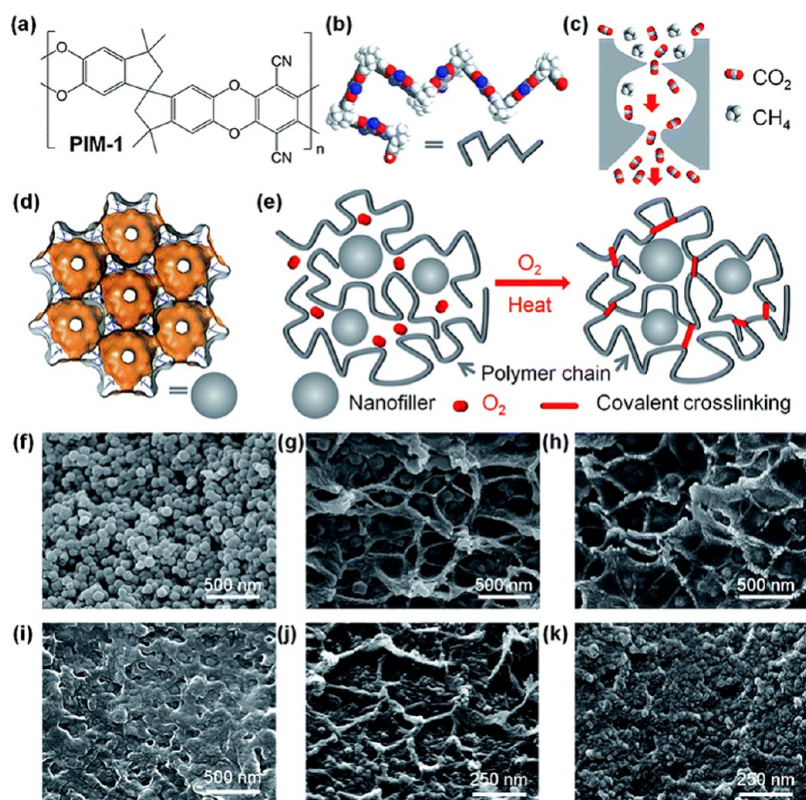


Figure 16. (a) Chemical structure, (b) 3D representation, and (c) schematic illustrating molecular sieving nature of PIM-1. (d) Crystal structure of ZIF-8 nanofiller with yellow region indicating surface probed by H₂, (e) schematic illustrating covalent thermo-oxidative cross-linking of nanofiller dispersed in PIM-1 at high temperatures (350–450 °C) under oxygen. (f) SEM image of ZIF-8 nanoparticles, (g) cross-sectional SEM image of PIM-1/ZIF-8 with heat treatment at 120 °C for 1 day, (h) cross-sectional SEM image of thermo-oxidatively cross-linked PIM-1 (TOX-PIM-1)/ZIF-8 with heat treatment at 385 °C for 1 day, (i) cross-sectional SEM image of PIM-1/ZIF-8 with heat treatment at 300 °C for 2 days, (j) cross-sectional SEM image of PIM-1/SiO₂ with heat treatment at 120 °C for 1 day, and (k) cross-sectional SEM images of TOX-PIM-1/SiO₂ with heat treatment at 385 °C for 1 day. All membranes were annealed under vacuum. This figure was adapted from ref 196.

MAMS-1 (Mesh Adjustable Molecular Sieve, Ni₈(5-bbdc)₆(OH)₄) (5-bbdc = 5-*tert*-butyl-1,3-benzenedicarboxylic acid) nanosheets.¹⁹⁰ The layers of MOF sheets were loosely bound together via van der Waals interactions. Similar to the work by Kang et al., the MAMS-1 nanosheets had two pathways: the first in the (001) direction with 2.9 Å pores perpendicular to the plane of the monolayer and the second in the (100) direction with 5 Å pores parallel to the plane of the monolayer. The 12 nm thick membrane was tested for permeation properties using a H₂/CO₂ mixture (20:80 v/v) and showed an extraordinary H₂ permeance of 6516 GPU and an H₂/CO₂ separation factor of 34, which is better performance than 2D graphene oxide (GO) membranes, which will be discussed later in this Perspective, despite being thicker. Such an approach indicates the promise with 2D MOF materials for separations: pores can be engineered and aligned in the direction of transport, whereas with typical GO materials, transport occurs between sheets, thereby resulting in lower effective diffusion coefficients for membranes of the same thickness.

8.3. Control of Interfacial Interactions between Continuous Phase and Filler in MMMs. MMMs with inorganic fillers, such as zeolites or carbons, often have a defective polymer–filler interfaces due to the lack of compatibility between the two components. These interfacial voids in MMMs create nonselective gas transport pathways adversely effecting gas selectivity. In contrast to zeolites or carbons, MOFs contain organic functionality in their bridging ligands. Such chemical characteristics make this class of materials

intriguing, since the organic functionality in the MOF can potentially interact favorably with the organic functionality in polymers. However, MOFs are still rigid, crystalline materials, so organic functionality does not completely eliminate this compatibility challenge. Therefore, various strategies have been pursued to improve interfacial interactions.

Within these efforts, improvements in both chemical and physical interactions have been pursued, including pre- and postsynthetic modifications to MOF ligands, chemically functionalizing the polymer, and employing cross-linking-type reactions to tether the MOF frameworks to the polymer. Lin et al. pursued a cross-linking-type approach by first synthesized hexagonally shaped [Cd₂L(H₂O)]₂·5H₂O (Cd-6F) using a 6FDA-based organic linker, which was also used for in the polymer matrix, 6FDA-oxidianiline (ODA). Introduction of Cd-6F in the polymer reaction solution resulted in a covalently cross-linked polymer–MOF network, thereby eliminating poor adhesion issues typically found with composite materials.¹⁹¹ In addition, –NH₂ end groups on 6FDA-ODA provide good chemical interaction with Cd-6F crystals, reducing nonideal interfacial void spaces between the MOF and polymer. Shahid et al. suggested a “controlled fusion” approach, which was based on chemically modifying the surface of precipitated Matrimid particles with compatible imidazole groups, followed by in-situ growth of ZIF-8 particles from an aqueous solution to form a two-phase system.¹⁹² The resulting Matrimid/MOF solution was cast onto a substrate by knife casting, and the resulting film was annealed in a DMF vapor environment for various amounts of

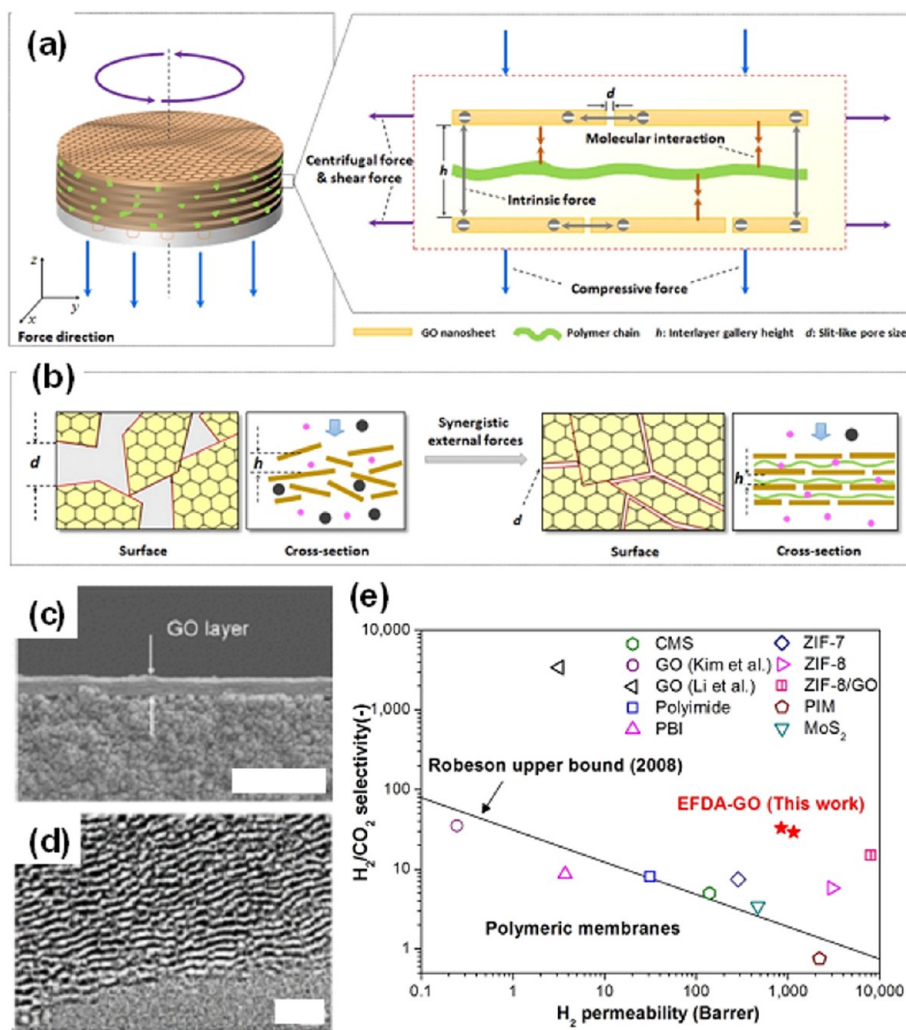


Figure 17. (a) Schematic illustrating 2D channels assembled via the so-called external force driven assembly (EFDA) method. The arrows indicate external forces applied to the layers resulting from vacuum and spinning, (b) the magnified image illustrates how polymer chains (green) create a repulsive internal force to space apart the GO nanosheets (yellow). (c) Cross-sectional SEM (scale bar = 5 μm) image of EFDA-GO membrane and (d) magnified TEM (scale bar = 4 nm) images of EFDA-GO membrane. (e) H_2/CO_2 separation performance of EFDA-GO membranes with the Robeson upper bound including data from several literature references. This figure was reproduced from refs 208 and 209.

time (e.g., 0, 2, 4, and 5 days). After sufficiently long annealing (i.e., 5 days), the polymer densified and sealed interfacial defects leading to selective MMMs. Chi et al. pursued an approach that targeted improved physical interactions by employing amphiphilic graft copolymers composed of poly(vinyl chloride)-*g*-poly(oxyethylene methacrylate) (PVC-*g*-POEM) to disperse ZIF-8 nanoparticles in THF solvent by secondary interactions between the POEM side chains and the imidazole moieties in the ZIF-8 organic linker, resulting in significant improvements in gas separation performance.¹⁹³ Wang et al. used a MOF surface modification approach by coating thin polydopamine (PD) layers on ZIF-8 nanoparticles.¹⁹⁴ The ZIF-8 nanoparticles were dispersed in a dopamine solution (0.5 g/L) of methanol and water (1:1) at a pH = 8.5, followed by different reaction times (1, 5, and 10 h) to modify the PD layer thickness. The performance of the ZIF-8@PD/polyimide MMM surpassed the upper bound limit for H_2/N_2 and H_2/CH_4 due to excellent interfacial interactions. Japip et al. fabricated cross-linked 6FDA-Durene/ZIF-71 MMMs using three vapor-phase cross-linkers of different chain lengths (ethylenediamine, diethylenetriamine, tris(2-aminoethyl)amine) to study the effect of restricted chain motion

and free volume on transport performance.¹⁹⁵ ZIF-71 fillers provided additional sites to form cross-links. Shorter chain length cross-linkers (e.g., ethylenediamine) restricted polymer chain motion, resulting in increased H_2/CO_2 selectivity at elevated temperature (150 $^\circ\text{C}$).

While most research focuses on the compatibility of the MOF-polymer interface to seal defects, MOFs can also be used to control the packing structure of surrounding polymer matrices, thereby tuning free volume. Song et al. demonstrated this feature by incorporating either ZIF-8 (70–100 nm diameter particles) or nonporous SiO_2 nanoparticles (12 nm diameter) into a polymer of intrinsic microporosity (i.e., PIM-1) that could be thermo-oxidatively cross-linked (TOX) (cf. Figure 16).¹⁹⁶ Thermo-oxidative cross-linking transformed linear polymer chains into cross-linked networks to improve gas selectivity. Moreover, the nanoscale fillers, either ZIF-8 or SiO_2 , regardless of internal pores, disrupted polymer chain packing and increased free volumes and permeability. Although this approach did not specifically focus on chemically or physically improving compatibility of these hybrid materials, it did demonstrate the ability to tune free volume within a MMM by cross-linking a

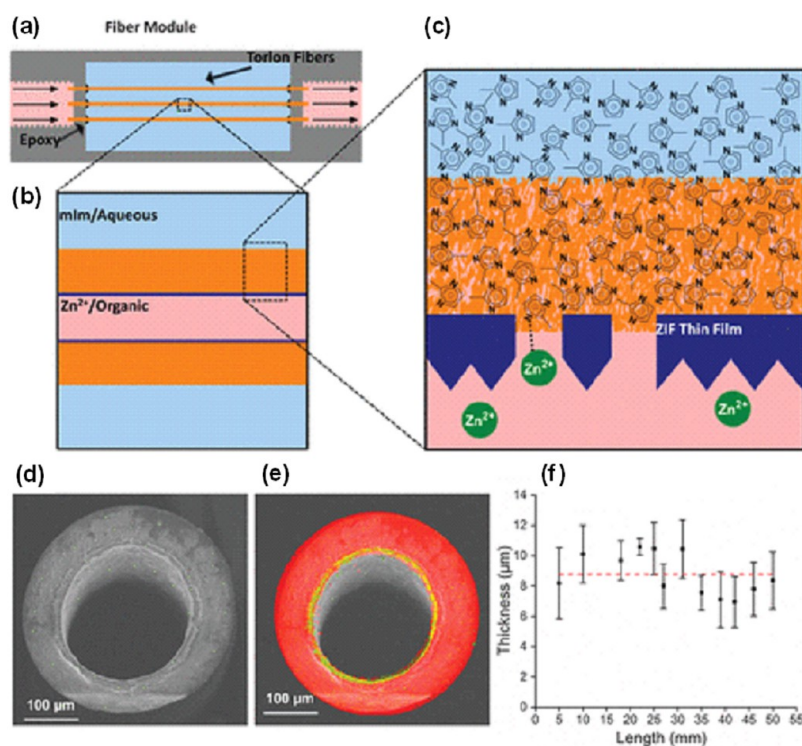


Figure 18. Schematic illustrating the IMMP technique for ZIF-8 hollow fiber membranes. (a) Side view of IMMP with Torlon fiber membranes. (b) The Zn^{2+} ions in a 1-octanol solution are supplied from the bore of the Torlon fiber (pink), while the 2-methylimidazole linkers in an aqueous solution are supplied from the outside of the Torlon fiber (light blue). (c) Enlarged section of the intermediate layer where the Zn^{2+} ions and the 2-methylimidazole linkers react to synthesize a ZIF-8 thin layer onto the inner surface of the Torlon fiber membrane (navy). (d) Cross-sectional SEM image of ZIF-8 hollow fiber membrane. (e) Energy-dispersive X-ray spectroscopy (EDX), elemental analysis of cross-sectional SEM image including carbon (red) and zinc (green). (f) ZIF-8 membrane thickness obtained at different lengths along the hollow fiber membrane (average thickness of ZIF-8 film is around $8.8 \mu\text{m}$, which is marked by red dashed line). This figure was reproduced from ref 211.

polymer that has its packing structure disrupted by MOF fillers. The property sets for these cross-linked MMMs are beyond the upper bound limit for CO_2/CH_4 , O_2/N_2 , H_2/N_2 , and H_2/CH_4 .

8.4. Graphene-Based Materials. Graphene-based materials are a unique platform of materials for small molecule separations based on transport through controlled pore sizes and interlayer spaces. The recent and rapid development of these materials, which resulted in a Nobel Prize in 2010, has driven research in the membrane community to develop these materials as atomically thin, layered membrane sheets.¹⁹⁷ The promise of these materials is that proper design and engineering could permit access to transformative transport property sets, since unprecedented permeance could be achieved if few-layer graphene sheets could be fabricated at an industrial scale.^{198,199} However, the development of these materials is still in its infancy, and many practical limitations need to be addressed.²⁰⁰

A common method for modifying the packing structure of graphene sheets is to use functionalized graphene, typically in the form of GO, which contains oxidized carbonyl and hydroxyl groups. A common method for preparing GO is Hummer's method, which oxidizes graphite with potassium permanganate in a suspension of sodium nitrate and concentrated sulfuric acid.^{201,202} Such approaches have led to encouraging membrane materials, but property sets are extraordinarily sensitive to membrane fabrication methods. Kim et al. investigated the sensitivity of membrane formation for designing selective GO membranes.²⁰³ In one case, passively contacting a membrane support with a GO solution resulted in Knudsen diffusion and nanoporous membrane-type behavior, whereas in another case,

spin coating the GO solution onto a membrane support formed a molecular-sieving membrane. In the latter case, the GO stacking structures could be modified by temperature with molecular-level precision to form membranes with exceptional H_2/CO_2 separation performance.²⁰³ Li et al. reported ultrathin (1.8, 9, and 18 nm) GO membranes prepared via a filtration process.²⁰⁴ Through incorporation of selective structure defects, GO membranes with H_2/CO_2 and H_2/N_2 gas separation selectivities as high as 3400 and 900, respectively, were formed.

The oxidized functionality of GO also creates chemical interactions with polymers that enables the formation of GO-polymer hybrid membranes with interesting diffusion, solubility, and morphological characteristics. Shen et al. leveraged polymer functionality to control molecular-sieving channels with GO MMMs.²⁰⁵ A commercial polyether-*block*-amide (PEBAX) copolymer formed hydrogen bonds with neighboring GO nanosheets, and these interactions resulted in the assembly of GO laminates, thereby increasing the rate of gas transport. The interlayer spacing between graphene layers was approximately 0.35 nm, enabling these materials to selectively separate CO_2 from CO_2/N_2 mixtures. The combination of interlayer channels of GO sheets and the favorable interactions between CO_2 with polar functional groups (i.e., $-\text{COOH}$ and $-\text{OH}$) on GO sheets increased CO_2 gas adsorption so that GO membranes had CO_2 permeabilities and CO_2/N_2 selectivities of 100 barrer and 91, respectively, for stable, long-term testing (>6000 min). Li et al. fabricated MMMs using GO nanosheets functionalized with poly(ethylene oxide) and polyethylenimine, providing high sorption properties due to enhanced CO_2 solubility selectivity

resulting from the introduction of ethylene oxide groups and amine groups as well as tortuous diffusion pathway generated by the rigidified interface between GO sheets and the polymer matrix.²⁰⁶

The packing nature of GO sheets is critical when forming a membrane, so naturally the field has investigated several chemical and physical strategies for controlling interlayer spacing. Wang et al. constructed nanochannels for CO₂ separations in GO membranes through borate-cross-linked GO nanosheets.²⁰⁷ The borate ions assisted in tuning the interlayer spacing and reversible CO₂ sorption in GO sheets when associated with water molecules under humid conditions. Shen et al. used a layer-by-layer approach to modify the GO packing structure. In contrast to the work by Kim et al.,²⁰³ which modified GO spacing by thermal treatment, the work by Shen et al. involved repetitive coating and washing steps of GO and PEI solutions on a porous ceramic substrate (i.e., Al₂O₃). During the formation of each membrane layer, vacuum and centrifugal forces were simultaneously applied during spinning. With PEI supported between GO layers, this approach allowed for the controlled growth of interlayer height. Figures 17a,b demonstrate schematically the concept behind this approach, Figures 17c,d present SEM images of the formed layers, and Figure 17e highlights the outstanding H₂/CO₂ separation performance achieved with these materials.^{208,209}

Of fundamental interest, permeation of individual gas molecules can also be regulated at the molecular level. Wang et al. used nanometer-sized gold clusters to partially block discrete angstrom-sized pores in graphene monolayers, thereby regulating gas permeance.²¹⁰ The migration of gold nanoclusters, and therefore the spacing between gold clusters and pores in the graphene sheets, could be stimulated via a laser-induced heating process in a vacuum. This technique permitted repeatable and reversible cycling of gas flux through this so-called “molecular valve”.

8.5. Hollow Fiber Membranes. Polymer hollow fibers have been widely used for industrial gas separation membranes.³⁷ In terms of engineering design, these types of membranes provide very high accessible surface area and contain an asymmetric structure to mechanically support a dense, selective polymer thin film.³⁷ Leveraging industrially accepted hollow fibers as supports for hybrid materials has been a growing area of interest for scaling up MOFs as films. Brown et al. developed an interfacial microfluidic membrane processing (IMMP) method presented in Figure 18 to form crystalline MOF structures (e.g., ZIF-8) supported on polymeric hollow fibers.²¹¹ In a reaction chamber, a solution of zinc nitrate hexahydrate/1-octanol flows through the bore side of a Torlon hollow fiber and an immiscible solution of 2-methylimidazole/water flows across the shell side. By proper choice of solvents and injection positions of precursor solutions to the reaction zone, a continuous molecular sieving 8.8 μm thick ZIF-8 hollow fiber membrane was formed and exhibited H₂/C₃H₈ and C₃H₆/C₃H₈ separation factors of 370 and 12, respectively. Recently, Eum et al. performed additional work on reducing defects in ZIF-8 films on Torlon hollow fibers by modifying the IMMP process. Typically, high concentrations of 2-methylimidazole (1.37 mol/L) flow from the shell side, which accelerates penetration of 2-methylimidazole into the bore, resulting in overgrowth of ZIF-8 crystals and membrane defects. After reducing the concentration of 2-methylimidazole (0.69 mol/L), uniform ZIF-8 membranes were formed with improved C₃H₆/C₃H₈ separation factors as high as 180.²¹² Others have continued to develop this type of approach for additional gas

separation applications, including Marti et al., who grew a thin ZIF-8 film (2.5 μm thick) from aqueous solutions that exhibited a CO₂ permeance of 22 GPU and a CO₂/N₂ selectivity of 52.²¹³ Hou et al. produced ultrathin (~400 nm in effective thickness) and continuous ZIF-8 films on (3-aminopropyl)triethoxysilane (APTES)-functionalized and TiO₂-coated PVDF hollow fibers.²¹⁴ The ultrathin ZIF-8 membrane showed H₂ permeance of 6.0 × 10⁴ GPU and H₂/CO₂ selectivity of 7, which is approaching the theoretically predicted permeation properties of ZIF-8.

In addition to forming films, other have investigated dispersing nanoparticles into hollow fibers. Dai et al. report a successful asymmetric dual-layer hollow-fiber MMM formed from ZIF-8 and Ultem for CO₂/N₂ separation using core and sheath dopes containing ZIF-8 nanoparticles.²¹⁵ Hybrid hollow fiber membranes were prepared with 17 vol % of ZIF-8 fillers and showed a CO₂ permeance of 26 GPU and CO₂/N₂ selectivity of 36 at 35 °C, both of which are higher than that of the neat Ultem hollow fibers (CO₂ permeance of 14 GPU and CO₂/N₂ selectivity of 30).

9. INORGANIC MEMBRANES

Compared to organic membranes and organic–inorganic hybrid materials, wholly inorganic materials have potential advantages such as high temperature stability, high permeation rates, and high selectivities. Despite this potential, decades of research in this area has not resulted in large-scale industrial adaption, largely due to issues with poor mechanical properties and capillary condensation.³⁷ Nevertheless, the introduction of new materials as alternatives to polymer-based membranes has begun to reinvigorate research.

9.1. Carbon Membranes. Early carbon membranes were developed in the 1960–1970s by Ash et al. using compressed graphite,^{216,217} and a refined understanding of the mechanism of transport in these materials (i.e., adsorption and activated transport) was developed by Koresh and Soffer in the 1980s.^{218,219} Carbon molecular sieve (CMS) membranes are typically formed by controlled pyrolysis of a polymer precursor at high temperatures. Numerous polymer precursors such as polyacrylonitrile (PAN),²²⁰ polyfurfuryl alcohol (PFA),²²¹ phenolic resin,²²² and polyimide^{223,224} have been used to create highly efficient CMS membranes. Among these polymer precursors, polyimides have been extensively studied owing to their intrinsic temperature stability and high modulus. These material properties are used to identify polymers that form molecular sieving structures during pyrolysis that do not easily succumb to pore collapse. CMS membranes have a slitlike pore structure, generated by a disordered sp²-hybridized carbon, which consists of small pores (ultramicropores <7 Å) and larger pores (micropores ~7–20 Å), which can provide beneficial permeability and selectivity property sets.^{40,225} Based on their simple preparation process and high separation performance, CMS membranes have been of great interest for many years.

In terms of polyimide precursors, Matrimid and 6FDA-based polyimides have been a particular focus. Rungta et al. pyrolyzed Matrimid under vacuum and inert argon atmosphere to produce CMS membrane for ethylene/ethane separation.⁴⁰ High ethylene/ethane selectivity was attributed to entropically driven separation performance. Very recently, Koros and Zhang described the preparation and application of dense-walled CMS hollow fiber membranes (~32 μm wall thickness) with excellent mechanical strength derived from Matrimid under argon atmosphere at high temperature (from 750 to 900 °C),

overcoming previous issues of brittleness typically found in CMS films.²²⁶ The CMS hollow fiber membrane showed a CO₂ permeability of over 100 barrer with a CO₂/CH₄ selectivity over 1000 and O₂ permeability of 10 barrer with O₂/N₂ selectivities over 20. Xu et al. explored the formation of asymmetric CMS hollow fiber membranes using 6FDA-DAM and 6FDA/BPDA-DAM polymer precursors for olefin/paraffin separation.²²⁷ These polymers have a higher glass transition temperature than Matrimid, thereby making them more rigid and resistant to substructural collapse.²²⁷ Qiu et al. fabricated a CMS membrane from 6FDA-mPDA/DABA (3:2) polyimide for CO₂/CH₄ separation.²²⁸ The DABA moieties in polyimide precursor created a cross-linked microvoid structure through a decarboxylation reaction, leading to a significant improvement in transport performance (e.g., CO₂ permeability of 14750 barrer and CO₂/CH₄ selectivity of 52).

Poly(vinylidene fluoride) (PVDF) has also been investigated as a CMS precursor. Koh et al. pyrolyzed a cross-linked PVDF polymer precursor to target applications in organic solvent nanofiltration of *p*-xylene/*o*-xylene mixtures.²²⁹ Compared to typical losses of meso- and macroporosity from neat PVDF polymer precursors, the cross-linked PVDF fibers maintained a mechanically robust modulus above the glass transition temperature of non-cross-linked PVDF, thereby preventing pore collapse and maintaining an asymmetric porous structure after pyrolysis (>500 °C). The carbon hollow fiber membranes derived from cross-linked PVDF polymer precursors have bimodal pore distributions of 6.0–6.3 Å and 8.0–8.4 Å and are suitable for separating *p*-xylene (5.8 Å) from *o*-xylene (6.8 Å). The CMS hollow fiber membranes have exceptional *p*-xylene/*o*-xylene diffusion selectivities of 25 for single-component experiments at room temperature with gas pressure of 3.4–13.8 bar. Moreover, binary (*p*-xylene/*o*-xylene) and ternary (*p*-xylene/*o*-xylene/*m*-xylene) mixtures were also investigated and had separation efficiencies with high pressures (~100 bar) beyond those of zeolite membranes.

9.2. MOF Membranes. MOFs are not only used as a filler in MMMs but also to produce polycrystalline membranes. Even though fabrication of pure MOF membranes is extremely sensitive to the experimental conditions, their outstanding separation performance contributes to invigorate research interest for this class of materials. Kwon et al. fabricated monolithic, defect-free ZIF-8 membranes on porous alumina support using a counter-diffusion-based in-situ method.²³⁰ Diffusion of metal and organic ligand precursors toward the interface between the porous alumina support and a solution was exploited to produce crystalline ZIF-8 membranes. These membranes exhibited promising propylene/propane (50/50 mixture gas) separation performance, with a propylene permeance of 60 GPU and a separation factor of 50. Kwon et al. also reported heteroepitaxially grown ZIF-8/ZIF-67 membranes using microwave-assisted seeding of ZIF-8 and secondary growth of ZIF-67 methods.²³¹ ZIF-67 and ZIF-8 have the same crystalline structure, but the former contains cobalt instead zinc. Membranes based on ZIF-8/ZIF-67 exhibited improved propylene/propane separation properties, with a separation factor of 85. More surprisingly, the ZIF-8/ZIF-67 membrane, after a ligand treatment for minimizing defect at the interface, exhibited a further improvement in its performance, with a propylene/propane separation factor of 200.

Nan et al. formed a seed layer of HKUST-1 on a porous alumina support through step-by-step deposition of metal and organic ligand molecules.²³² The successful seeding of precursors

allowed formation of a continuous HKUST-1 membrane via a secondary hydrothermal growth process. The HKUST-1 membrane was evaluated for H₂/CH₄, H₂/N₂, and H₂/CO₂ separation at 25 °C. Selectivities of 3, 3.7, and 4.6 were reported, respectively.

9.3. Ceramic Membranes. Ceramic membranes such as microporous silica membranes are of particular interest for high-temperature applications such as high-purity hydrogen generation (up to 99.99%).^{233,234} Microporous silica is a common ceramic material for these separations, since it can be deposited as a selective layer onto porous ceramic supports (i.e., α -alumina) via a sol-gel process^{235–237} or deposited via chemical vapor deposition (CVD).^{238,239} Tsapatsis et al. prepared SiO₂ layers in porous Vycor tubes for hydrogen-permeable membranes via atmospheric pressure chemical vapor deposition (APCVD) with SiCl₄ reactants. The SiO₂ membrane showed an H₂ permeance of 22 GPU and a He/N₂ selectivity above 500 at 500 °C.²⁴⁰ Industrially, Air Products worked for several decades on commercializing ceramic membranes through their ion transport membrane (ITM) systems. ITM ceramic materials are based on engineered conductors with complex formulation of metal oxides (e.g., perovskites), which exhibit both oxygen ion and electron conductivity at high temperatures (800–900 °C). The driving force for oxygen separation is the relative oxygen partial pressure difference across the membrane, with a pressured air feed at 100–300 psia, and a subatmospheric permeate side. In terms of separation mechanism, oxygen sorbed by the feed side of the ITM is ionized, providing an electron to the ceramic lattice. After diffusing through the ITM under the driving force, ionized oxygen recombines with an electron from ceramic lattice and desorbs from the permeate side. Air Products successfully designed full-size ITM modules in a scale of approximately 0.5 ton per day (STPD) with thin, cost-effective, multistacks of ceramic membranes, exceeding commercial separation performance targets.²⁴¹ Moreover, ITM membranes were integrated with a specifically developed gas turbine for conventional IGCC, which could reduce the plant power consumption during air separation.²⁴¹ Although the ITM technology reached semi-commercial development, this project was abandoned, and there has been less activity in ceramic membranes for gas separation in recent years.^{242–244} It is challenging for microporous silica membranes to overcome the severe loss of separation performance under humid conditions since humidity coupled with high temperatures assists in the formation of new –Si–O–Si bonds from –Si–OH surface sites through a condensation reaction, thereby leading to densification and reducing the number of accessible pores.^{245–248}

10. CONCLUSIONS

Membrane gas separation is a mature and expanding technology. Since 1979, when the first membrane separation unit based on polysulfone hollow fibers was built by Monsanto, hundreds of new polymeric, inorganic, and hybrid materials were introduced. Although several new materials show outstanding properties in the laboratory, plasticization and physical aging hamper their industrial use. However, some of these materials such as TR polymers, polyacetylenes, PIMs, and mixed-matrix membranes based on MOFs look promising, so they could be likely candidates to replace conventional glassy polymers in large scale gas separations. Synthesis and fabrication routes as well as transport and mechanical properties of these materials were reviewed in this paper.

Thirty-five years of academic and industrial practice in membrane science gave us an important lesson: development of next-generation membrane materials for large scale separations will rely on a multidisciplinary approach that embraces the broad fields of chemical and materials engineering, polymer science, and materials chemistry.

AUTHOR INFORMATION

Corresponding Author

*(B.D.F.) E-mail freeman@che.utexas.edu; Ph (512) 232-2803.

ORCID

Won Seok Chi: 0000-0002-0422-0495

Benny D. Freeman: 0000-0003-2779-7788

Notes

The authors declare no competing financial interest.

Biographies



Michele Galizia is an Assistant Professor of Chemical Engineering at the University of Oklahoma. He received a Ph.D. in Chemical Engineering from the University of Bologna under the supervision of Prof. Giulio Sarti. In 2013 he joined the Benny Freeman–Don Paul Research Group at the University of Texas at Austin as a Research Associate. In 2006, he was awarded from the Italian Ministry of Education with a Graduate Fellowship which funded his PhD project. Prof. Galizia's research focuses on membrane science, with special emphasis on small molecules sorption and transport in polymer-based materials for gas, vapor, and liquid separation as well as water purification. His research interests include (i) fundamental transport property–structure relationships of polymers, (ii) modeling and simulation of thermodynamic and transport properties of polymers, (iii) polymer–penetrant and penetrant–penetrant interactions, and (iv) design of new materials for separations in harsh environments, such as OSN, pervaporation, and vapor permeation. He is coauthor of 30 contributions as peer-reviewed papers on international journals and book chapters and over 60 conference proceedings. In 2013, he received the Best Reviewer Award from the *Journal of Membrane Science* “for the excellence in paper reviewing and for an ongoing contribution to the quality of the journal”. Since 2012, he has been member of the editorial boarding of *Frontiers in Polymer Chemistry* (Nature Publishing Group).



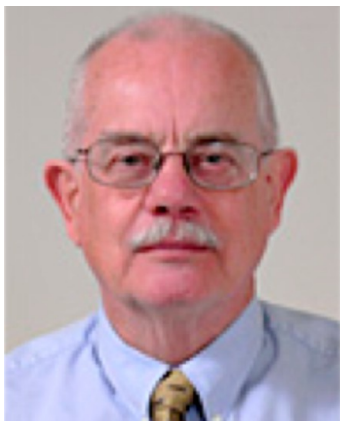
“Lucas” Won Seok Chi received both his B.S. (2010) and Ph.D. (2015) degrees in Chemical Engineering at Yonsei University under the supervision of Prof. Jong Hak Kim. He focused on membrane sciences for energy application and gas separation with synthesis of graft copolymers and ionic liquids. He is currently working in Chemical Engineering at the Massachusetts Institute of Technology under the supervision of Prof. Zachary Smith. His research interests include the design of mixed-matrix membranes based on highly permeable polyimides and metal–organic frameworks using strategies to reduce interfacial defects to increase compatibility.



Zachary P. Smith is an Assistant Professor and the Joseph R. Mares Career Development Chair in the Department of Chemical Engineering at the Massachusetts Institute of Technology. He earned his bachelor's degree in Chemical Engineering from the Penn State Schreyer Honors College and completed his graduate training in Chemical Engineering under the guidance of Profs. Benny Freeman and Don Paul at the University of Texas at Austin. His postdoctoral training was in the Department of Chemistry at the University of California, Berkeley, under the guidance of Prof. Jeffrey Long. Prof. Smith focuses on the molecular level design, synthesis, and characterization of polymers and inorganic materials for applications in membrane and adsorption-based separations. In particular, his group develops nanostructured, functional, and porous materials to reduce the energy consumption and environmental footprint of processes involving gas-phase separations and gas storage. Prof. Smith was a U.S. delegate to the Lindau Nobel Laureate Meeting on Chemistry in 2013, has been awarded the North American Membrane Society Young Membrane Scientist Award, and is a cofounder of Flux Technologies.



Timothy C. Merkel received his B.S. in Chemical Engineering from Polytechnic University (Brooklyn) and his M.S. and Ph.D. in Chemical Engineering from North Carolina State University. Dr. Merkel joined Membrane Technology and Research, Inc. (MTR), full-time as a Senior Research Scientist in January 2003 and became Director of MTR's Research and Development Group in 2009 and Vice-President of Technology in 2013. In his current role, Dr. Merkel leads a team of researchers developing new membrane materials and processes for use in industrial gas separations. Some of his group's recent work includes an industry-leading program on use of membranes for carbon capture from power and industrial exhaust gases. Dr. Merkel has published over 30 peer-reviewed articles and has given numerous presentations at academic and industrial meetings internationally. He is coauthor on 23 patents in the fields of membrane materials and process design.



Richard W. Baker founded Membrane Technology and Research, Inc. (MTR), in 1982 and served as President for 25 years. In that time, MTR became a leading membrane research, development, engineering, and production company, concentrating on the development of membranes and membrane systems for industrially and environmentally significant separations. He is currently leading MTR's new development program for membrane-based biomass/biofuel ethanol separations. Dr. Baker is the author of more than 100 papers and over 100 patents, all in the membrane area. Three editions of his book, *Membrane Technology and Applications*, were published in 2000, 2004, and 2012. He serves on the editorial board of the *Journal of Membrane Science* and was previously on the editorial boards of *Industrial and Engineering Chemistry Research*, the *Journal of Controlled Release*, and *Separation and Purification Technology*. He served as editor of the NAMS quarterly newsletter for several years. Dr. Baker is founder and past president of the International Controlled Release Society and cofounder of the North American Membrane Society (NAMS). In 2002, he was recipient of the first NAMS Alan S. Michaels Award for Innovation in Membrane Science and Technology.



Benny D. Freeman is the Richard B. Curran Centennial Chair in Engineering at The University of Texas at Austin. He completed graduate training in Chemical Engineering at the University of California, Berkeley, earning a Ph.D. in 1988. In 1988 and 1989, he was a postdoctoral fellow at the Ecole Supérieure de Physique et de Chimie Industrielles de la Ville de Paris (ESPCI), Laboratoire Physico-Chimie Structurale et Macromoléculaire in Paris, France. Dr. Freeman's research is in polymer science and engineering and, more specifically, in mass transport of small molecules in solid polymers. His research group focuses on structure/property correlation development for liquid and gas separation membrane materials. He has won a number of awards, including a Fulbright Distinguished Chair (2017), Fellow of the North American Membrane Society (NAMS) (2017), the Distinguished Service Award from the Polymeric Materials: Science and Engineering (PMSE) Division of the American Chemical Society (ACS) (2015), Joe J. King Professional Engineering Achievement Award from The University of Texas (2013), American Institute of Chemical Engineers (AIChE) Clarence (Larry) G. Gerhold Award (2013), Society of Plastics Engineers International Award (2013), Roy W. Tess Award in Coatings from the PMSE Division of ACS (2012), the ACS Award in Applied Polymer Science (2009), AIChE Institute Award for Excellence in Industrial Gases Technology (2008), and the Strategic Environmental Research and Development Program Project of the Year (2001). He is a Fellow of the AAAS, AIChE, ACS, and the PMSE and IECR Divisions of ACS. He has served as chair of the PMSE Division of ACS, Chair of the Gordon Research Conference on Membranes: Materials and Processes, President of the North American Membrane Society, Chair of the Membranes Area of the Separations Division of the AIChE, and Chair of the Separations Division of AIChE.

■ ACKNOWLEDGMENTS

We gratefully acknowledge partial support by the Australian–American Fulbright Commission for the award to B.D.F. of the U.S. Fulbright Distinguished Chair in Science, Technology and Innovation sponsored by the Commonwealth Scientific and Industrial Research Organization (CSIRO). Z.P.S. and W.S.C. thank Dr. Hiroyasu Furukawa for providing the high-resolution images of MOF crystal structures.

■ REFERENCES

- (1) Baker, R. W.; Lokhandwala, K. Natural gas processing with membranes: an overview. *Ind. Eng. Chem. Res.* **2008**, *47*, 2109–2121.
- (2) Bollinger, W.; MacLean, D.; Narayan, R. Separation systems for oil refining and production. *Chem. Eng. Prog.* **1982**, *78* (10).
- (3) Wijmans, J. G.; Baker, R. W. The solution-diffusion model: A review. *J. Membr. Sci.* **1995**, *107*, 1–21.
- (4) Paul, D. R. Reformulation of the solution-diffusion theory of reverse osmosis. *J. Membr. Sci.* **2004**, *241*, 371–386.

- (5) Baker, R. W.; Low, B. T. Gas Separation Membrane Materials: A Perspective. *Macromolecules* **2014**, *47*, 6999–7013.
- (6) Galizia, M.; Benedetti, F. M.; Paul, D. R.; Freeman, B. D. Monovalent and divalent ion sorption in a cation exchange membrane based on cross-linked poly(p-styrene sulfonate-co-divinylbenzene). *J. Membr. Sci.* **2017**, *535*, 132–142.
- (7) Robeson, L. M. The upper bound revisited. *J. Membr. Sci.* **2008**, *320*, 390–400.
- (8) Robeson, L. M. Correlation of separation factor versus permeability for polymeric membranes. *J. Membr. Sci.* **1991**, *62*, 165–185.
- (9) Freeman, B. D. Basis of Permeability/Selectivity Tradeoff Relations in Polymeric Gas Separation Membranes. *Macromolecules* **1999**, *32*, 375–380.
- (10) Vu, D. Q.; Koros, W. J.; Miller, S. J. Mixed matrix membranes using carbon molecular sieves. *J. Membr. Sci.* **2003**, *211*, 311–334.
- (11) Puleo, A. C.; Paul, D. R.; Kelley, S. S. The effect of degree of acetylation on gas sorption and transport behavior in cellulose acetate. *J. Membr. Sci.* **1989**, *47*, 301–332.
- (12) Koros, W. J.; Fleming, G. K.; Jordan, S. M.; Kim, T. H.; Hoehn, H. H. Polymeric membrane materials for solution-diffusion based permeation separations. *Prog. Polym. Sci.* **1988**, *13*, 339–401.
- (13) Muruganandam, N.; Koros, W. J.; Paul, D. R. Gas sorption and transport in substituted polycarbonates. *J. Polym. Sci., Part B: Polym. Phys.* **1987**, *25*, 1999–2026.
- (14) Pinnau, I.; Toy, L. G. Transport of organic vapors through poly(1-trimethylsilyl-1-propyne). *J. Membr. Sci.* **1996**, *116*, 199–209.
- (15) Chiou, J. S.; Barlow, J. W.; Paul, D. R. Plasticization of glassy polymers by CO₂. *J. Appl. Polym. Sci.* **1985**, *30*, 2633–2642.
- (16) Wind, J. D.; Staudt-Bickel, C.; Paul, D. R.; Koros, W. J. The effects of crosslinking chemistry on CO₂ plasticization of polyimide gas separation membranes. *Ind. Eng. Chem. Res.* **2002**, *41*, 6139–6148.
- (17) Donohue, M. D.; Minh, B. S.; Lee, S. Y. Permeation behavior of carbon dioxide-methane mixtures in cellulose acetate membranes. *J. Membr. Sci.* **1989**, *42*, 197–214.
- (18) Merkel, T. C.; Pinnau, I.; Prabhakar, R.; Freeman, B. D. Gas and vapor transport properties of perfluoropolymers. *Materials science of membranes for gas and vapor separation* **2006**, 251–270.
- (19) Rowe, B. W.; Freeman, B. D.; Paul, D. R. Physical aging of ultrathin glassy polymer films tracked by gas permeability. *Polymer* **2009**, *50*, 5565–5575.
- (20) Hillock, A. M. W.; Koros, W. J. Cross-Linkable Polyimide Membrane for Natural Gas Purification and Carbon Dioxide Plasticization Reduction. *Macromolecules* **2007**, *40*, 583–587.
- (21) Liu, Y.; Wang, R.; Chung, T.-S. Chemical cross-linking modification of polyimide membranes for gas separation. *J. Membr. Sci.* **2001**, *189*, 231–239.
- (22) Eldridge, R. B. Olefin/paraffin separation technology: a review. *Ind. Eng. Chem. Res.* **1993**, *32*, 2208–2212.
- (23) Merkel, T. C.; Zhou, M.; Baker, R. W. Carbon dioxide capture with membranes at an IGCC power plant. *J. Membr. Sci.* **2012**, *389*, 441–450.
- (24) Kohl, A.; Nielsen, R. *Gas Purification*; Elsevier: Houston, TX, 1997.
- (25) Lin, H.; Van Wagner, E.; Freeman, B. D.; Toy, L. G.; Gupta, R. P. Plasticization-enhanced hydrogen purification using polymeric membranes. *Science* **2006**, *311*, 639–642.
- (26) Stern, S. A. Polymers for gas separations: the next decade. *J. Membr. Sci.* **1994**, *94*, 1–65.
- (27) Ohya, H.; Kudryavsev, V.; Semenova, S. I. *Polyimide Membranes: Applications, Fabrications and Properties*; CRC Press: 1997.
- (28) Kumbharkar, S. C.; Liu, Y.; Li, K. High performance polybenzimidazole based asymmetric hollow fibre membranes for H₂/CO₂ separation. *J. Membr. Sci.* **2011**, *375*, 231–240.
- (29) Valtcheva, I. B.; Kumbharkar, S. C.; Kim, J. F.; Bhole, Y.; Livingston, A. G. Beyond polyimide: Crosslinked polybenzimidazole membranes for organic solvent nanofiltration (OSN) in harsh environments. *J. Membr. Sci.* **2014**, *457*, 62–72.
- (30) Borjigin, H.; Stevens, K. A.; Liu, R.; Moon, J. D.; Shaver, A. T.; Swinnea, S.; Freeman, B. D.; Riffle, J. S.; McGrath, J. E. Synthesis and characterization of polybenzimidazoles derived from tetraaminodiphenylsulfone for high temperature gas separation membranes. *Polymer* **2015**, *71*, 135–142.
- (31) da Silva Burgal, J.; Peeva, L.; Livingston, A. Negligible ageing in poly(ether-ether-ketone) membranes widens application range for solvent processing. *J. Membr. Sci.* **2017**, *525*, 48–56.
- (32) Vogel, H.; Marvel, C. S. Polybenzimidazoles, new thermally stable polymers. *J. Polym. Sci.* **1961**, *50*, 511–539.
- (33) Tena, A.; Marcos-Fernández, A.; Palacio, L.; Prádanos, P.; Lozano, A. E.; de Abajo, J.; Hernández, A. On the influence of the proportion of PEO in thermally controlled phase segregation of copoly(ether-imide)s for gas separation. *J. Membr. Sci.* **2013**, *434*, 26–34.
- (34) Luo, S.; Stevens, K. A.; Park, J. S.; Moon, J. D.; Liu, Q.; Freeman, B. D.; Guo, R. Highly CO₂-Selective Gas Separation Membranes Based on Segmented Copolymers of Poly(Ethylene oxide) Reinforced with Pentiptycene-Containing Polyimide Hard Segments. *ACS Appl. Mater. Interfaces* **2016**, *8*, 2306–2317.
- (35) Tena, A.; Marcos-Fernández, A.; Lozano, A. E.; de la Campa, J. G.; de Abajo, J.; Palacio, L.; Prádanos, P.; Hernández, A. Thermally Segregated Copolymers with PPO Blocks for Nitrogen Removal from Natural Gas. *Ind. Eng. Chem. Res.* **2013**, *52*, 4312–4322.
- (36) Stern, S.; Shah, V.; Hardy, B. Structure-permeability relationships in silicone polymers. *J. Polym. Sci., Part B: Polym. Phys.* **1987**, *25*, 1263–1298.
- (37) Baker, R. W. *Membrane Technology and Applications*; John Wiley and Sons: London, 2004.
- (38) Ghanem, B. S.; McKeown, N. B.; Budd, P. M.; Selbie, J. D.; Fritsch, D. High-performance membranes from polyimides with intrinsic microporosity. *Adv. Mater.* **2008**, *20*, 2766–2771.
- (39) Tanaka, K.; Kita, H.; Okano, M.; Okamoto, K.-i. Permeability and permselectivity of gases in fluorinated and non-fluorinated polyimides. *Polymer* **1992**, *33*, 585–592.
- (40) Rungta, M.; Xu, L.; Koros, W. J. Carbon molecular sieve dense film membranes derived from Matrimid® for ethylene/ethane separation. *Carbon* **2012**, *50*, 1488–1502.
- (41) Pechar, T. W.; Kim, S.; Vaughan, B.; Marand, E.; Tsapatsis, M.; Jeong, H. K.; Cornelius, C. J. Fabrication and characterization of polyimide–zeolite L mixed matrix membranes for gas separations. *J. Membr. Sci.* **2006**, *277*, 195–202.
- (42) Budd, P. M.; Ghanem, B. S.; Makhseed, S.; McKeown, N. B.; Msayib, K. J.; Tattershall, C. E. Polymers of intrinsic microporosity (PIMs): robust, solution-processable, organic nanoporous materials. *Chem. Commun.* **2004**, *2*, 230–231.
- (43) Nagai, K.; Masuda, T.; Nakagawa, T.; Freeman, B. D.; Pinnau, I. Poly [1-(trimethylsilyl)-1-propyne] and related polymers: synthesis, properties and functions. *Prog. Polym. Sci.* **2001**, *26*, 721–798.
- (44) Masuda, T.; Takahashi, T.; Higashimura, T. Polymerization of 1-phenyl-1-alkynes by halides of niobium and tantalum. *Macromolecules* **1985**, *18*, 311–317.
- (45) Lau, C. H.; Nguyen, P. T.; Hill, M. R.; Thornton, A. W.; Konstas, K.; Doherty, C. M.; Mulder, R. J.; Bourgeois, L.; Liu, A. C. Y.; Sprouster, D. J.; Sullivan, J. P.; Bastow, T. J.; Hill, A. J.; Gin, D. L.; Noble, R. D. Ending Aging in Super Glassy Polymer Membranes. *Angew. Chem., Int. Ed.* **2014**, *53*, 5322–5326.
- (46) Kelman, S. D.; Matteucci, S.; Bielawski, C. W.; Freeman, B. D. Crosslinking poly(1-trimethylsilyl-1-propyne) and its effect on solvent resistance and transport properties. *Polymer* **2007**, *48*, 6881–6892.
- (47) Raharjo, R. D.; Freeman, B. D.; Sanders, E. S. Pure and mixed gas CH₄ and n-C₄H₁₀ sorption and dilation in poly(1-trimethylsilyl-1-propyne). *Polymer* **2007**, *48*, 6097–6114.
- (48) Raharjo, R. D.; Freeman, B. D.; Paul, D. R.; Sanders, E. S. Pure and mixed gas CH₄ and n-C₄H₁₀ permeability and diffusivity in poly(1-trimethylsilyl-1-propyne). *Polymer* **2007**, *48*, 7329–7344.
- (49) Starannikova, L.; Pilipenko, M.; Belov, N.; Yampolskii, Y.; Gringolts, M.; Finkelshtein, E. Addition-type polynorbornene with Si(CH₃)₃ side groups: Detailed study of gas permeation and thermodynamic properties. *J. Membr. Sci.* **2008**, *323*, 134–143.

- (50) Galizia, M.; De Angelis, M. G.; Finkelshtein, E.; Yampolskii, Y. P.; Sarti, G. C. Sorption and transport of hydrocarbons and alcohols in addition-type poly(trimethyl silyl norbornene). I: Experimental data. *J. Membr. Sci.* **2011**, *385-386*, 141–153.
- (51) Galizia, M.; De Angelis, M. G.; Sarti, G. C. Sorption of hydrocarbons and alcohols in addition-type poly(trimethyl silyl norbornene) and other high free volume glassy polymers. II: NELF model predictions. *J. Membr. Sci.* **2012**, *405-406*, 201–211.
- (52) Vaughn, J. T.; Harrigan, D. J.; Sundell, B. J.; Lawrence, J. A.; Yang, J. Reverse selective glassy polymers for C₃⁺ hydrocarbon recovery from natural gas. *J. Membr. Sci.* **2017**, *522*, 68–76.
- (53) Thomas, S.; Pinnau, I.; Du, N.; Guiver, M. D. Pure- and mixed-gas permeation properties of a microporous spirobisindane-based ladder polymer (PIM-1). *J. Membr. Sci.* **2009**, *333*, 125–131.
- (54) Robeson, L. M.; Dose, M. E.; Freeman, B. D.; Paul, D. R. Analysis of the transport properties of thermally rearranged (TR) polymers and polymers of intrinsic microporosity (PIM) relative to upper bound performance. *J. Membr. Sci.* **2017**, *525*, 18–24.
- (55) Du, N.; Park, H. B.; Robertson, G. P.; Dal-Cin, M. M.; Visser, T.; Scoles, L.; Guiver, M. D. Polymer nanosieve membranes for CO₂-capture applications. *Nat. Mater.* **2011**, *10*, 372–375.
- (56) Ghanem, B. S.; McKeown, N. B.; Budd, P. M.; Al-Harbi, N. M.; Fritsch, D.; Heinrich, K.; Starannikova, L.; Tokarev, A.; Yampolskii, Y. Synthesis, Characterization, and Gas Permeation Properties of a Novel Group of Polymers with Intrinsic Microporosity: PIM-Polyimides. *Macromolecules* **2009**, *42*, 7881–7888.
- (57) Ma, X.; Pinnau, I. A novel intrinsically microporous ladder polymer and copolymers derived from 1,1[prime or minute],2,2[prime or minute]-tetrahydroxy-tetraphenylethylene for membrane-based gas separation. *Polym. Chem.* **2016**, *7*, 1244–1248.
- (58) Swaidan, R.; Ghanem, B.; Litwiller, E.; Pinnau, I. Physical Aging, Plasticization and Their Effects on Gas Permeation in “Rigid” Polymers of Intrinsic Microporosity. *Macromolecules* **2015**, *48*, 6553–6561.
- (59) Li, P.; Chung, T. S.; Paul, D. R. Gas sorption and permeation in PIM-1. *J. Membr. Sci.* **2013**, *432*, 50–57.
- (60) Scholes, C. A.; Jin, J.; Stevens, G. W.; Kentish, S. E. Competitive permeation of gas and water vapour in high free volume polymeric membranes. *J. Polym. Sci., Part B: Polym. Phys.* **2015**, *53*, 719–728.
- (61) Scholes, C. A.; Jin, J.; Stevens, G. W.; Kentish, S. E. Hydrocarbon solubility, permeability, and competitive sorption effects in polymer of intrinsic microporosity (PIM-1) membranes. *J. Polym. Sci., Part B: Polym. Phys.* **2016**, *54*, 397–404.
- (62) Luo, S.; Liu, Q.; Zhang, B.; Wiegand, J. R.; Freeman, B. D.; Guo, R. Pentiptycene-based polyimides with hierarchically controlled molecular cavity architecture for efficient membrane gas separation. *J. Membr. Sci.* **2015**, *480*, 20–30.
- (63) Weidman, J. R.; Luo, S.; Zhang, Q.; Guo, R. Structure Manipulation in Triptycene-Based Polyimides through Main Chain Geometry Variation and Its Effect on Gas Transport Properties. *Ind. Eng. Chem. Res.* **2017**, *56*, 1868–1879.
- (64) Ghanem, B. S.; Swaidan, R.; Litwiller, E.; Pinnau, I. Ultra-Microporous Triptycene-based Polyimide Membranes for High-Performance Gas Separation. *Adv. Mater.* **2014**, *26*, 3688–3692.
- (65) Wolfe, J. F.; Arnold, F. E. Rigid-rod polymers. 1. Synthesis and thermal properties of para-aromatic polymers with 2,6-benzobisoxazole units in the main chain. *Macromolecules* **1981**, *14*, 909–915.
- (66) Park, H. B.; Jung, C. H.; Lee, Y. M.; Hill, A. J.; Pas, S. J.; Mudie, S. T.; Van Wagner, E.; Freeman, B. D.; Cookson, D. J. Polymers with Cavities Tuned for Fast Selective Transport of Small Molecules and Ions. *Science* **2007**, *318*, 254–258.
- (67) Sanders, D. F.; Smith, Z. P.; Ribeiro, C. P.; Guo, R.; McGrath, J. E.; Paul, D. R.; Freeman, B. D. Gas permeability, diffusivity, and free volume of thermally rearranged polymers based on 3,3'-dihydroxy-4,4'-diamino-biphenyl (HAB) and 2,2'-bis-(3,4-dicarboxyphenyl) hexafluoropropane dianhydride (6FDA). *J. Membr. Sci.* **2012**, *409-410*, 232–241.
- (68) Smith, Z. P.; Sanders, D. F.; Ribeiro, C. P.; Guo, R.; Freeman, B. D.; Paul, D. R.; McGrath, J. E.; Swinnea, S. Gas sorption and characterization of thermally rearranged polyimides based on 3,3'-dihydroxy-4,4'-diamino-biphenyl (HAB) and 2,2'-bis-(3,4-dicarboxyphenyl) hexafluoropropane dianhydride (6FDA). *J. Membr. Sci.* **2012**, *415-416*, 558–567.
- (69) Jiang, Y.; Willmore, F. T.; Sanders, D.; Smith, Z. P.; Ribeiro, C. P.; Doherty, C. M.; Thornton, A.; Hill, A. J.; Freeman, B. D.; Sanchez, I. C. Cavity size, sorption and transport characteristics of thermally rearranged (TR) polymers. *Polymer* **2011**, *52*, 2244–2254.
- (70) Galizia, M.; Stevens, K. A.; Smith, Z. P.; Paul, D. R.; Freeman, B. D. Nonequilibrium Lattice Fluid Modeling of Gas Solubility in HAB-6FDA Polyimide and Its Thermally Rearranged Analogues. *Macromolecules* **2016**, *49*, 8768–8779.
- (71) Galizia, M.; Stevens, K. A.; Paul, D. R.; Freeman, B. D. Modeling gas permeability and diffusivity in HAB-6FDA polyimide and its thermally rearranged analogs. *J. Membr. Sci.* **2017**, *537*, 83–92.
- (72) Gleason, K. L.; Smith, Z. P.; Liu, Q.; Paul, D. R.; Freeman, B. D. Pure- and mixed-gas permeation of CO₂ and CH₄ in thermally rearranged polymers based on 3,3'-dihydroxy-4,4'-diamino-biphenyl (HAB) and 2,2'-bis-(3,4-dicarboxyphenyl) hexafluoropropane dianhydride (6FDA). *J. Membr. Sci.* **2015**, *475*, 204–214.
- (73) Liu, Q.; Galizia, M.; Gleason, K. L.; Scholes, C. A.; Paul, D. R.; Freeman, B. D. Influence of toluene on CO₂ and CH₄ gas transport properties in thermally rearranged (TR) polymers based on 3,3'-dihydroxy-4,4'-diamino-biphenyl (HAB) and 2,2'-bis-(3,4-dicarboxyphenyl) hexafluoropropane dianhydride (6FDA). *J. Membr. Sci.* **2016**, *514*, 282–293.
- (74) Wang, H.; Chung, T.-S.; Paul, D. R. Physical aging and plasticization of thick and thin films of the thermally rearranged ortho-functional polyimide 6FDA-HAB. *J. Membr. Sci.* **2014**, *458*, 27–35.
- (75) Wang, H.; Chung, T.-S.; Paul, D. R. Thickness dependent thermal rearrangement of an ortho-functional polyimide. *J. Membr. Sci.* **2014**, *450*, 308–312.
- (76) Liu, Q.; Paul, D. R.; Freeman, B. D. Gas permeation and mechanical properties of thermally rearranged (TR) copolyimides. *Polymer* **2016**, *82*, 378–391.
- (77) Kushwaha, A.; Dose, M. E.; Smith, Z. P.; Luo, S.; Freeman, B. D.; Guo, R. Preparation and properties of polybenzoxazole-based gas separation membranes: A comparative study between thermal rearrangement (TR) of poly(hydroxyimide) and thermal cyclodehydration of poly(hydroxyamide). *Polymer* **2015**, *78*, 81–93.
- (78) Budd, P. M.; Msayib, K. J.; Tattershall, C. E.; Ghanem, B. S.; Reynolds, K. J.; McKeown, N. B.; Fritsch, D. Gas separation membranes from polymers of intrinsic microporosity. *J. Membr. Sci.* **2005**, *251*, 263–269.
- (79) Ma, X.; Swaidan, R.; Belmabkhout, Y.; Zhu, Y.; Litwiller, E.; Jouiad, M.; Pinnau, I.; Han, Y. Synthesis and Gas Transport Properties of Hydroxyl-Functionalized Polyimides with Intrinsic Microporosity. *Macromolecules* **2012**, *45*, 3841–3849.
- (80) Fritsch, D.; Bengtson, G.; Carta, M.; McKeown, N. B. Synthesis and Gas Permeation Properties of Spirobischromane-Based Polymers of Intrinsic Microporosity. *Macromol. Chem. Phys.* **2011**, *212*, 1137–1146.
- (81) Han, J. Y.; Lee, J. Y.; Kim, H. J.; Kim, M. H.; Han, S. G.; Jang, J. H.; Cho, E.; Yoo, S. J.; Henkensmeier, D. Synthesis and characterization of fluorene-based polybenzimidazole copolymer for gas separation. *J. Appl. Polym. Sci.* **2014**, *131*, 40521.
- (82) Cabasso, I.; Klein, E.; Smith, J. K. Polysulfone hollow fibers. I. Spinning and properties. *J. Appl. Polym. Sci.* **1976**, *20*, 2377–2394.
- (83) Scholes, C. A.; Ribeiro, C. P.; Kentish, S. E.; Freeman, B. D. Thermal rearranged poly(benzoxazole)/polyimide blended membranes for CO₂ separation. *Sep. Purif. Technol.* **2014**, *124*, 134–140.
- (84) Sur, G. S.; Sun, H. L.; Lyu, S. G.; Mark, J. E. Synthesis, structure, mechanical properties, and thermal stability of some polysulfone/organoclay nanocomposites. *Polymer* **2001**, *42*, 9783–9789.
- (85) Zhang, Y.; Musselman, I. H.; Ferraris, J. P.; Balkus, K. J. Gas permeability properties of Matrimid® membranes containing the metal-organic framework Cu-BPY-HFS. *J. Membr. Sci.* **2008**, *313*, 170–181.
- (86) Hägg, M.-B.; Quinn, R. Polymeric Facilitated Transport Membranes for Hydrogen Purification. *MRS Bull.* **2006**, *31*, 750–755.
- (87) Deng, L.; Kim, T.-J.; Hägg, M.-B. Facilitated transport of CO₂ in novel PVAm/PVA blend membrane. *J. Membr. Sci.* **2009**, *340*, 154–163.

- (88) LeBlanc, O. H.; Ward, W. J.; Matson, S. L.; Kimura, S. G. Facilitated transport in ion-exchange membranes. *J. Membr. Sci.* **1980**, *6*, 339–343.
- (89) Scholander, P. F. Oxygen Transport through Hemoglobin Solutions. *Science* **1960**, *131* (3400), 585.
- (90) Ward, W. J.; Robb, W. L. Carbon Dioxide-Oxygen Separation: Facilitated Transport of Carbon Dioxide across a Liquid Film. *Science* **1967**, *156*, 1481–1484.
- (91) Hughes, R.; Steigelmann, E. Process for separation of unsaturated hydrocarbons. Google Patents, 1973.
- (92) Huang, J.; Zou, J.; Ho, W. S. W. Carbon Dioxide Capture Using a CO₂-Selective Facilitated Transport Membrane. *Ind. Eng. Chem. Res.* **2008**, *47*, 1261–1267.
- (93) Peng, D.; Liu, Y.; Wang, S.; Tian, Z.; Xin, Q.; Wu, H.; Chen, J.; Jiang, Z. Facilitated transport membranes by incorporating different divalent metal ions as CO₂ carriers. *RSC Adv.* **2016**, *6*, 65282–65290.
- (94) Takht Ravanchi, M.; Kaghazchi, T.; Kargari, A. Application of membrane separation processes in petrochemical industry: a review. *Desalination* **2009**, *235*, 199–244.
- (95) Ryu, J. H.; Lee, H.; Kim, Y. J.; Kang, Y. S.; Kim, H. S. Facilitated Olefin Transport by Reversible Olefin Coordination to Silver Ions in a Dry Cellulose Acetate Membrane. *Chem. - Eur. J.* **2001**, *7*, 1525–1529.
- (96) Park, Y. S.; Won, J.; Kang, Y. S. Facilitated transport of olefin through solid PAAm and PAAm-graft composite membranes with silver ions. *J. Membr. Sci.* **2001**, *183*, 163–170.
- (97) Tome, L. C.; Mecerreyes, D.; Freire, C. S. R.; Rebelo, L. P. N.; Marrucho, I. M. Polymeric ionic liquid membranes containing IL-Ag⁺ for ethylene/ethane separation via olefin-facilitated transport. *J. Mater. Chem. A* **2014**, *2*, 5631–5639.
- (98) Merkel, T. C.; Blanc, R.; Ciobanu, L.; Firat, B.; Suwarlim, A.; Zeid, J. Silver salt facilitated transport membranes for olefin/paraffin separations: Carrier instability and a novel regeneration method. *J. Membr. Sci.* **2013**, *447*, 177–189.
- (99) Kuraoka, K.; Chujo, Y.; Yazawa, T. A novel inorganic-organic hybrid membrane for oxygen/nitrogen separation containing a cobalt(II) Schiff base complex as oxygen carrier using poly(N-vinylpyrrolidone) as mediator. *Chem. Commun.* **2000**, *24*, 2477–2478.
- (100) Drago, R. S.; Balkus, K. J., Jr. Cobalt (II)-facilitated transport of dioxygen in a polystyrene membrane. *Inorg. Chem.* **1986**, *25*, 716–718.
- (101) Yang, J. M.; Hsiue, G. H. Epoxidized styrene-butadiene-styrene block copolymer membrane complexes with cobalt schiff bases for oxygen permeation. *Macromolecules* **1991**, *24*, 4010–4016.
- (102) Park, S.; Mathur, V. K.; Planalp, R. P. Syntheses, solubilities and oxygen absorption properties of new cobalt(II) Schiff-base complexes. *Polyhedron* **1998**, *17*, 325–330.
- (103) Maxwell, J. C. *A Treatise on Electricity and Magnetism*; Clarendon Press: Oxford, 1873; p 2 v.
- (104) Vu, D. Q.; Koros, W. J.; Miller, S. J. Mixed matrix membranes using carbon molecular sieves: II. Modeling permeation behavior. *J. Membr. Sci.* **2003**, *211*, 335–348.
- (105) Gonzo, E. E.; Parentis, M. L.; Gottifredi, J. C. Estimating models for predicting effective permeability of mixed matrix membranes. *J. Membr. Sci.* **2006**, *277*, 46–54.
- (106) Hashemifard, S. A.; Ismail, A. F.; Matsuura, T. Prediction of gas permeability in mixed matrix membranes using theoretical models. *J. Membr. Sci.* **2010**, *347*, 53–61.
- (107) Keskin, S.; Sholl, D. S. Selecting metal organic frameworks as enabling materials in mixed matrix membranes for high efficiency natural gas purification. *Energy Environ. Sci.* **2010**, *3*, 343–351.
- (108) Zornoza, B.; Tellez, C.; Coronas, J.; Gascon, J.; Kapteijn, F. Metal organic framework based mixed matrix membranes: An increasingly important field of research with a large application potential. *Microporous Mesoporous Mater.* **2013**, *166*, 67–78.
- (109) Vinh-Thang, H.; Kaliaguine, S. Predictive Models for Mixed-Matrix Membrane Performance: A Review. *Chem. Rev. (Washington, DC, U. S.)* **2013**, *113*, 4980–5028.
- (110) Dong, G.; Li, H.; Chen, V. Challenges and opportunities for mixed-matrix membranes for gas separation. *J. Mater. Chem. A* **2013**, *1*, 4610–4630.
- (111) Rodenas, T.; Luz, I.; Prieto, G.; Seoane, B.; Miro, H.; Corma, A.; Kapteijn, F.; Llabrés i Xamena, F. X.; Gascon, J. Metal-organic framework nanosheets in polymer composite materials for gas separation. *Nat. Mater.* **2014**, *14*, 48–55.
- (112) Kang, D.-Y.; Jones, C. W.; Nair, S. Modeling molecular transport in composite membranes with tubular fillers. *J. Membr. Sci.* **2011**, *381*, 50–63.
- (113) Berean, K. J.; Ou, J. Z.; Nour, M.; Field, M. R.; Alsaif, M. M. Y. A.; Wang, Y.; Ramanathan, R.; Bansal, V.; Kentish, S.; Doherty, C. M.; Hill, A. J.; McSweeney, C.; Kaner, R. B.; Kalantar-zadeh, K. Enhanced Gas Permeation through Graphene Nanocomposites. *J. Phys. Chem. C* **2015**, *119*, 13700–13712.
- (114) Checchetto, R.; Miotello, A.; Nicolais, L.; Carotenuto, G. Gas transport through nanocomposite membrane composed by polyethylene with dispersed graphite nanoplatelets. *J. Membr. Sci.* **2014**, *463*, 196–204.
- (115) Tzeng, P.; Stevens, B.; Devlaming, I.; Grunlan, J. C. Polymer-Graphene Oxide Quadlayer Thin-Film Assemblies with Improved Gas Barrier. *Langmuir* **2015**, *31*, 5919–5927.
- (116) Japip, S.; Xiao, Y.; Chung, T.-S. Particle-Size Effects on Gas Transport Properties of 6FDA-Durene/ZIF-71 Mixed Matrix Membranes. *Ind. Eng. Chem. Res.* **2016**, *55*, 9507–9517.
- (117) Gheimasi, K. M.; Peydayesh, M.; Mohammadi, T.; Bakhtiari, O. Prediction of CO₂/CH₄ permeability through Sigma-1-Matrimid@5218 MMMs using the Maxwell model. *J. Membr. Sci.* **2014**, *466*, 265–273.
- (118) Barrer, R. M. 33. Synthesis of a zeolitic mineral with chabazite-like sorptive properties. *J. Chem. Soc.* **1948**, No. 0, 127–132.
- (119) Barrer, R. M. Zeolites and their synthesis. *Zeolites* **1981**, *1*, 130–140.
- (120) Mahajan, R.; Koros, W. J. Mixed matrix membrane materials with glassy polymers. Part 1. *Polym. Eng. Sci.* **2002**, *42*, 1420–1431.
- (121) Mahajan, R.; Koros, W. J. Mixed matrix membrane materials with glassy polymers. Part 2. *Polym. Eng. Sci.* **2002**, *42*, 1432–1441.
- (122) Hussain, M.; König, A. Mixed-Matrix Membrane for Gas Separation: Polydimethylsiloxane Filled with Zeolite. *Chem. Eng. Technol.* **2012**, *35*, 561–569.
- (123) Dahe, G. J.; Teotia, R. S.; Bellare, J. R. The role of zeolite nanoparticles additive on morphology, mechanical properties and performance of polysulfone hollow fiber membranes. *Chem. Eng. J.* **2012**, *197*, 398–406.
- (124) Zhang, Y.; Balkus, K. J., Jr.; Musselman, I. H.; Ferraris, J. P. Mixed-matrix membranes composed of Matrimid® and mesoporous ZSM-5 nanoparticles. *J. Membr. Sci.* **2008**, *325*, 28–39.
- (125) Jeong, B.-H.; Hoek, E. M. V.; Yan, Y.; Subramani, A.; Huang, X.; Hurwitz, G.; Ghosh, A. K.; Jawor, A. Interfacial polymerization of thin film nanocomposites: A new concept for reverse osmosis membranes. *J. Membr. Sci.* **2007**, *294*, 1–7.
- (126) Jia, M.-D.; Pleinmann, K.-V.; Behling, R.-D. Preparation and characterization of thin-film zeolite-PDMS composite membranes. *J. Membr. Sci.* **1992**, *73*, 119–128.
- (127) Wang, H.; Holmberg, B. A.; Yan, Y. Homogeneous polymer-zeolite nanocomposite membranes by incorporating dispersible template-removed zeolite nanocrystals. *J. Mater. Chem.* **2002**, *12*, 3640–3643.
- (128) Mohammad Gheimasi, K.; Mohammadi, T.; Bakhtiari, O. Modification of ideal MMMs permeation prediction models: Effects of partial pore blockage and polymer chain rigidification. *J. Membr. Sci.* **2013**, *427*, 399–410.
- (129) Paul, D. R.; Koros, W. J. Effect of partially immobilizing sorption on permeability and the diffusion time lag. *J. Polym. Sci., Polym. Phys. Ed.* **1976**, *14*, 675–685.
- (130) Paul, D. R.; Kemp, D. R. The diffusion time lag in polymer membranes containing adsorptive fillers. *J. Polym. Sci., Polym. Symp.* **1973**, *41*, 79–93.
- (131) Keizer, K.; Burggraaf, A. J.; Vroon, Z. A. E. P.; Verweij, H. Two component permeation through thin zeolite MFI membranes. *J. Membr. Sci.* **1998**, *147*, 159–172.

- (132) Thornton, A. W.; Dubbeldam, D.; Liu, M. S.; Ladewig, B. P.; Hill, A. J.; Hill, M. R. Feasibility of zeolitic imidazolate framework membranes for clean energy applications. *Energy Environ. Sci.* **2012**, *5*, 7637–7646.
- (133) Furukawa, H.; Cordova, K. E.; O’Keeffe, M.; Yaghi, O. M. The Chemistry and Applications of Metal-Organic Frameworks. *Science* **2013**, *341*, 1230444.
- (134) Park, K. S.; Ni, Z.; Côté, A. P.; Choi, J. Y.; Huang, R.; Uribe-Romo, F. J.; Chae, H. K.; O’Keeffe, M.; Yaghi, O. M. Exceptional chemical and thermal stability of zeolitic imidazolate frameworks. *Proc. Natl. Acad. Sci. U. S. A.* **2006**, *103*, 10186–10191.
- (135) Wong-Foy, A. G.; Matzger, A. J.; Yaghi, O. M. Exceptional H₂ Saturation Uptake in Microporous Metal–Organic Frameworks. *J. Am. Chem. Soc.* **2006**, *128*, 3494–3495.
- (136) Liu, Y.; Her, J.-H.; Dailly, A.; Ramirez-Cuesta, A. J.; Neumann, D. A.; Brown, C. M. Reversible Structural Transition in MIL-53 with Large Temperature Hysteresis. *J. Am. Chem. Soc.* **2008**, *130*, 11813–11818.
- (137) Llewellyn, P. L.; Bourrelly, S.; Serre, C.; Vimont, A.; Daturi, M.; Hamon, L.; De Weireld, G.; Chang, J.-S.; Hong, D.-Y.; Kyu Hwang, Y.; Hwa Jhung, S.; Férey, G. High Uptakes of CO₂ and CH₄ in Mesoporous Metal–Organic Frameworks MIL-100 and MIL-101. *Langmuir* **2008**, *24*, 7245–7250.
- (138) Geier, S. J.; Mason, J. A.; Bloch, E. D.; Queen, W. L.; Hudson, M. R.; Brown, C. M.; Long, J. R. Selective adsorption of ethylene over ethane and propylene over propane in the metal-organic frameworks M2(dobdc) (M = Mg, Mn, Fe, Co, Ni, Zn). *Chem. Sci.* **2013**, *4*, 2054–2061.
- (139) Kandiah, M.; Nilsen, M. H.; Usseglio, S.; Jakobsen, S.; Olsbye, U.; Tilset, M.; Larabi, C.; Quadrelli, E. A.; Bonino, F.; Lillerud, K. P. Synthesis and Stability of Tagged UiO-66 Zr-MOFs. *Chem. Mater.* **2010**, *22*, 6632–6640.
- (140) Katz, M. J.; Brown, Z. J.; Colon, Y. J.; Siu, P. W.; Scheidt, K. A.; Snurr, R. Q.; Hupp, J. T.; Farha, O. K. A facile synthesis of UiO-66, UiO-67 and their derivatives. *Chem. Commun.* **2013**, *49*, 9449–9451.
- (141) Queen, W. L.; Hudson, M. R.; Bloch, E. D.; Mason, J. A.; Gonzalez, M. L.; Lee, J. S.; Gygi, D.; Howe, J. D.; Lee, K.; Darwish, T. A.; James, M.; Peterson, V. K.; Teat, S. J.; Smit, B.; Neaton, J. B.; Long, J. R.; Brown, C. M. Comprehensive study of carbon dioxide adsorption in the metal-organic frameworks M2(dobdc) (M = Mg, Mn, Fe, Co, Ni, Cu, Zn). *Chem. Sci.* **2014**, *5*, 4569–4581.
- (142) Sumida, K.; Rogow, D. L.; Mason, J. A.; McDonald, T. M.; Bloch, E. D.; Herm, Z. R.; Bae, T.-H.; Long, J. R. Carbon Dioxide Capture in Metal–Organic Frameworks. *Chem. Rev.* **2012**, *112*, 724–781.
- (143) Yang, Q.; Wiersum, A. D.; Jobic, H.; Guillerm, V.; Serre, C.; Llewellyn, P. L.; Maurin, G. Understanding the Thermodynamic and Kinetic Behavior of the CO₂/CH₄ Gas Mixture within the Porous Zirconium Terephthalate UiO-66(Zr): A Joint Experimental and Modeling Approach. *J. Phys. Chem. C* **2011**, *115*, 13768–13774.
- (144) Peralta, D.; Chaplais, G.; Simon-Masseron, A.; Barthelet, K.; Pirngruber, G. D. Separation of C6 Paraffins Using Zeolitic Imidazolate Frameworks: Comparison with Zeolite 5A. *Ind. Eng. Chem. Res.* **2012**, *51*, 4692–4702.
- (145) Casco, M. E.; Cheng, Y. Q.; Daemen, L. L.; Fairen-Jimenez, D.; Ramos-Fernandez, E. V.; Ramirez-Cuesta, A. J.; Silvestre-Albero, J. Gate-opening effect in ZIF-8: the first experimental proof using inelastic neutron scattering. *Chem. Commun.* **2016**, *52*, 3639–3642.
- (146) Fairen-Jimenez, D.; Moggach, S. A.; Wharmby, M. T.; Wright, P. A.; Parsons, S.; Düren, T. Opening the Gate: Framework Flexibility in ZIF-8 Explored by Experiments and Simulations. *J. Am. Chem. Soc.* **2011**, *133*, 8900–8902.
- (147) Zhang, C.; Dai, Y.; Johnson, J. R.; Karvan, O.; Koros, W. J. High performance ZIF-8/6FDA-DAM mixed matrix membrane for propylene/propane separations. *J. Membr. Sci.* **2012**, *389*, 34–42.
- (148) Song, Q.; Nataraj, S. K.; Roussanova, M. V.; Tan, J. C.; Hughes, D. J.; Li, W.; Bourgoin, P.; Alam, M. A.; Cheetham, A. K.; Al-Muhtaseb, S. A.; Sivaniah, E. Zeolitic imidazolate framework (ZIF-8) based polymer nanocomposite membranes for gas separation. *Energy Environ. Sci.* **2012**, *5*, 8359–8369.
- (149) Japip, S.; Wang, H.; Xiao, Y.; Shung Chung, T. Highly permeable zeolitic imidazolate framework (ZIF)-71 nano-particles enhanced polyimide membranes for gas separation. *J. Membr. Sci.* **2014**, *467*, 162–174.
- (150) Chui, S. S.-Y.; Lo, S. M.-F.; Charmant, J. P. H.; Orpen, A. G.; Williams, I. D. A Chemically Functionalizable Nanoporous Material [Cu₃(TMA)₂(H₂O)₃]_n. *Science* **1999**, *283*, 1148–1150.
- (151) Al-Janabi, N.; Hill, P.; Torrente-Murciano, L.; Garforth, A.; Gorgojo, P.; Siperstein, F.; Fan, X. Mapping the Cu-BTC metal–organic framework (HKUST-1) stability envelope in the presence of water vapour for CO₂ adsorption from flue gases. *Chem. Eng. J.* **2015**, *281*, 669–677.
- (152) Sorribas, S.; Kudasheva, A.; Almendro, E.; Zornoza, B.; de la Iglesia, Ó.; Téllez, C.; Coronas, J. Pervaporation and membrane reactor performance of polyimide based mixed matrix membranes containing MOF HKUST-1. *Chem. Eng. Sci.* **2015**, *124*, 37–44.
- (153) Kim, H. K.; Yun, W. S.; Kim, M.-B.; Kim, J. Y.; Bae, Y.-S.; Lee, J.; Jeong, N. C. A Chemical Route to Activation of Open Metal Sites in the Copper-Based Metal–Organic Framework Materials HKUST-1 and Cu-MOF-2. *J. Am. Chem. Soc.* **2015**, *137*, 10009–10015.
- (154) Basu, S.; Cano-Odena, A.; Vankelecom, I. F. J. Asymmetric Matrimid@[Cu₃(BTC)₂] mixed-matrix membranes for gas separations. *J. Membr. Sci.* **2010**, *362*, 478–487.
- (155) Lin, R.; Ge, L.; Diao, H.; Rudolph, V.; Zhu, Z. Ionic Liquids as the MOFs/Polymer Interfacial Binder for Efficient Membrane Separation. *ACS Appl. Mater. Interfaces* **2016**, *8*, 32041–32049.
- (156) DeCoste, J. B.; Denny, M. S., Jr.; Peterson, G. W.; Mahle, J. J.; Cohen, S. M. Enhanced aging properties of HKUST-1 in hydrophobic mixed-matrix membranes for ammonia adsorption. *Chem. Sci.* **2016**, *7*, 2711–2716.
- (157) Boutin, A.; Coudert, F.-X.; Springuel-Huet, M.-A.; Neimark, A. V.; Férey, G.; Fuchs, A. H. The Behavior of Flexible MIL-53(Al) upon CH₄ and CO₂ Adsorption. *J. Phys. Chem. C* **2010**, *114*, 22237–22244.
- (158) Bourrelly, S.; Moulin, B.; Rivera, A.; Maurin, G.; Devautour-Vinot, S.; Serre, C.; Devic, T.; Horcajada, P.; Vimont, A.; Clet, G.; Daturi, M.; Lavalley, J.-C.; Loera-Serna, S.; Denoyel, R.; Llewellyn, P. L.; Férey, G. Explanation of the Adsorption of Polar Vapors in the Highly Flexible Metal Organic Framework MIL-53(Cr). *J. Am. Chem. Soc.* **2010**, *132*, 9488–9498.
- (159) Llewellyn, P. L.; Horcajada, P.; Maurin, G.; Devic, T.; Rosenbach, N.; Bourrelly, S.; Serre, C.; Vincent, D.; Loera-Serna, S.; Filinchuk, Y.; Férey, G. Complex Adsorption of Short Linear Alkanes in the Flexible Metal-Organic-Framework MIL-53(Fe). *J. Am. Chem. Soc.* **2009**, *131*, 13002–13008.
- (160) Chen, L.; Mowat, J. P. S.; Fairen-Jimenez, D.; Morrison, C. A.; Thompson, S. P.; Wright, P. A.; Düren, T. Elucidating the Breathing of the Metal–Organic Framework MIL-53(Sc) with ab Initio Molecular Dynamics Simulations and in Situ X-ray Powder Diffraction Experiments. *J. Am. Chem. Soc.* **2013**, *135*, 15763–15773.
- (161) Volkringer, C.; Loiseau, T.; Guillou, N.; Férey, G.; Elkaim, E.; Vimont, A. XRD and IR structural investigations of a particular breathing effect in the MOF-type gallium terephthalate MIL-53(Ga). *Dalton Trans.* **2009**, *12*, 2241–2249.
- (162) Serre, C.; Millange, F.; Thouvenot, C.; Noguès, M.; Marsolier, G.; Louër, D.; Férey, G. Very Large Breathing Effect in the First Nanoporous Chromium(III)-Based Solids: MIL-53 or Cr^{III}(OH)·{O₂C–C₆H₄–CO₂}·xH₂O. *J. Am. Chem. Soc.* **2002**, *124*, 13519–13526.
- (163) Loiseau, T.; Serre, C.; Huguénard, C.; Fink, G.; Taulelle, F.; Henry, M.; Bataille, T.; Férey, G. A Rationale for the Large Breathing of the Porous Aluminum Terephthalate (MIL-53) Upon Hydration. *Chem. - Eur. J.* **2004**, *10*, 1373–1382.
- (164) Boutin, A.; Springuel-Huet, M.-A.; Nossov, A.; Gédéon, A.; Loiseau, T.; Volkringer, C.; Férey, G.; Coudert, F.-X.; Fuchs, A. H. Breathing Transitions in MIL-53(Al) Metal–Organic Framework Upon Xenon Adsorption. *Angew. Chem., Int. Ed.* **2009**, *48*, 8314–8317.
- (165) Serre, C.; Bourrelly, S.; Vimont, A.; Ramsahye, N. A.; Maurin, G.; Llewellyn, P. L.; Daturi, M.; Filinchuk, Y.; Leynaud, O.; Barnes, P.; Férey, G. An Explanation for the Very Large Breathing Effect of a

Metal–Organic Framework during CO₂ Adsorption. *Adv. Mater.* **2007**, *19*, 2246–2251.

(166) Coudert, F.-X.; Boutin, A.; Fuchs, A. H.; Neimark, A. V. Adsorption Deformation and Structural Transitions in Metal–Organic Frameworks: From the Unit Cell to the Crystal. *J. Phys. Chem. Lett.* **2013**, *4*, 3198–3205.

(167) Férey, G.; Mellot-Draznieks, C.; Serre, C.; Millange, F.; Dutour, J.; Surblé, S.; Margiolaki, I. A Chromium Terephthalate-Based Solid with Unusually Large Pore Volumes and Surface Area. *Science* **2005**, *309*, 2040–2042.

(168) Férey, G.; Mellot-Draznieks, C.; Serre, C.; Millange, F. Crystallized Frameworks with Giant Pores: Are There Limits to the Possible? *Acc. Chem. Res.* **2005**, *38*, 217–225.

(169) Bhattacharjee, S.; Chen, C.; Ahn, W.-S. Chromium terephthalate metal-organic framework MIL-101: synthesis, functionalization, and applications for adsorption and catalysis. *RSC Adv.* **2014**, *4*, 52500–52525.

(170) Henschel, A.; Gedrich, K.; Kraehnert, R.; Kaskel, S. Catalytic properties of MIL-101. *Chem. Commun.* **2008**, *35*, 4192–4194.

(171) Rodenas, T.; van Dalen, M.; García-Pérez, E.; Serra-Crespo, P.; Zornoza, B.; Kapteijn, F.; Gascon, J. Visualizing MOF Mixed Matrix Membranes at the Nanoscale: Towards Structure-Performance Relationships in CO₂/CH₄ Separation Over NH₂-MIL-53(Al)@PI. *Adv. Funct. Mater.* **2014**, *24*, 249–256.

(172) Sabetghadam, A.; Seoane, B.; Keskin, D.; Duim, N.; Rodenas, T.; Shahid, S.; Sorribas, S.; Guillouzer, C. L.; Clet, G.; Tellez, C.; Daturi, M.; Coronas, J.; Kapteijn, F.; Gascon, J. Metal Organic Framework Crystals in Mixed-Matrix Membranes: Impact of the Filler Morphology on the Gas Separation Performance. *Adv. Funct. Mater.* **2016**, *26*, 3154–3163.

(173) Xin, Q.; Ouyang, J.; Liu, T.; Li, Z.; Li, Z.; Liu, Y.; Wang, S.; Wu, H.; Jiang, Z.; Cao, X. Enhanced Interfacial Interaction and CO₂ Separation Performance of Mixed Matrix Membrane by Incorporating Polyethylenimine-Decorated Metal–Organic Frameworks. *ACS Appl. Mater. Interfaces* **2015**, *7*, 1065–1077.

(174) Rosi, N. L.; Kim, J.; Eddaoudi, M.; Chen, B.; O’Keeffe, M.; Yaghi, O. M. Rod Packings and Metal–Organic Frameworks Constructed from Rod-Shaped Secondary Building Units. *J. Am. Chem. Soc.* **2005**, *127*, 1504–1518.

(175) Millward, A. R.; Yaghi, O. M. Metal–Organic Frameworks with Exceptionally High Capacity for Storage of Carbon Dioxide at Room Temperature. *J. Am. Chem. Soc.* **2005**, *127*, 17998–17999.

(176) Britt, D.; Furukawa, H.; Wang, B.; Glover, T. G.; Yaghi, O. M. Highly efficient separation of carbon dioxide by a metal-organic framework replete with open metal sites. *Proc. Natl. Acad. Sci. U. S. A.* **2009**, *106*, 20637–20640.

(177) Bae, Y.-S.; Lee, C. Y.; Kim, K. C.; Farha, O. K.; Nickias, P.; Hupp, J. T.; Nguyen, S. T.; Snurr, R. Q. High Propene/Propane Selectivity in Isostructural Metal–Organic Frameworks with High Densities of Open Metal Sites. *Angew. Chem., Int. Ed.* **2012**, *51*, 1857–1860.

(178) Wu, H.; Zhou, W.; Yildirim, T. High-Capacity Methane Storage in Metal–Organic Frameworks M2(dhtp): The Important Role of Open Metal Sites. *J. Am. Chem. Soc.* **2009**, *131*, 4995–5000.

(179) Bachman, J. E.; Long, J. R. Plasticization-resistant Ni₂(dobdc)/polyimide composite membranes for the removal of CO₂ from natural gas. *Energy Environ. Sci.* **2016**, *9*, 2031–2036.

(180) Bachman, J. E.; Smith, Z. P.; Li, T.; Xu, T.; Long, J. R. Enhanced ethylene separation and plasticization resistance in polymer membranes incorporating metal-organic framework nanocrystals. *Nat. Mater.* **2016**, *15*, 845–849.

(181) McDonald, T. M.; Mason, J. A.; Kong, X.; Bloch, E. D.; Gygi, D.; Dani, A.; Crocella, V.; Giordanino, F.; Odoh, S. O.; Drisdell, W. S.; Vlaisavljevich, B.; Dzubak, A. L.; Poloni, R.; Schnell, S. K.; Planas, N.; Lee, K.; Pascal, T.; Wan, L. F.; Prendergast, D.; Neaton, J. B.; Smit, B.; Kortricht, J. B.; Gagliardi, L.; Bordiga, S.; Reimer, J. A.; Long, J. R. Cooperative insertion of CO₂ in diamine-appended metal-organic frameworks. *Nature* **2015**, *519*, 303–308.

(182) Cavka, J. H.; Jakobsen, S.; Olsbye, U.; Guillou, N.; Lamberti, C.; Bordiga, S.; Lillerud, K. P. A New Zirconium Inorganic Building Brick

Forming Metal Organic Frameworks with Exceptional Stability. *J. Am. Chem. Soc.* **2008**, *130*, 13850–13851.

(183) Nguyen, H. G. T.; Schweitzer, N. M.; Chang, C.-Y.; Drake, T. L.; So, M. C.; Stair, P. C.; Farha, O. K.; Hupp, J. T.; Nguyen, S. T. Vanadium-Node-Functionalized UiO-66: A Thermally Stable MOF-Supported Catalyst for the Gas-Phase Oxidative Dehydrogenation of Cyclohexene. *ACS Catal.* **2014**, *4*, 2496–2500.

(184) Piscopo, C.; Polyzoidis, A.; Schwarzer, M.; Loebbecke, S. Stability of UiO-66 under acidic treatment: Opportunities and limitations for post-synthetic modifications. *Microporous Mesoporous Mater.* **2015**, *208*, 30–35.

(185) Liu, X.; Demir, N. K.; Wu, Z.; Li, K. Highly Water-Stable Zirconium Metal–Organic Framework UiO-66 Membranes Supported on Alumina Hollow Fibers for Desalination. *J. Am. Chem. Soc.* **2015**, *137*, 6999–7002.

(186) Anjum, M. W.; Vermoortele, F.; Khan, A. L.; Bueken, B.; De Vos, D. E.; Vankelecom, I. F. J. Modulated UiO-66-Based Mixed-Matrix Membranes for CO₂ Separation. *ACS Appl. Mater. Interfaces* **2015**, *7*, 25193–25201.

(187) Venna, S. R.; Lartey, M.; Li, T.; Spore, A.; Kumar, S.; Nulwala, H. B.; Luebke, D. R.; Rosi, N. L.; Albenze, E. Fabrication of MMMs with improved gas separation properties using externally-functionalized MOF particles. *J. Mater. Chem. A* **2015**, *3*, 5014–5022.

(188) Su, N. C.; Sun, D. T.; Beavers, C. M.; Britt, D. K.; Queen, W. L.; Urban, J. J. Enhanced permeation arising from dual transport pathways in hybrid polymer-MOF membranes. *Energy Environ. Sci.* **2016**, *9*, 922–931.

(189) Kang, Z.; Peng, Y.; Hu, Z.; Qian, Y.; Chi, C.; Yeo, L. Y.; Tee, L.; Zhao, D. Mixed matrix membranes composed of two-dimensional metal-organic framework nanosheets for pre-combustion CO₂ capture: a relationship study of filler morphology versus membrane performance. *J. Mater. Chem. A* **2015**, *3*, 20801–20810.

(190) Wang, X.; Chi, C.; Zhang, K.; Qian, Y.; Gupta, K. M.; Kang, Z.; Jiang, J.; Zhao, D. Reversed thermo-switchable molecular sieving membranes composed of two-dimensional metal-organic nanosheets for gas separation. *Nat. Commun.* **2017**, *8*, 14460.

(191) Lin, R.; Ge, L.; Hou, L.; Strounina, E.; Rudolph, V.; Zhu, Z. Mixed Matrix Membranes with Strengthened MOFs/Polymer Interfacial Interaction and Improved Membrane Performance. *ACS Appl. Mater. Interfaces* **2014**, *6*, 5609–5618.

(192) Shahid, S.; Nijmeijer, K.; Nehache, S.; Vankelecom, I.; Deratani, A.; Quemener, D. MOF-mixed matrix membranes: Precise dispersion of MOF particles with better compatibility via a particle fusion approach for enhanced gas separation properties. *J. Membr. Sci.* **2015**, *492*, 21–31.

(193) Chi, W. S.; Kim, S. J.; Lee, S.-J.; Bae, Y.-S.; Kim, J. H. Enhanced Performance of Mixed-Matrix Membranes through a Graft Copolymer-Directed Interface and Interaction Tuning Approach. *ChemSusChem* **2015**, *8*, 650–658.

(194) Wang, Z.; Wang, D.; Zhang, S.; Hu, L.; Jin, J. Interfacial Design of Mixed Matrix Membranes for Improved Gas Separation Performance. *Adv. Mater.* **2016**, *28*, 3399–3405.

(195) Japip, S.; Liao, K.-S.; Chung, T.-S. Molecularly Tuned Free Volume of Vapor Cross-Linked 6FDA-Durene/ZIF-71 MMMs for H₂/CO₂ Separation at 150 °C. *Adv. Mater.* **2017**, *29*, 1603833.

(196) Song, Q.; Cao, S.; Pritchard, R. H.; Qiblawey, H.; Terentjev, E. M.; Cheetham, A. K.; Sivaniah, E. Nanofiller-tuned microporous polymer molecular sieves for energy and environmental processes. *J. Mater. Chem. A* **2016**, *4*, 270–279.

(197) Geim, A. K.; Novoselov, K. S. The rise of graphene. *Nat. Mater.* **2007**, *6*, 183–191.

(198) Celebi, K.; Buchheim, J.; Wyss, R. M.; Droudian, A.; Gasser, P.; Shorubalko, I.; Kye, J.-I.; Lee, C.; Park, H. G. Ultimate Permeation Across Atomically Thin Porous Graphene. *Science* **2014**, *344*, 289–292.

(199) Turchanin, A.; Beyer, A.; Nottbohm, C. T.; Zhang, X.; Stosch, R.; Sologubenko, A.; Mayer, J.; Hinze, P.; Weimann, T.; Götzhäuser, A. Thin Films: One Nanometer Thin Carbon Nanosheets with Tunable Conductivity and Stiffness. *Adv. Mater.* **2009**, *21*, 1233–1237.

- (200) Park, H. B.; Yoon, H. W.; Cho, Y. H., Graphene Oxide Membrane for Molecular Separation. In *Graphene Oxide*; John Wiley & Sons, Ltd.: 2016; pp 296–313.
- (201) Marcano, D. C.; Kosynkin, D. V.; Berlin, J. M.; Sinititskii, A.; Sun, Z.; Slesarev, A.; Alemany, L. B.; Lu, W.; Tour, J. M. Improved Synthesis of Graphene Oxide. *ACS Nano* **2010**, *4*, 4806–4814.
- (202) Yeh, C.-N.; Raidongia, K.; Shao, J.; Yang, Q.-H.; Huang, J. On the origin of the stability of graphene oxide membranes in water. *Nat. Chem.* **2015**, *7*, 166–170.
- (203) Kim, H. W.; Yoon, H. W.; Yoon, S.-M.; Yoo, B. M.; Ahn, B. K.; Cho, Y. H.; Shin, H. J.; Yang, H.; Paik, U.; Kwon, S.; Choi, J.-Y.; Park, H. B. Selective Gas Transport Through Few-Layered Graphene and Graphene Oxide Membranes. *Science* **2013**, *342*, 91–95.
- (204) Li, H.; Song, Z.; Zhang, X.; Huang, Y.; Li, S.; Mao, Y.; Ploehn, H. J.; Bao, Y.; Yu, M. Ultrathin, Molecular-Sieving Graphene Oxide Membranes for Selective Hydrogen Separation. *Science* **2013**, *342*, 95–98.
- (205) Shen, J.; Liu, G.; Huang, K.; Jin, W.; Lee, K.-R.; Xu, N. Membranes with Fast and Selective Gas-Transport Channels of Laminar Graphene Oxide for Efficient CO₂ Capture. *Angew. Chem., Int. Ed.* **2015**, *54*, 578–582.
- (206) Li, X.; Cheng, Y.; Zhang, H.; Wang, S.; Jiang, Z.; Guo, R.; Wu, H. Efficient CO₂ Capture by Functionalized Graphene Oxide Nanosheets as Fillers To Fabricate Multi-Permeable Mixed Matrix Membranes. *ACS Appl. Mater. Interfaces* **2015**, *7*, 5528–5537.
- (207) Wang, S.; Wu, Y.; Zhang, N.; He, G.; Xin, Q.; Wu, X.; Wu, H.; Cao, X.; Guiver, M. D.; Jiang, Z. A highly permeable graphene oxide membrane with fast and selective transport nanochannels for efficient carbon capture. *Energy Environ. Sci.* **2016**, *9*, 3107–3112.
- (208) Shen, J.; Liu, G.; Huang, K.; Chu, Z.; Jin, W.; Xu, N. Subnanometer Two-Dimensional Graphene Oxide Channels for Ultrafast Gas Sieving. *ACS Nano* **2016**, *10*, 3398–3409.
- (209) Liu, G.; Jin, W.; Xu, N. Two-Dimensional-Material Membranes: A New Family of High-Performance Separation Membranes. *Angew. Chem., Int. Ed.* **2016**, *55*, 13384–13397.
- (210) Wang, L.; Drahushuk, L. W.; Cantley, L.; Koenig, S. P.; Liu, X.; Pellegrino, J.; Strano, M. S.; Scott Bunch, J. Molecular valves for controlling gas phase transport made from discrete ångström-sized pores in graphene. *Nat. Nanotechnol.* **2015**, *10*, 785–790.
- (211) Brown, A. J.; Brunelli, N. A.; Eum, K.; Rashidi, F.; Johnson, J. R.; Koros, W. J.; Jones, C. W.; Nair, S. Interfacial microfluidic processing of metal-organic framework hollow fiber membranes. *Science* **2014**, *345*, 72–75.
- (212) Eum, K.; Ma, C.; Rownaghi, A.; Jones, C. W.; Nair, S. ZIF-8 Membranes via Interfacial Microfluidic Processing in Polymeric Hollow Fibers: Efficient Propylene Separation at Elevated Pressures. *ACS Appl. Mater. Interfaces* **2016**, *8*, 25337–25342.
- (213) Marti, A. M.; Wickramanayake, W.; Dahe, G.; Sekizkardes, A.; Bank, T. L.; Hopkinson, D. P.; Venna, S. R. Continuous Flow Processing of ZIF-8 Membranes on Polymeric Porous Hollow Fiber Supports for CO₂ Capture. *ACS Appl. Mater. Interfaces* **2017**, *9*, 5678–5682.
- (214) Hou, J.; Sutrisna, P. D.; Zhang, Y.; Chen, V. Formation of Ultrathin, Continuous Metal–Organic Framework Membranes on Flexible Polymer Substrates. *Angew. Chem., Int. Ed.* **2016**, *55*, 3947–3951.
- (215) Dai, Y.; Johnson, J. R.; Karvan, O.; Sholl, D. S.; Koros, W. J. Ultem®/ZIF-8 mixed matrix hollow fiber membranes for CO₂/N₂ separations. *J. Membr. Sci.* **2012**, *401–402*, 76–82.
- (216) Ash, R.; Barrer, R. M.; Lowson, R. T. Transport of single gases and of binary gas mixtures in a microporous carbon membrane. *J. Chem. Soc., Faraday Trans. 1* **1973**, *69*, 2166–2178.
- (217) Ash, R.; Barrer, R. M.; Pope, C. G. Flow of Adsorbable Gases and Vapours in a Microporous Medium. II. Binary Mixtures. *Proc. R. Soc. London, Ser. A* **1963**, *271*, 19–33.
- (218) Koresh, J. E.; Soffer, A. Mechanism of permeation through molecular-sieve carbon membrane. Part I.-The effect of adsorption and the dependence on pressure. *J. Chem. Soc., Faraday Trans. 1* **1986**, *82*, 2057–2063.
- (219) Koresh, J.; Soffer, A. Study of molecular sieve carbons. Part I.-Pore structure, gradual pore opening and mechanism of molecular sieving. *J. Chem. Soc., Faraday Trans. 1* **1980**, *76*, 2457–2471.
- (220) David, L. I. B.; Ismail, A. F. Influence of the thermastabilization process and soak time during pyrolysis process on the polyacrylonitrile carbon membranes for O₂/N₂ separation. *J. Membr. Sci.* **2003**, *213*, 285–291.
- (221) Song, C.; Wang, T.; Jiang, H.; Wang, X.; Cao, Y.; Qiu, J. Gas separation performance of C/CMS membranes derived from poly-(furfuryl alcohol) (PFA) with different chemical structure. *J. Membr. Sci.* **2010**, *361*, 22–27.
- (222) Centeno, T. A.; Fuertes, A. B. Supported carbon molecular sieve membranes based on a phenolic resin. *J. Membr. Sci.* **1999**, *160*, 201–211.
- (223) Tin, P. S.; Chung, T.-S.; Liu, Y.; Wang, R. Separation of CO₂/CH₄ through carbon molecular sieve membranes derived from P84 polyimide. *Carbon* **2004**, *42*, 3123–3131.
- (224) Shao, L.; Chung, T.-S.; Wensley, G.; Goh, S. H.; Pramoda, K. P. Casting solvent effects on morphologies, gas transport properties of a novel 6FDA/PMDA–TMMDA copolyimide membrane and its derived carbon membranes. *J. Membr. Sci.* **2004**, *244*, 77–87.
- (225) Kiyono, M.; Williams, P. J.; Koros, W. J. Effect of pyrolysis atmosphere on separation performance of carbon molecular sieve membranes. *J. Membr. Sci.* **2010**, *359*, 2–10.
- (226) Koros, W. J.; Zhang, C., Ultra-selective carbon molecular sieve membranes and methods of making. Google Patents, 2016.
- (227) Xu, L.; Rungta, M.; Brayden, M. K.; Martinez, M. V.; Stears, B. A.; Barbay, G. A.; Koros, W. J. Olefins-selective asymmetric carbon molecular sieve hollow fiber membranes for hybrid membrane-distillation processes for olefin/paraffin separations. *J. Membr. Sci.* **2012**, *423–424*, 314–323.
- (228) Qiu, W.; Zhang, K.; Li, F. S.; Zhang, K.; Koros, W. J. Gas Separation Performance of Carbon Molecular Sieve Membranes Based on 6FDA-mPDA/DABA (3:2) Polyimide. *ChemSusChem* **2014**, *7*, 1186–1194.
- (229) Koh, D.-Y.; McCool, B. A.; Deckman, H. W.; Lively, R. P. Reverse osmosis molecular differentiation of organic liquids using carbon molecular sieve membranes. *Science* **2016**, *353*, 804–807.
- (230) Kwon, H. T.; Jeong, H.-K. In Situ Synthesis of Thin Zeolitic–Imidazolate Framework ZIF-8 Membranes Exhibiting Exceptionally High Propylene/Propane Separation. *J. Am. Chem. Soc.* **2013**, *135* (29), 10763–10768.
- (231) Koh, H. T.; Jeong, H.-K.; Lee, A. S.; An, H. S.; Lee, J. S. Heteroepitaxially Grown Zeolitic Imidazolate Framework Membranes with Unprecedented Propylene/Propane Separation Performances. *J. Am. Chem. Soc.* **2015**, *137* (38), 12304–12311.
- (232) Nan, J.; Dong, X.; Wang, W.; Jin, W.; Xu, N. Step-by-Step Seeding Procedure for Preparing HKUST-1 Membrane on Porous α -Alumina Support. *Langmuir* **2011**, *27* (8), 4309–4312.
- (233) Adhikari, S.; Fernando, S. Hydrogen Membrane Separation Techniques. *Ind. Eng. Chem. Res.* **2006**, *45*, 875–881.
- (234) Ockwig, N. W.; Nenoff, T. M. Membranes for Hydrogen Separation. *Chem. Rev.* **2007**, *107*, 4078–4110.
- (235) Kusakabe, K.; Sakamoto, S.; Saie, T.; Morooka, S. Pore structure of silica membranes formed by a sol-gel technique using tetraethoxysilane and alkyltriethoxysilanes. *Sep. Purif. Technol.* **1999**, *16*, 139–146.
- (236) Nair, B. N.; Yamaguchi, T.; Okubo, T.; Suematsu, H.; Keizer, K.; Nakao, S.-I. Sol-gel synthesis of molecular sieving silica membranes. *J. Membr. Sci.* **1997**, *135*, 237–243.
- (237) Cao, G.; Lu, Y.; Delattre, L.; Brinker, C. J.; López, G. P. Amorphous silica molecular sieving membranes by sol-gel processing. *Adv. Mater.* **1996**, *8*, 588–591.
- (238) Araki, S.; Mohri, N.; Yoshimitsu, Y.; Miyake, Y. Synthesis, characterization and gas permeation properties of a silica membrane prepared by high-pressure chemical vapor deposition. *J. Membr. Sci.* **2007**, *290*, 138–145.
- (239) Lee, D.; Zhang, L.; Oyama, S. T.; Niu, S.; Saraf, R. F. Synthesis, characterization, and gas permeation properties of a hydrogen

permeable silica membrane supported on porous alumina. *J. Membr. Sci.* **2004**, *231*, 117–126.

(240) Tsapatsis, M.; Gavalas, G. Structure and aging characteristics of H₂-permselective SiO₂-Vycor membranes. *J. Membr. Sci.* **1994**, *87*, 281–296.

(241) Bose, A. C. *Inorganic Membranes for Energy and Environmental Applications*; Springer: 2008.

(242) Carolan, M.; Chen, C.; Chen, J.; Miller, C.; Minford, E.; Waldron, W. ITM Ceramic Membrane Technology to Produce Synthesis Gas. *ECS Trans.* **2008**, *13*, 319–325.

(243) Carolan, M. F.; Chen, C. M.; Rynders, S. W.; Waldron, W. Development of the ceramic membrane ITM syngas/ITM hydrogen process. *Fuel Chem. Div Prepr.* **2003**, *48*, 344.

(244) Carolan, M. F.; Chen, C. M.; Rynders, S. W. In ITM Syngas and ITM H₂: Engineering Development of Ceramic Membrane Reactor Systems for Converting Natural Gas to Hydrogen and Synthesis Gas for Liquid Transportation Fuels (DE-FC26-97FT96052), Citeseer.

(245) de Lange, R. S. A.; Keizer, K.; Burggraaf, A. J. Aging and Stability of Microporous Sol-Gel-Modified Ceramic Membranes. *Ind. Eng. Chem. Res.* **1995**, *34*, 3838–3847.

(246) Yong Ha, H.; Woo Nam, S.; hong, S.-A.; Kook Lee, W. Chemical vapor deposition of hydrogen-permselective silica films on porous glass supports from tetraethylorthosilicate. *J. Membr. Sci.* **1993**, *85*, 279–290.

(247) Qi, H.; Han, J.; Xu, N.; Bouwmeester, H. J. M. Hybrid Organic–Inorganic Microporous Membranes with High Hydrothermal Stability for the Separation of Carbon Dioxide. *ChemSusChem* **2010**, *3*, 1375–1378.

(248) Scholze, H. Chemical durability of glasses. *J. Non-Cryst. Solids* **1982**, *52*, 91–103.